ADDIS ABABA UNIVERSITY

SCHOOL OF GRADUATE STUDIES

EVALUATION OF TARO BOLOSO-I (*Colocasia esculenta* Cultivar) NATIVE STARCH AS DISINTEGRANT AND ITS PRE-GELATINIZED FORM AS DIRECT COMPRESSION DILUENT IN PARACETAMOL TABLETS

By: Tamrat Balcha (B. Pharm)

January, 2016

Addis Ababa, Ethiopia

Evaluation of Taro Boloso-I Native (*Colocasia esculenta* Cultivar) Starch as Disintegrant and Its Pre-Gelatinized form as Direct Compression Diluent in Paracetamol Tablets

Tamrat Balcha Balla (B. Pharm)

A Thesis Submitted to the School of Graduate Studies of Addis Ababa University, in partial fulfillment of the requirements for the Degree of Master of Science in Pharmaceutics, in the Department of Pharmaceutics and Social Pharmacy, School of Pharmacy, College of Health Sciences, Addis Ababa University

ADDIS ABABA UNIVERSITY

SCHOOL OF GRADUATE STUDIES

This is to certify that the thesis investigated by Tamrat Balcha Balla, Entitled: "Evaluation of Taro Boloso-I (*Colocasia esculenta* Cultivar) Native Starch as Disintegrant and Its Pre-Gelatinized form as Direct Compression Diluent in Paracetamol Tablets" and submitted in partial fulfillment of the requirements for the Degree of Master of Science in Pharmaceutics complies with the regulations of the University and meets the accepted standards with respect to originality and quality.

Signed by the following Examining Committee:

Name	Signature	Date
Dr. Anteneh Belete (Advisor)	_____	_____
Dr Nisha Mary Joseph (Advisor)	_____	_____
Prof Tsige Gebre-Mariam (Examiner)	_____	_____
Dr Kaleab Asres (Examiner)	_____	_____

ACKNOWLEDGEMENTS

Most of all, I thank His Omnipotency Lord with my full-length passion for all.

I am glad to express my heart depth gratitude and admirations to my advisors: Dr Anteneh Belete and Dr Nisha Mary Joseph, for advisory, encouragement, constructive mentorships and technical backings. I extend my thanks to Prof Tsige Gebre-mariam for initial confirmatory comments on the plant, facilitating morphological study of starches and providing standard amylose and amylopectin.

I would like to thank Martin Luther University, Germany; Diya Labs, India; Ethiopian Pharmaceutical Manufacturing Share Company (EPHARM); Ethiopian Public Health Institute and Areka Agricultural Research Center for material donations, technical supports and access to laboratory facilities.

I am glad to grant Dr Fitsum Feleke, Mr Tesfa Marew, Mr Efrem Nigusu, Mr Getahun Paulos, Mr Yonas Birhane, Mr Fekade Tefera, Mrs Ademech Goshu, Mrs Yetnayet Berhanu and some of my friends for the official and friendly contributions. I am equally indebted to acknowledge my friends Dr Birhanetsehay Teklewold, Dr Alemayehu Yohanis, Mr Nigatu Mathewes, Mr Tilahun Saol and Mr Girma Workneh as well as my sister Mrs Beletech Balcha and Brother Mr Nigatu Balcha for their invaluable contributions on the material procurement to processing in the laboratory.

Last but not least, I thank Areka Town Administration and Addis Ababa University for sponsoring my whole MSc studies and this research in particular.

TABLE OF CONTENTS

CONTENTS Page

LIST OF TABL

LIST OF FIGUR

LIST OF ACRONYMS

ANOVA	Analysis of Variance
CCD	Central composite design
CV	Coefficient of variation
DSC	Differential Scanning Calorimetry
DT	Tablet disintegration time
FI	Factor interaction

FTIR	Fourier Transform Infra-red spectroscopy
ΔH	Enthalpy
LOF	Lack of Fit
OOP	Out-of-plane
%RH	Percent relative humidity
RSM	Response surface Methodology
SP	Swelling power
NTB1S	Native *Taro Boloso-I* starch
PGTB1S	Pregelatinized *Taro Boloso-I* starch
PRESS	Predicted Residual Sum of Squares
UV/Vis	Ultraviolet-visible
WSI	Water solubility index
XRD	X-Ray Diffraction

ABSTRACT

Taro *Boloso-I* is a new variety of *Colocasia esculenta* (L. Schott) officially released from Areka Agricultural Research Center, Areka, Ethiopia. Its cultivation out yields 67% more than a previously reported variety (Godare) in Ethiopia. It contains 85.65 ± 0.07% of carbohydrate on dry basis and higher gross energy than the existing cultivars of taro reflecting its difference from the preexisting varieties of taro. The aim of this study was to isolate, characterize the starch from this plant and evaluate its potential applications. It was also to evaluate the tablet disintegrant properties and direct compressibility of the pre-gelatinized form using paracetamol as a model drug. Starch was extracted from the *C. esculenta* by using saline solution (0.1N) and sodium hydroxide (0.03 N). Various

experimental methods were applied for characterization of the starch. Central composite design was used for optimization of the levels and hence the responses. Yield of starch from Taro *Boloso-I* on dry weight basis was 83.5 ± 1.6%. The native Taro *Boloso-I* starch (NTB1S) was characterized by lower amylose to amylopectin ratio (20.7 ± 1.8% to 77.3 ± 2.1%, w/w) higher onset, peak and endset temperatures of gelatinization than potato starch. Its granules were found to exhibit polyhedral/angular shape and A-type polymorphism comprising powder of poor flow. In all of these properties, Taro *Boloso-I* starch not only significantly differs from the previously reported taro varieties in Ethiopia but also shares more of cereal starches (rice starch) than the tuber starches. Paracetamol tablet (350mg) prepared by wet granulation using NTB1S (9.80%) as disintegrant and compression force of 15kN had hardness of 117.1 ± 4.93N, friability of 0.159 ± 0.02% and disintegration time of 1.31 ± 0.02 min. The hardness, friability and balance between binding and disintegration were better than potato starch, 58.1 ± 2.57 N, 1.01 ± 0.06% and 46.4 ± 4, respectively. Moreover, the tablets fulfill the disintegrant time requirements for fast dissolving tablets. The modified (optimized) Taro *Boloso-I* starch (PGTB1S) has comparable flow property but higher compressibility and compactibility. If used as a disintegrant in paracetamol tablets, NTB1S can result not only in better hardness and friability than the corresponding tablets with potato starch but also a kind of fast dissolving tablet. Also it was revealed that PGTB1S can be used as efficient direct compression diluent with magnesium stearate tolerance of 0.5%. Its dilution potential was also better than Starch 1500®.

Key words: Starch, tablet, compression, gelatinization, disintegrant, Taro *Boloso-I,* Kawakita, Heckel

1. INTRODUCTION

1.1. Starch

Starch is the most abundant biopolymer next to cellulose. It is a polymer of glucose joined by glycosidic bonds. Structurally, it comprises α-D-glucopyranosyl residues straightly linked 1 → 4 or those with 1 → 6 extra linkages at the branch points besides 1 → 4: the amylose and amylopectin, respectively (Fig. 1.1) (Belitz *et al.,* 2009).

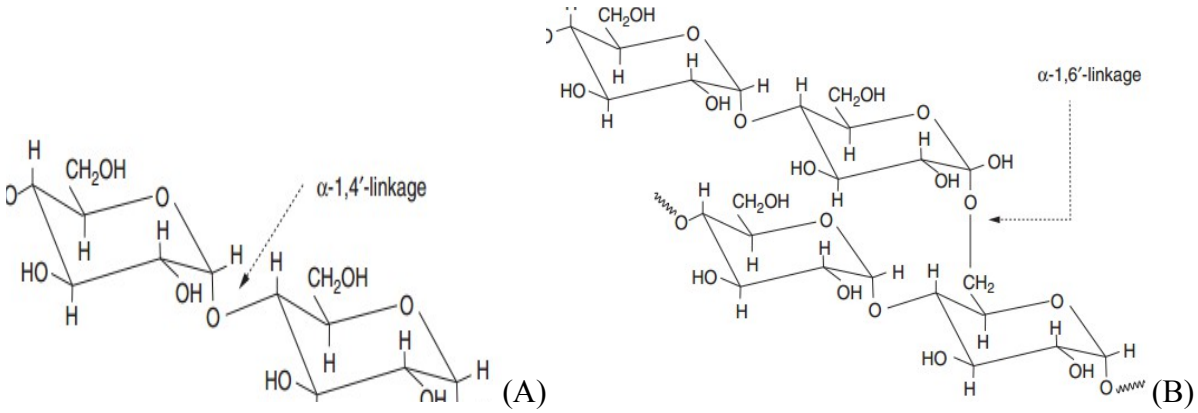

Fig. 1.1. Molecular structure of amylose (A) and amylopectin (B) (Sangwan *et al.*, 2014).

Starches are obtained from plants, where they are energy stores, of which the foremost are cereals (rice, maize and wheat) and roots (potatoes, cassava, taro etc.). The source plants contain blends of sugars, starches, mucilages, proteins, pectins, cellulose, gums, inorganic salts, fixed and volatile oils, resins, tannins, coloring materials, alkaloids and glycosides, among others. This necessitates appropriate selection of the solvent for desired constituents to sediment while dissolving the undesired constituents. The major challenges in tuber starch extraction, mucilage and latex related quality and quantity loss, are overcome through various chemicals capable of forming complexes with mucilage and latex and fasten sedimentation, e.g., $NH_4OH_{(aq)}$ and $NaOH_{(aq)}$ (Belitz *et al.,* 2009; Sionkowska, 2011).

1.2. The Physicochemical Properties of Starch

Starches obtained from the sources exist in separate, simple or compound, concentric or eccentric granules of polygonal, round, elliptical, or oval shapes typical to the sources (Swarbrik, 2007). The physicochemical properties such as morphology, granule size, crystallinity, moisture-uptake, swelling, gelatinization, viscosity, etc. of starches vary still with botanical source even from variety to variety ((Hoover, 2001; Roy *et al.*, 1984). The native starch granules vary in size as small (2-40 μm) or large

(50-150 µm) (Flickinger and Drew, 1999). Though amylose to amylopectin ratio (20: 80% - 30: 70%, mostly) is core structural factor for applications, starch granules contain proteins and lipids. Composition, molecular length and branching density of starch make basis for the rest of physicochemical and functional properties and define types of applications of the starches.

1.2.1. Crystallinity

Starch is a semi-crystalline polymer. Its crystallinity decreases with amylose content (Tan and Halley, 2014). Degree of crystallinity, which also decreases with moisture content, affects the gelatinization and retrogradation (Dalonso and Petkowicz, 2014; Moraes *et al.,* 2014). Native starches exist as types A (largely in cereal starches), B (largely in potatoes, amaylomaize and retrograded starches), C (largely in corn and legumes) and V (in swollen starches: V_a water free and V_h hydrated). A and B-type polymorphs are real crystalline whereas C is mixed or intermediate between A and B (Belitz *et al.,* 2009). For a starch as a pharmaceutical excipient, certain degree of crystallinity is desired to keep some desired attributes. Amorphization or crystalline transformation can occur during storage besides tableting at drying, granulation, compression, temperature changes and humidity changes. A-type crystalline structure is associated with low amylose content than B-type (Yong-an *et al.,* 2012; Zhou *et al.,* 2014).

1.2.2. Behavior in Water

1.2.2.1. Swelling and Solubility

Air dried starch reversibly swells 30–40% of diameter in cold water though it doesn't dissolve due to extensive hydrogen bonding. Swelling rate is very important characteristic of tablet disintegrants (Shayne, 2008). Swelling power (SP) as well as solubility of starches increases with temperature (Nawab *et al.,* 2014). For disintegrants whose mechanism is swelling, the rate, force and extent of swelling define the disintegrating efficiency (Alfonso, 2000). Moreover, the susceptibility of starch to structural change on heat-moisture treatment or gelatinization varies with botanical source (larger for tuber and root origin starches) (Gunaratne and Hoover, 2002).

1.2.2.2. Gelatinization

When starch suspension is heated, an irreversible order-disorder phase transition called gelatinization occurs at a typical temperature (50–75 ˚C), gelatinization temperature (Belitz *et al.,* 2009). The process of gelatinization causes significant changes because of granular disruption. It has been proven and

published that gelatinization renders starches directly compressible, for example corn starch (Widodo and Hassan, 2015). A contrast of pregelatinization of starches to other modifications is that it retains their capillary activity and swelling to some degree when in contact with water (Odeku and Picker-Freyer, 2010).

1.3. Applications of Starch

Innumerable starch sources, modifications and derivatives provide vital inputs for pharmaceutical, food, paper and textile manufacturing *inter alia* for starch is renewable, biodegradable, low cost polymer and most abundant biopolymer next to cellulose (Flickinger and Drew, 1999). It is available, non-irritant, ecofriendly, modifiable, potentially degradable and biocompatible by virtue of design by - nature (Sionkowska, 2011). An early form of modifications was slight hydrolysis by vinegar of 1500-1900 AD. It was scaled up by carbohydrate chemists starting from 1930s on wards, e.g., production of waxy corn starch (Deborah and Roy, 2009). These tendencies have continued to grow to suit the starch for settings such as high heat and shear, low pH, freeze/thaw and cooling. This is with possible aim of using it as sweetener, binder, disintegrant, thickener, emulsifier, inhibiting moisture (stabilizer); producing cuttable texture; developing a soft or crisp coating; or stabilizing an emulsion. Starch modifications, for example, cross-linking, affects gelatinization temperature and swelling capacity of the starch proportionally (Belitz *et al.,* 2009). Because of its abundance, high density and limited pretreatments while preparing, starch is the most practiced natural resource for fermentation. Above and beyond, newer starches are looked for and will continue to be sought after evermore further than foregoing reviews. This is because of the scaling up fashion of versatility of starch applications, modifications, derivatizations and demands along with advances in biotechnology. Thus, any notable progress, even slight, of a starch will bring about great societal impact with so immense and diverse consumption (Flickinger and Drew, 1999).

1.4. Taro *Boloso-I* (*Colocasia esculenta*)

Taro (*Colocasia esculenta*) is a tropical and subtropical herbaceous monocotyledonous, perennial stem root crop with large heart shaped leaves. Worldwide, it is among top five in terms of area and production with cassava, potato, sweet potato and yam. It is one of the top three in South, South Western and Western Ethiopia where it is widely cultivated and used. This calls for its high yield, pest and disease resistance, ecological adaptation and storage for longer period of time. Some of the vernacular names of taro include “godare” in Amharic and “Boyna” in Wolaitta languages which are

equivalent to “taro” in English. Eight local land race cultivars of taro grow in Wolaitta Zone (Dagne *et al.*, 2014) before the era of Taro *Boloso-I*.

Taro *Boloso-I* (Fig. 1.2) is an improved new variety of *C. esculenta* officially released from Areka Agricultural Research Center for mid altitude and similar growing areas of Southern Ethiopia with wet heavy fertile soil. It was developed by collecting 87 accessions of taro during 1996 - 1997 cropping seasons from Southern, South western and Western Ethiopia which are the major taro growing areas of the country. It was selected among from these accessions in terms of yield, relative resistance towards major diseases and pests and agronomic merits for the growing areas. It was released and named “Taro Boloso-I” by National Variety Releasing Committee (NVRC) for mid altitude agro-ecology and similar growing areas of Southern Nations, Nationalities and People’s Region with heavy fertile soil (Dagne *et al.,* 2014). The specific vernacular name of Taro *Boloso-I* cultivar in Wolaitta is “Barakata” for “blessed” named after its high yield.

 (A)  (B)  (C)

Fig. 1.2. Taro *Boloso-I* in the field (A), dug out from soil (B) and after harvesting the tuber stems (C) (Photograph by Tamrat Balcha).

The marketable yield of Taro Boloso-I outweighs the other cultivar by average of 67% (Dagne *et al.,* 2014). Raw Taro *Boloso-I* contains 85.65 ± 0.07% of carbohydrate on dry basis. It has gross energy content comparable to that of maize, higher than that of cassava, Irish potato, yam, sweet potato and other taro cultivars and lower than rice and sorghum. Because of its higher productivity and gross energy content it is claimed it can endow the efforts of the Ethiopian Government to improve food and nutrition security (Adane *et al.,* 2013). These facts of Taro *Boloso-I* reveal it is different from the existing varieties of taro including the plant investigated by Adane *et al.,* (2006b).

1.5. Pharmaceutical Applications of Starch

1.5.1. Tablet Disintegrants

Besides therapeutic ingredients, pharmaceutical dosage forms contain excipients for biopharmaceutical advantages (e.g., tablet disintegrants), technological augments (e.g., directly compressible vehicles) or both purposes. Especially for tablet disintegrating and binding properties, starch is the most striking excipient in pharmaceutical industries. Unless rapid disintegration is intended where the starch added as disintegrant might total up to 20%, 5 - 10% is appropriate. Of all the starch powder as tablet disintegrant, often a portion (e.g., half) is added as intra-granular disintegrant and the rest reserved and added to finished granulation ahead of tablet compression. This sometimes doubles the disintegration of tablet, *i.e.*, the second portion fragments the tablet into smaller pieces (may be granules) and the first portion extends into finer. As it is difficult to judge best of intra-granular, extra-granular or portioned method of incorporation, preferably, all the data are taken and optimized. In the case of corn starch, liability of disintegrating property is of amylose and that of binding/gummy property is of amylopectin (Alfonso, 2000; Swarbrick, 2007). Disintegrant action of starch is stated to be capillary action (wicking). However, swelling is also claimed though the spherical shape of the starch grains is associated with the former mechanism by increasing the porosity of the tablet (Shayne, 2008). The disintegration time of tablets depends on the nature and concentration of disintegrants used (Gebre-mariam and Schmidt, 1996a).

~~**1.5.2. Tablet Disintegrants**~~

1.5.3. ~~Disintegrants are needed because the strength rendered to tablets so that the tablets tolerate stressful manufacturing processes blocks the dissolution of the tablets after ingestion by patients. Disintegrants are the right excipients, in the presence of water, to overcome this cohesive force by swelling, capillary (wicking or internal pressure), gas release and enzymatic mechanisms which may be mixed or indistinct to rightly acclaim (James, 2007; Shayne C, 2008).~~

1.5.4. ~~Starch, the oldest disintegrant, is still the most common for its highly branched, water insoluble, major constituent, the amylopectin, is very hydrophilic and hence swells when moistened, among other mechanisms. Disintegrant action of starch is stated to be capillary action (wicking). However, swelling is also claimed though, increasing the porosity of the tablet, the spherical shape of the starch grains is associated with the former mechanism, capillary action (Alfonso, 2000; Shayne, 2008).~~

1.5.5. ~~Unless more hurried tablet disintegration is intended in which case the total of starch added as disintegrant might be up to 20%, 5 - 10% is appropriate. But for that super-disintegrants bypass the high concentration demand and the low efficiency of intra-granular starches as disintegrants, starch is still widely used tablet disintegrant (James, 2007). Of all the starch powder as tablet disintegrant, often a portion (e.g. half) is added as endo-disintegrant and the rest reserved and added to finished granulation ahead of tablet compression. This sometimes doubles the disintegration of tablet, i.e. the second portion fragments the tablet into smaller pieces (may be granules) and the first portion extends into finer. As it is difficult to judge best of intra-granular, extra-granular or portioned method of incorporation, preferably, all the data are taken and optimized (Alfonso, 2000; James, 2007).~~

1.5.6. Directly Compressible Diluents

Besides, starch can be used as filler (diluent) for direct compression of tablets. Despite the paradoxes and complexity of tableting as only a few materials are there fitting the quality attributes, tablet is the commonest dosage form. Tableting, changing the powder into a low porosity compact which can disintegrate on ingestion as rapidly as possible, involves compressing uniform volumes of particles directly or following either wet or dry granulation. Consolidation also takes place during compression (Murakami *et al.,* 2001; Dale *et al.,* 2009). On the other hand, direct compression is preferred method of tableting. This is because, wet granulation method has been used for long while it has drawbacks in terms of achieving batch-to-batch reproducibility and higher productivity, especially in low particle size range. Moreover, it is energy and time consuming besides exposing thermolabile and moisture sensitive drug molecules. Direct compression overcomes these problems. It is more economic as it requires fewer unit operations and, in this way, second advantage of which is reducing chances of contamination and steps to be validated and documented. It also avoids stability problems of especially moisture and heat sensitive drugs, drugs whose dissolution profile is likely to change on storage and drugs under the risk of microbial growth. Moreover, it favors faster dissolution as the tablet disintegrates directly into API particles than into granules. Furthermore, it reduces wear & tear of punches due to exemption of high compaction pressure involved in the production of tablets by slugging or roller compaction. The reason is that direct compression is preferable for hygroscopic drugs, e.g., as orodispersibles. It is also method of choice for low dose tablets and tablets of high loading with poor compactibility. It is because of this besides the advent of emergence of new

excipients, new grades of the existing excipients and state-of-art mechanized technologies such as positive die feeding and the precompression stages, that tableting is focusing more on direct compression (Ahmada *et al.,* 2012). Nevertheless, it needs warranty of flow and compactibility (ability to form robust tablets) of powders, main challenges for adequate productivity and quality. Pregelatinization and particle size adjustment make starches directly compressible (Odeku and Picker-Freyer, 2010). The reason is betterment of flow property following changes in particle density, particle size and shape, and moisture content (Chaudhuri *et al.,* 2006).

1.5.6.1. Flowability

In tablet manufacturing, for acceptable weight uniformity the powder should have better fluidity as cohesiveness of powders affects scale up and scale down of unit operations such as blending, sampling discharge, fluidization and granulation (Chaudhuri *et al.,* 2006). Carr's index and Hausner ratio (Kojima and Eliott, 2012), flow rate and direct observation are used to characterize powder flowability. The powders of angles of repose values < 30, 30-45, 45-55 and > 55 ° are categorized as good flowing, some cohesive, true cohesive and sluggish (very cohesive)/very limited flowing. Similarly, the Carr's index values 5-10, 12-16, 18-21 and 23-35 correspond to excellent, good, fair and poor flowability classes. The Hausner ratio of below 1.25 shows good flowability. Flow rates of different materials depend upon many particle related and process related factors. It is advantageous for investigating any pulsating flow of free flowing bulk solids. Nevertheless, no single powder flow method can satisfactorily or completely characterize and explain the wide range of flow properties practiced in the industry (USP 30 / NF 25, 2007).

1.5.6.2. ~~Compactibility:~~ Compressibility~~and Consolidation~~

Compressibility is the ability of a powder to deform under pressure and compactibility is its ability to form mechanically strong compact with certain resistance towards stress. If small size particles are pressed against each other by external forces, the interparticular compressive stress increases leading to increase in adhesive force and plastic deformation of the particles in contact areas which are very small. The compression force both compresses and consolidates the bulk solid *(Dale et al., 2009)*. Bonding mechanisms include formation of solid bridges, intermolecular forces and shape related bonding (mechanical interlocking). The higher compressible the powder particles are the closer the particles to each other generating more contact points and result in higher number of bonding and

stronger compacts (Santl *et al.,* 2011; ElShaer *et al.,* 2013). Compressibility is usually defined by relative density, porosity, or volume and applied pressure by using the Heckel or Kawakita models.

Kawakita equation with the use of tapping/pressure is used for analyzing powder compressibility (Shayne, 2008). The basic concept of Kawakita model which analyzes the dependence of degree of volume reduction on applied taps or pressure is described in eq 1.1 commonly used in practice as eq. 1.2.

$$C = \frac{V_0 - V_N}{V_0} = \frac{abN}{1+b} \qquad \text{eq. 1.1}$$

$$\frac{N}{C} = \frac{N}{a} + \frac{1}{ab} \qquad \text{eq. 1.2}$$

Where , C, V_0, V_N and N stand for degree of volume reduction, loose volume, tapped volume and the number of taps (can be replaced by pressure) whereas 'a' and 'b' are constants.

The constants of Kawakita equation are calculated from slope and intercept of the line from number of taps divided by degree of volume reduction before tapping versus number of taps (eq. 1.2). Constant 'a' is the fluidity which describes the minimum porosity before compression and constant 'b' is related to plasticity of the material and is called coefficient of compression. The constant '1/b' describes interparticulate cohesiveness and it corresponds to the amount of tapping or pressure that would make degree of volume reduction equal to half of 'a' (Swarbrick, 2007; Bakre and Ayodele, 2013; Widodo and Hassan, 2015).

Heckel model is the most commonly used method of studying powder compressibility. It involves plotting tablet densification (natural logarithm of reciprocal of porosity) versus applied pressure. The linear potion of the plot has slope 'k' and intercept 'A' both of which are material constants (eq. 1.3).

$$\ln\left(\frac{1}{1-D_{rel}}\right) = kP + \qquad \text{eq. 1.3}$$

Where k is Heckel constant, A is powder bed densification.

The plot may have three different regions dominated by different mechanisms of densification. These are: initial non-linear part where the densification is dominated by particle rearrangement, a linear part where the data obey the Heckel equation and final non-linear region dominated by elastic deformation. It is the linear region that represents plastic deformation of a powder particles. The reciprocal of its slope (k), is equal to the mean yield pressure (Gabaude *et al.,* 1999; Bakre and Ayodele, 2013). In this

regard, the shape of Heckel plot is used to determine the type of deformation mechanism the material undergoes (brittle/ or elastic/plastic) during compaction.

The linear portion of the plot is obtained by a line that fits the highest number of points on the graph, mostly in the range of the compression pressure 50-150 MPa, such that the correlation coefficient reasonably closcer to ~~1, e.g. not less than 0.95 in a study conducted by Mitrevej *et al.* (1996)~~ 1. The constant 'A' (intercept of the straight portion of the Heckel slope) is related to the particle rearrangement and die filling just before deformation and bonding of particles and used to calculate a relative density (D_A) (eq. 1.4).

$$D_A = 1 - e^{-A} \qquad \text{eq. 1.4}$$

D_A per se, along with relative density at a point applied pressure equals zero (D_0) is used to calculate phase of densification at low pressure, D_b (eq. 1.5) (Widodo and Hassan, 2015).

$$D_b = D_A - D_0 \qquad \text{eq. 1.5}$$

D_0 can be determined either from the plot (eq. 1.6), or experimentally (ratio of bulk density to true density).

$$D_0 = 1 - e^{-A_0} \qquad \text{eq. 1.6}$$

Importantly, D_b exhibits phase of densification at low pressure and shows further densification due to particle fragmentation (Mitrevej *et al.*, 1996).

1.6. The Present Study

Starch, as a natural polymer, is sought preferentially after either to semi-synthetic or synthetic ones in drug delivery. In this regard, Ethiopia is importing apt industrial starches while there are tremendous potential domestic sources of starches. This has negative consequences on the national income and economic development of the country. On the way to confront with these issues, there are some basic characterizations and studies of local starches including *Ensete ventricosum (Gebre-Mariam and Schmidt, 1996b)*, *Dioscorea abyssinica* (Gebre-Mariam and Schmidt, 1998)**,** Cassava starch (Paulos *et al.,* 2009) and Godare starch (Adane *et al.,* 2006) as important and critical pavements for further renascent explorations and researches. Nevertheless, in the literature, there is no relevant body of knowledge regarding the distinctive physicochemical properties, potential for pharmaceutical applications of either native or modified starch from Taro *Boloso-I*. Parallel to these, Taro *Boloso-I* is known for its higher yield, *i.e.*, 67% out yielding the other taro varieties on harvest, and its high gross

energy content reflecting its carbohydrate content excellence. Thus, isolation, physicochemical characteristization, potential application of its native starch as tablet disintegrant and its pregelatinized form as direct compression excipient were performed using paracetamol as a model drug. The physicochemical parameters investigated include proximate composition, amylose to amylopectin ratio, bulk powder properties, crystallinity, hydrothermal property and properties in water. The concentration of this starch as formulation factor and compression force as process factor (Riippia *et al.,* 1998) were optimized using CCD-RSM for their critical influences on the disintegrant properties. It has been shown that native taro *Boloso-I* starch (NTB1S) used as extra granular disintegrant in paracetamol tablet has ever increasing effect on the hardness with increasing concentration. This fact prompted and backed up the potential of NTB1S to have good compressibility and compactibility but poor flowability ~~(Mîinea *et al.*, 2011)~~. With this consideration, pre/gelatinization (in terms of temperature and time) has been optimized using CCD-RSM method to enhance the flow property of starch without impairing its compressibility/compactibility. Direct compression property of the optim~~u~~i~~m~~zed pregelatinized starch was evaluated.

1.7. The Objectives of Study

1.7.1. General Objective

To isolate, characterize and evaluate native (as a disintegrant) and pregelatinized (as direct compression diluent) starch from Taro Boloso-I (*Colocasia esculenta*).

1.7.2. Specific Objectives

- To isolate starch from Taro *Boloso-I* cultivar
- To characterize the physicochemical properties of NTB1S and the pregelatinized starch
- To optimize the disintegrant properties of NTB1S
- To optimize the NTB1S pregelatinization for direct compressibility
- To evaluate the direct compression properties of optimized pregelatinized starch

2. EXPERIMENTAL

2.1. Materials

Taro *Boloso-I* was obtained from Areka Agricultural Research institute, located at Areka (300 km South of Addis Ababa), Wolaitta, Ethiopia. Pure paracetamol (China Associate Co Ltd, China) was donated by the Ethiopian Pharmaceutical Manufacturing Share Company (EPHARM). Sodium hydroxide, magnesium stearate, potassium chloride and magnesium chloride hexahydrate (BDH Poole Co, UK); potassium monobasic phosphate and sodium chloride (Sörensen, Leuren, Denmark), potassium bromide (Research Lab fine industries, India); Ac-Di-Sol® (FMC, Co., USA), Iodine Resublimed (Reagent Chemicals Services Ltd., UK), hydrochloric acid 37% (Riedel-deHaën®, Germany) and potassium iodide (UNI-CHEM Chemical Reagents, USA) were used as obtained.

2.2. Methods

2.2.1. Isolation of Starch from Taro *Boloso-I*

Taro *Boloso-I* starch (NTB1S) was extracted as per the methods described by Gebre-Mariam and Schmidt (1996b) with slight modifications. First, fresh Taro *Boloso-I* tuber was washed to remove surface soil, cleaned, peeled and trimmed into small pieces and then crushed with 1% (w/v) $NaCl_{(aq)}$ solution using a blender machine (Blender-888A, Germany). The resulting mass was then repeatedly washed with the same saline solution containing 0.01 N NaOH although sedimentation did not take place. To improve this, a series of NaOH concentrations of (0.02, 0.03, 0.04, 0.05, 0.06 and 0.08 N) with the NaCl kept at 1% (w/v) were attempted. The sedimenting behavior increased with increasing concentration of NaOH up to 0.03 N and then decreased at 0.04 N and beyond most likely because of solublization. Therefore, 0.03 N NaOH was used for sedimenting the starch which was further washed with distilled water until the supernatant was clear and pH became neutral. Finally, the starch was dried at 40˚C in an oven (KOTTERMANN® 2711, Germany), milled until fine using laboratory grinder (Pulberisette 2, Fritsch, Germany) and sieved through 224 µm mesh size and kept in a tight sealing bottle for further use (Gebre-Mariam and Schmidt, 1996b; Subhadhirasakul *et al.,* 2001; Adane *et al.,* 2006).

2.2.2. Determination of Percent Yield

For determination of percent yield on dry mass basis of starch from Taro *Boloso-I*, the standard method described by ~~Paulos *et al* (2009) was used~~Association of Official Analytical Chemists (AOAC, 2000) was employed. Accordingly, 1 kg of fresh tubers was cleaned, peeled and cut into small pieces and wet milled, air dried into fine powder prior to getting dried at 130 ˚C overnight in drying oven. The resulting dry mass was accurately weighed and extracted by using normal saline (1%, w/v) and 0.03 N $NaOH_{(aq)}$ washing, muslin straining and sedimenting until the supernatant was clear and transparent. The sediment was then washed with distilled water three times so that it became neutral. Finally, it was sieved, dried at 40 ºC in an oven (KOTTERMANN® 2711, Germany), percent yield on dry basis was calculated.

2.2.3. Determination of Chemical Composition

2.2.3.1. Amylose Content

Amylose content was determined by a colorimetric assay method (Gebre-Mariam and Schmidt, 1996b). Stock solutions of amylose and amylopectin were prepared by dissolving 50 mg of each in 50 ml of 1.8% HCl. From each solution, 2 ml was taken and diluted to 10 ml using 1.8% HCl. Then, appropriate aliquots were taken and diluted with 1.8% HCl. Mixtures of amylose and amylopectin solutions were prepared to provide a starch concentration of 50 µg in 10 ml in any mixture. Various mixtures were prepared to contain 100, 80, 60, 40, 20, or 0% amylose or amylopectin, respectively. The absorbance reading of the resulting solutions were taken at 600 nm (for amylose) and 540 nm (for amylopectin) using a spectrophotometer (CM 2203, Solar, Belarus, Russia), immediately after staining with Lugol's solution (diluted 1:3). 100 µl of the diluted Lugol's solution were used for staining 2 ml of the mixture and also the blank HCl. Likewise, absorbance readings of each of the pure amylose and amylopectin solutions of the same concentration and solutions of native *taro Boloso-I* starch were taken at the same wavelengths. The amylose and amylopectin concentrations were calculated using standard calibration curves. The experiment was performed 5 repetitions and the mean values were taken.

2.2.3.2. Ash Content

For determination of ash value, FAO manual of food quality control (FAO, 1986) was used. Accordingly, the starch was weighed (2.5 g) into crucible and the sample was incinerated in a furnace

at 550˚C, for 1 h. The crucible was then taken out of the furnace and cooled in desiccator and weighed soon after reaching room temperature. These weights were used for calculation of ash content of the starch. The experiment was performed 3 ~~five~~ times and mean values were taken.

2.2.3.3. Protein Content

Protein content was determined by using the method of Association of Official Analytical Chemists (2000). First, weighed amount (0.5 g) of the sample was placed in 500 ml digestion flask into which 6 ml acid mixture (2:1 ratio of concentrated $H_2SO_{4\ (aq)}$ to concentrated ortho-$H_3PO_{4\ (aq)}$) was added. The flask was placed on heater and the violent reaction was observed. Immediately after the end of this reaction, heat was applied until the content became light green for 1 h. Then, it was cooled, diluted with distilled water, transferred into the sample compartment of the distiller and distilled till NH_3 was entirely collected. The excess standard acid in the distillate was titrated with standard NaOH solution for the determination of the amount of nitrogen (N_2). The protein content was reported by multiplying the percent nitrogen by 6.25.

2.2.3.4. Lipid Content

Lipid content was determined by using the method of Association of Official Analytical Chemists (2000) involving acid hydrolysis. Two milliliters of 85% methanol was added to 2 g of sample and cooled to prevent burning on addition of acid. The next step was addition of 10 ml of 24% HCl into the beaker held at 75˚C and moving the mixture to extraction kit where 25 ml of petroleum ether was added later and shaken exhaustively for 1 min. Then, it was let to stand so that the supernatant was clear. The liquid remaining after filtering the ether fat solution was re-extracted twice, each time with 15 ml of petroleum ether. The petroleum ether fraction was evaporated slowly on steam bath; the remaining was dried in oven at 100˚C to constant weight. It was allowed to settle in air to constant weight and measured with weighing balance and reported as percent total lipid AOAC, 2000).

2.2.4. Determination of Moisture Content

The moisture content was determined by oven drying method. Accordingly, a clean drying dish was dried in oven to 130 ˚C for 1 h. Then, the drying dish was covered with lid and it was let to cool in a desiccator for 30 min and weighed. After cooling, 2.00 g starch sample was accurately weighed and added into it. This was kept at 130 ˚C overnight. Then, the dry sample in the dish was taken out of oven and let to cool in the desiccator for 30 min covered with lid to prevent atmospheric moisture. As

soon as the temperature reached room temperature, it was weighed and percent weight loss of the sample was taken as its moisture content.

2.2.5. Preparation of Pregelatinized Starch

Pregelatinized starch was prepared using a method used by Odeku *et al* (2008) with slight modification. A preliminary study showed that pre/gelatinization of NTB1S resulted in better flowability and compressibility at starch to water ratio of 15% (w/v) and this was followed throughout this study. Accordingly, a total of 13 aqueous suspensions (15%, w/v) of NTB1S were heated in water bath at specified temperatures (61-89 °C) with continuous and uniform stirring for specified periods of time (12-68 min). The pregelatinized starches were then dried at 40 ºC for 48 h, powdered in a laboratory grinder (Pulberisette 2, Fritsch, Germany), so that all the powders passed through a 224 µm aperture sieve. Finally, the samples were stored separately in tightly sealed glass containers.

2.2.6. Physicochemical Characterization

2.2.6.1. Laser Light Diffractometry

The granule size and size distributions and specific surface area were studied by using laser light diffractometer (Malvern Mastersizer 2000, Germany) with Mastersizer S, PSS0003-01 software (2002). It was set at 2.4 mm active beam length; 0.05-900 µm (300RF) size range; small volume polydisperse standard-wet sample dispersion unit; 3 OHD presentation and 30 s measurement time. A small amount of starch samples were dispersed in 5 ml of cold distilled water and added in drops into sample port beaker containing cold distilled water until obscuration reading was within 15-20%. These determinations were performed in triplicates and averages were reported.

2.2.6.2. Scanning Electron Microscopy (SEM)

Scanning electron microscopy (SEM) was used for morphological study of native taro *Boloso-I* starch granules (Gebre-Mariam and Schmidt 1996b). To this end, a DSM 940 scanning electron microscope (Carl Zeiss, Oberkochen, Germany) set at an accelerating voltage of 5 kV was used. The starch sample was mounted and sputter coated with gold to a thickness of about 30 nm in a sputter coater (Sputter Coater Type E 5100, Biorad GmbH, Munich Germany). Then, the scanning electron micrographs were taken.

2.2.6.3. Fourier Transform Infra-red Spectroscopy

Fourier transform infra-red spectroscopy (FTIR) was used for both identification of starch and study of drug-excipient compatibility. For the starch samples, FTIR spectra were obtained with infrared spectrophotometer (Shimazu-8400S, Japan) in transmittance mode using KBr method at resolution of 8 cm^{-1}. For each run 20 scans were used in the range of wavenumber from 4000-500 cm^{-1}. For data translation IR solution software was used. The procedure was repeated with paracetamol as well as the paracetamol-starch physical mixture (1:1) for the case of compatibility study (John, 2000).

2.2.6.4. X-Ray Diffractometry (XRD)

For determination of starch crystallinity, XRD method was used (Gebre-Mariam and Schmidt 1996b). The X-ray diffraction machine (D8 Advance, BRUKER, Germany) whose source is Dermic X-ray tube of 2.2 kW Cu anode with Lynux eye detector was used**.** A Cu source X-ray tube target, voltage and current being 40 kV and 30 mA, respectively. Divergence, scatter and receiving slits were at 1, 1 and 0.3˚ values, respectively. The sample was scanned continuously within a 2θ range of 10-30˚at 5 ˚/min scan speed with sampling pitch of 0.02˚.

2.2.6.5. Densities and Related Properties

A sample weighing 30 g was put in 250 ml measuring cylinder calibrated into 0.5 ml volume and the resulting volume reading was used for calculation of bulk density (g/ml) (eq. 2.1).

$$\text{Bulk denisty} = \frac{\text{The weight of powde}}{\text{Bulk volume of the pow}} \qquad \text{eq. 2.1}$$

A tapped densitometer (ERWEKA, type SVM, Germany) which provided a fixed drop of one-half inch at a rate of 250 taps/min was used for 2 min to read the tapped volume to calculate the tapped density (eq. 2.2). Both measurements were performed in triplicates. The Carr's index (% compressibility) and Hausner ratio were calculated using the eq. 2.3 and 2.4, respectively.

$$\text{Tapped denisty} = \frac{\text{The weight of powder}}{\text{Tapped volume of the powde}} \qquad \text{eq. 2.2}$$

$$\%\text{compressibility} = \frac{\text{[illegible]}}{\text{Tapped Density}} \times 10 \qquad \text{eq. 2.3}$$

$$\text{Hausner's Ratio} = \frac{\text{Tapped Density}}{\text{Bulk Density}} \qquad \text{eq. 2.4}$$

For determination of true density, fluid (xylene) displacement method was used. A cleaned volumetric flask filled with xylene was weighed. Having added 2 g starch into the empty flask, it was nearly filled with xylene. After letting bubbles to be released for 10 min, it was carefully filled with xylene. Then, the starch's true density (ρ) was calculated using eq. 2.5. This was performed in triplicates and the average was taken.

$$\rho = \frac{ws}{(x+w)-y} \qquad \text{eq. 2.5}$$

Where- w, s, x and y stand for weight of starch, specific gravity of xylene = 0.855, weight of the flask plus filled xylene and weight of the flask plus starch plus xylene filled, respectively.

2.2.6.6. Flow Properties

The Carr's indexes and Hausner ratios calculated from the bulk and tapped density were used as parameters of flow property. Moreover, angle of repose and flow rate were determined by using funnel method. Accordingly, 30 g of starch was taken and let to pass via a stemless funnel having 15 mm aperture from a 10 cm height. The powder pile formed was carefully measured for its average diameter and height. Angle of repose was calculated by applying eq. 2.6. Flow rate was calculated from the time required for the sample to flow through the funnel.

$$\text{Angle of repose}(\theta) = \tan^{-1} \qquad \text{eq. 2.6}$$

Where h is the height of starch powder pile and r is the radius of the starch powder pile.

2.2.6.7. Moisture Sorption Pattern

Moisture sorption behavior was determined by using the method used by Paulos *et al* (*2009)* with slight modification. It involves preparation of saturated salt solutions of magnesium chloride hexahydrate ($MgCl_2.6H_2O$), sodium nitrite ($NaNO_2$), sodium chloride (NaCl) and potassium chloride (KCl) to obtain relative humidity (RH) chambers of 32.7%, 65.4%, 75.6% and 85.1%, respectively.

Pure distilled water was used to obtain 100% RH. Then, 5 g sample, oven dried at 120 ˚C for 4 h, was kept spread evenly on Petri dishes in each RH% chambers for 4 weeks. The increment in weights in percent of initial weight was reported as moisture sorption.

2.2.6.8. Differential Scanning Calorimetry (DSC)

Gelatinization properties in water and drug-excipient studies of starches were analyzed by using thermal analyzer (NETZSCH, Selb, Germany). For the determination of gelatinization properties, starch sample was thoroughly mixed with distilled water (at 1:2 ratio) and allowed to equilibrate in closed glass jars for 24 h at room temperature. Then, accurately weighed 3 mg samples were hermetically sealed in flat bottom aluminum pans. Placing the pan in a DSC cell, it was heated and cooled at ramps of 10˚C /min from 20˚C to 110˚C and scanned parallel to an empty sealed reference pan. From the DSC trace, onset (T_o), peak (T_p) and end set (T_e) temperature (˚C) of the gelatinization, were obtained (Adane *et al.,* 2006). Enthalpy of gelatinization (ΔH, mJ/mg) was obtained by integrating the respective endotherms (Swarbrick, 2007). For assessment of the drug-starch compatibility, the procedures were repeated with the drug alone, and the drug-starch physical mixture (1:1). The only differences were that samples were not mixed with water and the range of scanning was from 30 - 200 ˚C. Then, the thermographs were observed for any appearance, disappearance or shift of exothermic or endothermic reactions.

2.2.6.9. Swelling Power and Solubility Determinations

The swelling power and the solubility index were determined using the method described by ~~Paulos *et a*~~Bello-Pérez ~~*l*~~ (2009~~0~~) with slight modifications. It involves introduction of 0.1 g of the samples into three pre-weighed test tubes containing 10 ml of distilled water and heated in water bath at temperature of 25, 35, 45, 55, 65, 75 and 85 ˚C for 30 min with uniform shaking. The contents of test-tubes were centrifuged at 8000 rpm for 15 min to facilitate the removal of the supernatant, which was carefully decanted and the weight of the starch paste taken. Water solubility index (WSI) was calculated from the supernatant using eq. 2.7. Similarly, swelling power (SP) was calculated from the starch paste (precipitate) (eq. 2.8). All tests were performed in triplicates and the average was taken.

$$\mathrm{WSI} = \frac{w_1}{w_3} \times 100 \qquad \text{eq. 2.7}$$

$$\mathrm{SP} = \frac{100 w_2}{(100 - S) w_3} \qquad \text{eq. 2.8}$$

Where w1 is weight (g) of soluble material in the supernatant, w2 is the weight (g) of precipitate and w3 is the weight (g) of the starch sample.

2.2.7. Evaluation of NTB1S as Tablet Disintegrant

After conducting a preliminary study using NTB1S as 100% exo-disintegrant, 50% by 50% exo-endo-disintegrant and 100% endo-disintegrant, NTB1S was used only as exo-disintegrant in paracetamol tablets as it showed better disintegrant effects.

2.2.7.1. Preparation of Paracetamol Granules

Paracetamol granules were prepared by wet granulation method using a blender (Erweka D-63150 LK5, Germany). Accordingly, an aqueous 3% (w/w) polyvinyl pyrollidone (PVP) solution was added to the drug powder and the mixture was blended for 20 min. The resulting wet mass was passed through 1.6 mm sieve and dried in an oven (KOTTERMANN® 2711, Germany) at 40 ˚C overnight. The dry granules were screened by passing through a 1 mm sieve.

2.2.7.2. Characterization of Granules

To determine the size distribution of the granules, 30 g of the samples were shaken in a set of sieves (ISO 3310-1) arranged from top to bottom at constant intensity for 2 min using an ERWEKA universal drive unit (Type AR 401, Germany). The average granule size (in µm) on any sieve was the average of mesh size of the sieve through which the granules passed and that upon which the granules were retained. Overall mean size of granules was computed using averages of the mean sizes in each sieve weighed in terms of percent weight. Similarly, to measure the friability, 10 g (larger than 315 µm) was put in friability tester and rotated for 4 min at 25 rpm dropping the granules a distance of 6 inches. It was sieved using the 315 µm sieve and the loss was calculated as percent friability. This was done in triplicates and reported as mean ± SD. The same procedure was used for determination of the tablet friability on 20 tablets in each batch.

2.2.7.3. Compression of Paracetamol Granules

Formulations of granules of the study were as shown in Table 2.1.

Table 2.1.The formulae of 350 mg paracetamol tablets using NTB1S as disintegrant.

	Paracetamol + PVP	Starch
	mg (%)	mg (%)

F1	330.75 (94.5)	17.5 (5)
F2	295.75 (84.5)	52.5 (15)
F3	330.75 (94.5)	17.5 (5)
F4	295.75 (84.5)	52.5 (15)
F5	337.75 (96.5)	10.5 (3)
F6	288.75 (82.5)	59.5 (17)
F7-F13	313.25 (89.5)	35.0 (10)

The granules were mixed with specified amount of disintegrant (3-17%) in a tumble mixer (Willy A. Bachofen AG, Turbula® 2TF, Basel, Switzerland) at 49 rpm for 10 min. Then, 0.5 % of magnesium stearate was added and mixing process continued for further 5 min (Table 2.1).~~The granules were mixed with specified amount of disintegrant (3-17%) in a tumble mixer (Willy A. Bachofen AG, Turbula® 2TF, Basel, Switzerland) at 49 rpm for 10 min. Then, 0.5 % of magnesium stearate was added and mixing process continued for further 5 min (Table 2.1). The resulting mixtures were compressed into target weight of 350 mg tablets with instrumented tablet machine (Korsch AG XP1 K0010288, Germany) at various compression forces. All tablets were kept for 24 h for elastic recovery.~~

Table 2.2.**The formulae of 350 mg paracetamol tablets using NTB1S as disintegrant.**

	~~**Paracetamol + PVP**~~	~~**Starch**~~	~~**Magnesium stearate**~~
	mg (%)	~~mg (%)~~	~~mg (%)~~
~~F1~~	~~330.75 (94.5)~~	~~17.5 (5)~~	~~1.75 (0.5)~~
~~F2~~	~~295.75 (84.5)~~	~~52.5 (15)~~	~~1.75 (0.5)~~
~~F3~~	~~330.75 (94.5)~~	~~17.5 (5)~~	~~1.75 (0.5)~~
~~F4~~	~~295.75 (84.5)~~	~~52.5 (15)~~	~~1.75 (0.5)~~
~~F5~~	~~337.75 (96.5)~~	~~10.5 (3)~~	~~1.75 (0.5)~~
~~F6~~	~~288.75 (82.5)~~	~~59.5 (17)~~	~~1.75 (0.5)~~
~~F7~~	~~313.25 (89.5)~~	~~35.0 (10)~~	~~1.75 (0.5)~~
~~F8~~	~~313.25 (89.5)~~	~~35.0 (10)~~	~~1.75 (0.5)~~
~~F9~~	~~313.25 (89.5)~~	~~35.0 (10)~~	~~1.75 (0.5)~~
~~F10~~	~~313.25 (89.5)~~	~~35.0 (10)~~	~~1.75 (0.5)~~
~~F11~~	~~313.25 (89.5)~~	~~35.0 (10)~~	~~1.75 (0.5)~~
~~F12~~	~~313.25 (89.5)~~	~~35.0 (10)~~	~~1.75 (0.5)~~
~~F13~~	~~313.25 (89.5)~~	~~35.0 (10)~~	~~1.75 (0.5)~~

2.2.8. ~~*Optimization of Disintegrant Property*~~Optimization of Disintegrant Property

2.2.8.1. Experimental Designs

For the study of tablet disintegrant effects of NTB1S, while concentration of NTB1S and compression force were factors, responses were tablet hardness, friability and disintegration time (DT). Central composite design (CCD) was used for the optimization of the factors targeting the best combination of the responses. Number of experimental runs was obtained by using eq. 1.8 described in the Section 1.7. Accordingly, there were 13 experimental runs (4 factorial points, 4 axial points and 5 central points) as shown in Table 2.2. For ease of statistical handling of the coefficients, the levels of the factors were transformed using eq. 2.9 (Dale *et al.,* 2009; Adedokun and Itiola, 2011).

$$\text{Transformed Value} = \frac{[2A-(\text{Max}+\text{M}}{\text{Max}-\text{Min}} \qquad \text{eq. 2.9}$$

Where: A is actual value of factors; Max and Min show maximum and minimum values, respectively.

Table 2.3. Experimental design for the disintegrant effect study.

No	Factor 1		Factor 2		
	Coded	Actual	Coded	Actual	
	X_1	NTB1SC	X_2	CF	
F1	-1	5	-1	15	
F2	+1	15	-1	15	Factorial
F3	-1	5	+1	25	design points
F4	+1	15	+1	25	
F5	-1.414	3	0	20	
F6	+1.414	17	0	20	Axial design
F7	0	10	-1.414	13	points
F8	0	10	+1.414	27	
F9-F13	0	10	0	20	Central points

*Where NTB1SC and CF stand for NTB1S concentration and compression force, respectively.

Then, the values of the responses of each of the 13 formulations were fed into a statistical software (Design-Expert 8.0.7.1, Stat-ease, Corp. Australia). The respective polynomial regression algorithms

(eq. 2.9) were created using the ANOVA output used to relate and optimize the factors to responses (Lewis *et al.,* 1999).

$$Y = \beta_0 + \beta_1 X_1 + \beta_2 X_2 + \beta_{12} X_1 X_2 + \beta_{11} X_1^{\,2} + \beta_{22} X_2^{\,2} + \qquad \text{eq. 2.10}$$

Where X_1 is factor 1 and X_2 is factor 2, β_0 is the intercept, β_1, β_2, β_{12}, β_{11} and β_{22} are the coefficients of factor 1, factor 2, the interaction, the quadratic terms of factors 1 and 2, respectively.

2.2.8.2. Evaluation and Validation of Optimum Formulation

For validation, tablet formulations at three points different from the design points were prepared in three batches and evaluated. The results were compared with the predicted values. The relative error (%) was calculated by using eq. 2.11.

$$\%\text{Relative error} = \frac{\text{Predicted Value} - \text{Experimental Value}}{\text{Predicted Value}} \times 100 \qquad \text{eq. 2.11}$$

For evaluation of the optimized formulation, using NTB1S and potato starch were prepared in three batches in parallel with all the other conditions kept at optimization values.

2.2.8.3. Evaluation of Tablets

2.2.8.3.1. Crushing strength (H)

From each batch, 10 tablets were tested for hardness by using a tablet hardness tester (CALEVA, G.B., Caleva Ltd., UK) and each value was recorded. The average of 10 force recordings was reported as tablet hardness.

2.2.8.3.2. Tablet thickness and porosity

Ten tablets were taken and thickness was measured using sliding caliper scale (Nippon, Sokuti, Japan). The porosity was calculated by using eq. 2.12 (Riyanto and Aziz, 2015).

$$\epsilon = (1 - P_f) \times 100\% \qquad \text{eq. 2.12}$$

Where: ϵ is tablet porosity and P_F - packing fraction (eq. 2.13).

$$P_f = \qquad \text{eq. 2.13}$$

Where, ρ is particle (true) density obtained by using the method described in Section 2.2.6.5 (eq. 2.5) and ρ_0 is bulk density of tablet in g/ml calculated by using eq. 2.14.

$$\rho_0 = 4W/\pi$$ eq. 2.14

Where h, w and d stand for thickness of tablets (cm), weight of tablet (g) and diameter of tablet (cm), respectively.

2.2.8.3.3. Tablet tensile strength

The radial tensile strength of tablets was calculated from hardness, diameter and thickness data using eq. 2.15 (Riyanto and Aziz, 2015).

$$\delta_x =$$ eq. 2.15

Where, δ_x, F_δ, d and t stand for radial tensile strength, the maximum radial force to bring about fracture, the diameter and the thickness of the tablets, respectively.

2.2.8.3.4. Disintegration time (DT)

DT test was carried out as per USP 30/NF 25 (2007). Six tablets were placed in a disintegration tester (Erweka ZT504, Germany) filled with distilled water at 37 ± 2 °C and the apparatus was operated. The tablets were considered completely disintegrated when all the particles passed through the wire mesh.

2.2.8.3.5. Crushing strength/Friability/Disintegration Ratio

The hardness/friability/DT ratio was calculated according to the method used elsewhere by using the eq. 2.16 (Alebiowu and Itiola, 2003; Puttewar *et al.,* 2010).

$$\frac{\left(\frac{C\delta}{F\gamma}\right)}{DT} = \frac{\frac{\text{Hardness}}{\text{Friability}}}{\text{Disintegration ti}}$$ eq. 2.16

Where, $C\delta$, $F\gamma$, and DT stand for the hardness, friability and the disintegration time of the tablet, respectively.

2.2.8.3.6. Calibration Curve

A stock solution of paracetamol (200 µg/ml) in phosphate buffer of pH 5.8 was prepared and respectively diluted to six different concentrations (2, 4, 6, 8, 10 and 12 µg/ml). Before the absorbance of any paracetamol solution was read, phosphate buffer of pH 5.8 was used as blank at 243 nm. The UV absorbance of each of these concentrations were read in UV/Vis spectrophotometer (CM 2203,

Solar, Belarus, Russia) and the Beer Lambert curve was plotted and the correlation coefficient was calculated.

2.2.8.3.7. Dissolution Test

Dissolution test was done as per USP 30 /NF 25 (2007) using the apparatus II (ERWEKA, DT600, Germany), with 900 ml phosphate buffer (pH 5.8) medium at 37 ± 0.5 ºC with stirring rate of 50 rpm. Five ml of aliquots were removed with blank replacement at 5, 10, 15, 20, 30, 45 and 60 min and filtered using Whatman No.1 filter paper. One ml of the filtered samples was diluted to 25 ml and absorbance readings were taken with a spectrofluorometer CM 2203 (Solar, Belarus, Russia) at 243 nm. Phosphate buffer (pH 5.8) was used as a blank. The necessary corrections for dilution were made when calculating the drug dissolution.

2.2.9. Evaluation of Pregelatinized TB1S as Direct Compression Excipient

2.2.9.1. Flowability and Density Related Properties

Angle of repose, flow rate, density, compressibility index and Hausner ratio were analyzed per the procedures described in the Sections 2.2.6.5 and 2.2.6.6.

2.2.9.2. Compressibility Studies

2.2.9.2.1. Kawakita Equations

Thirty grams of sample powder were tapped using a~~the~~ tapping densitometer (ERWEKA, Germany) 5, 10, 20, 30, 40, 50, 75, 100, 300, 400 and 500 times and the volume was measured after each of these numbers of taps and eq. 1.2 was used to perform Kawakita analysis.

2.2.9.2.2. Heckel Plots

A single punch machine (Korsch AG XP1 K0010288, Germany) equipped with a round flat-faced stainless steel die cavity with a diameter of 10 cm was used in the preparation of compacts. In advance of the compression, the punch faces as well as the die wall was lubricated with magnesium stearate suspension in 95% alcohol. Eight tablets of manually weighed 300 ± 3 mg samples were prepared at each of 8 different compression forces (3, 6, 9, 12, 15, 18, 21, and 24 kN). C~~The c~~ompact weight, hardness, ~~and the dimensions of~~ diameter and thickness of out-of-die tablets were measured 24 h after compression ~~-~~(Widodo and Hassan, 2015). Tablet true density (ρ_t) was computed as the weighted

average of the component true densities. Compact density or tablet density (ρ_c) was calculated using its weight (w), diameter (d) and thickness (t) as shown in eq. 2.17.

$$\rho_c = 4w / \pi d^2 t \qquad \text{eq. 2.17}$$

Out-of-die tablet relative density (D_{rel}) at any compression pressure was calculated by using eq. 2.18 and used for calculation of the tablet densification (eq. 2.19). Similarly, compression pressure was calculated from compression force in kN and tablet diameter (d) eq. 2.20.

$$D_{rel} = \rho_c / \rho_t \qquad \text{eq. 2.18}$$

$$\text{Densification} = -\ln(1 - D_{rel}) \qquad \text{eq. 2.19}$$

$$\text{Compression pressure} : 4\text{Compression force} / \pi d^2 \qquad \text{eq. 2.20}$$

Finally, graph of –ln –(1-D_{rel}) versus pressure (in MPa) was plotted to analyze ~~the~~ compression properties of the powder compacts. The linear portion of the plot was obtained from the line that fits the largest number of points on the graph (eq. 1.3 described in the Section 1.6.2.2) using the Origin Software such that the correlation coefficient was not less than 0.9905. For calculation of D_A, D_0 and D_b values eq. 1.4, eq. 1.5 and eq. 1.6 described in the Section 1.6.2.2 were used~~The value of D_A was calculated from the intercept A and D_b was calculated using D_A value and D_0 value obtained from the graph (eq. 1.5 and eq. 1.7, respectively, described in the section 1.9)~~.

2.2.10. Optimization of Pregelatinization

2.2.10.1. Experimental Designs

For the pre/gelatinization study, temperature and time of pre/gelatinization were factors whereas angle of repose, Hausner ratio. Kawakita compressibility, Heckel number and hardness of the tablets compressed at 12 kN were responses. Central composite design (CCD) was used for optimization of the factors targeting the optimum combination~~s~~ of the responses. Number of experimental runs was obtained by using eq. 1.4. Accordingly, there were 13 experimental runs (4 factorial points, 4 axial points and 5 central points) as shown in Table 2.3. For ease of statistical handling of the coefficients, the levels of factors were transformed using eq. 2.9 described in the S~~s~~ection 2.2.8.1 –(Dale *et al.*, 2009; Adedokun and Itiola, 2011).

Table 2.4. Experimental design for the pre/gelatinization study.

No	Factor 1		Factor 2		
	Coded	Actual	Coded	Actual	
	X1	Temperature (˚C)	X2	Time (min)	
F1	-1	65	-1	20	Factorial design points
F2	+1	85	- 1	20	
F3	-1	65	+1	60	
F4	+1	85	+1	60	
F5	-1.414	61	0	40	Axial design points
F6	+1.414	89	0	40	
F7	0	75	-1.414	12	
F8	0	75	+1.414	68	
F9-F13	0	75	0	40	Central points

Then, the values of the responses of each of the 13 formulations were fed into a statistical software (Design-Expert 8.0.7.1 software, Stat-ease, Corp. Australia). The respective polynomial regression algorithms were created using the ANOVA output and used to relate the factors to the responses (Lewis *et al.,* 1999).

2.2.10.2. Evaluation and Validation of Optimum Formulation

For validation of the optimization, tablet formulations at three points different from the design points were prepared and evaluated. The results were compared with the predicted values and the comparator formulations. R~~The r~~elative error (%) was calculated by using eq. 2.10 described in the ~~s~~Section 2.2.8.2. For evaluation, the ~~the~~ optimized product~~the~~ was compared as powder and in tablet formulations with Starch 1500® and the native starch.

2.2.11. Compactibility and Lubricant Sensitivity Study

Tablets of PGTB1S were prepared with magnesium stearate at various concentrations from 0.00, 0.25, 0.50, 0.75, 1.00, 1.50 and 2.00% (w/w). Forty grams batch of each mixture was mixed for 5 min in Turbula mixer (Willy A. Bachofen AG, Turbula 2 TF, Basel, Switzerland) and compressed to produce

10 mm flat surfaced compacts of starches with 300 mg size at a compression force of 17 kN with instrumented tablet machine (Korsch AG XP1 K0010288, Germany). The tablet properties were determined 24 h after compression.

2.2.12. Dilution Potential Study

Tablets of 300 mg weight containing 20%, 30%, 40% and 50% paracetamol were prepared using NTB1S, PGTB1S or Starch 1500® by direct compression method (Table 2.4). Briefly, paracetamol, Ac-Di-Sol® and starch were mixed for 10 min in the Turbula mixer and after addition of 0.5% magnesium stearate, mixing was continued for 5 min. Paracetamol tablets were then compressed using instrumented single punch tablet machine (Korsch AG XP1 K0010288, Germany) at compression force of 17 kN (Morris *et al.,* 1996). In all cases, the tablet properties were determined 24 h after production.

Table 2.5.Tablet formation for dilution potential study.

Ingredients	Formulations											
	1			2			3			4		
Paracetamol (%)	20	20	20	30	30	30	40	40	40	50	50	50
NTB1S (%)	75.5	-	-	65.5	-	-	55.5	-	-	45.5	-	-
PGTB1S (%)	-	75.5	-	-	65.5	-	-	55.5	-	-	45.5	-
Starch 1500® (%)	-	-	75.5	-	-	65.5	-	-	55.5	-	-	45.5
Ac-Di-Sol® (%)	4	4	4	4	4	4	4	4	4	4	4	4
Magnesium Stearate (%)	0.5	0.5	0.5	0.5	0.5	0.5	0.5	0.5	0.5	0.5	0.5	0.5

2.2.13. Statistical analyses

Statistical analyses including one way ANOVA were applied by using Design-Expert 8.0.7.1 software (Stat-ease, Corp. Australia) for the optimizations. The responses of the disintegrant effect and pre/gelatinization studies were expressed in polynomial models in terms of compression force and concentration and, temperature and time of the pre/gelatinization, respectively. All the results of direct measurements were presented as arithmetic mean ± standard deviation $(\mu \pm \sigma)$. Origin version 7 (Origin Lab™ Corporation, USA) was used to show the trend of dependence of responses on factors. The target significance of statistical data was within 95% CI.

3. RESULTS AND DISCUSSIONS

3.1. Isolation and Physicochemical Characterization of Taro *Boloso-I* Starch

3.1.1. Isolation and Yield

~~Taro *Boloso-one* s~~Starch was extracted successfully from ~~washed, cleaned, peeled, trimmed and crushed~~ tuber of ~~the plant~~Taro *Boloso-I* cultivar. The extraction process came into effect ~~with the use~~using ~~of saline solution (~~1% (w/v) of $NaCl_{(aq)}$ ~~which was required~~ to remove soluble substances, sugar and mucilage. Moreover, soaking with 0.03 N NaOH solution was needed to fasten ~~the~~ sedimentation and improve quality and quantity of its yield (Gebre-Mariam and Schmidt, 1996b; Subhadhirasakul *et al.,* 2001; Adane *et al.,* 2006). The y~~The y~~ield on dry weight basis of native t~~T~~aro *Boloso-I* starch (NTB1S) was ~~determined to be~~ 83.5 ± 1.6% which indicates that Taro *Boloso-I* is a promising plant as an alternative source of starch.

3.1.2. Physicochemical Properties

3.1.2.1. Composition

A~~The a~~mylose and amylopectin contents of NTB1S and potato starch were determined using ~~the~~ the standard linear curves (Fig. 3.1) of absorbances at wavelengths 600 nm for amylose and 540 nm for amylopectin versus concentrations. This method is based on the ~~the~~ difference between ~~the~~ iodine binding capacities of amylose and amylopectin. (Gebre-Mariam and Schmidt, 1996b). Linear regression fits of the curves were as shown in eq. 3.1 and 3.2 with the R^2 values of 0.9995 and 0.9998, respectively.~~For applications in pharmaceutical industries, the lower protein content and ash value of NTB1S is desirable since high purity starches are preferable (Belitz *et al.*, 2009; Makowska *et al.*, 2014).Moisture content affects the properties of dosage forms favorably or unfavorably, e.g., flow, compaction, caking, disintegration, dissolution, chemical stability, compatibility via hydrolysis and die-wall friction. With increasing moisture content up to optimum, the yield pressure of powders increases up to maximum and then decreases (Müller *et al.*, 2013). At high temperatures, high moisture can cause the starch to gelatinize. The moisture content values of NTB1S and potato starch are shown in Table 3.1.~~

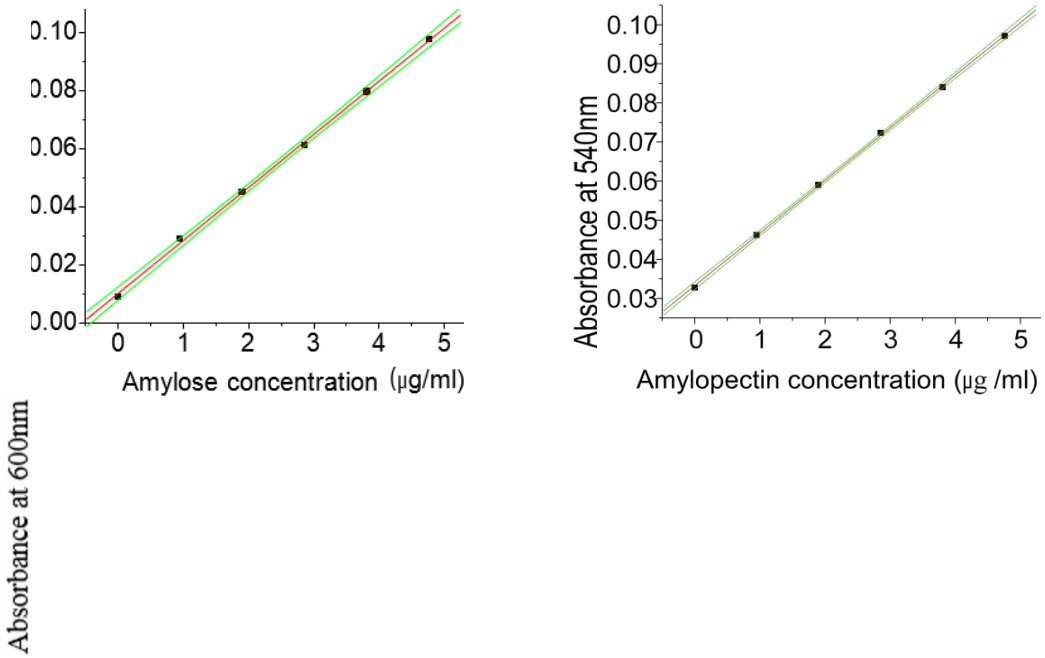

Fig. 3.3 Standard linear curve of amylose and amylopectin by colorimetry.

~~The linear regression fits of the curves were as shown in eq. 3.1 and 3.2 with the R^2 values of 0.9995 and 0.9998, respectively. The amylose and amylopectin contents of the starch samples were determined are shown in Table 3.1 along with lipid, protein and moisture contents and also ash values, of NTB1S and potato starch.~~

$$A_l = 0.00996 + 0.01835C \quad \text{eq. 3.1}$$

$$A_p = 0.03318 + 0.01346 \quad \text{eq. 3.2}$$

Where, A_l and A_p stand for color light absorbance at 600 and 540 nm, and C_l and C_p for concentrations in µg/ml of amylose and amylopectin, respectively.

High purity starches are preferable for applications in pharmaceutical industries (Belitz *et al.*, 2009; Makowska *et al.*, 2014). Moreover, moisture content also affects the properties of dosage forms containing the starches favorably or unfavorably, e.g., flow, compaction, caking, disintegration, dissolution, chemical stability, compatibility via hydrolysis and die-wall friction. Furthermore, with increasing moisture content up to optimum, the yield pressure of powders increases up to maximum and then decreases (Müller *et al.*, 2013). For these reasons, protein and lipid contents as well as ash values were determined to evaluate the starch purity and shown in Table 3.1 together with the amylose, amylopectin and moisture contents.

Table 3.6. Chemical compositions and moisture contents of NTB1S, potato and Godare starches.

Starch	Amylose (%)	Amylopectin (%)	Lipid (%)	Protein (%)	Ash value (%)	Moisture (%)
NTB1S	20.7 ± 1.8	77.3 ± 2.1	0.86 ± 0.01	0.23 ± 0.00	0.07 ± 0.00	10.43 ± 0.42
Potato starch	29.2 ± 2.0	68.5 ± 2.6	0.48 ±0.00	1.43 ± 0.02	0.27 ± 0.01	12.8 ± 0.70
Godare starch*	24.3*	75.7*	-	-	0.45*	11.81*

*Values adopted from the report by Adane *et al* (2006b).

Th~~is~~e results reveal~~s, that~~ amylose to amylopectin ratio of NTB1S is lower than potato starch and ~~also~~ Godare starch~~, *i.e.*, 24.3:75.7 (Adane *et al.*, 2006).~~ . Moreover, NTB1S has lower protein content than potato starch ($p < 0.05$) and higher amount of lipids than potato starch ($p < 0.05$) ~~(Belitz *et al.*, 2009)~~. A~~The a~~sh value of NTB1S was found to be 0.07~~ ± 0.00~~% indicating lower level of residual inorganic materials (sand, soil etc.) than potato starch ~~. This value was much lower ($p < 0.05$) than that of potato~~

~~starch~~ (~~0.27~~0.27 ~~± 0.01~~%) and Godare starch ~~indicating lower amount of residual inorganic material (sand, soil etc.)~~. ~~-~~Moreover, For applications in pharmaceutical industries, the lower protein content and ash value of NTB1S is desirable since high purity starches are preferable (Belitz *et al.,* 2009; Makowska *et al.,* 2014).

Moisture content affects the properties of dosage forms favorably or unfavorably, e.g., flow, compaction, caking, disintegration, dissolution, chemical stability, compatibility via hydrolysis and die-wall friction. With increasing moisture content up to optimum, the yield pressure of powders increases up to maximum and then decreases (Müller *et al.,* 2013). At high temperatures, high moisture can cause the starch to gelatinize. The moisture content values of NTB1S and potato starch are shown in Table 3.1. ~~This shows that moisture~~moisture content of NTB1S (10.43 ± 0.42%) was less than that of potato starch (12.80 ± 0.70%) ~~($p < 0.05$)~~ and Godare starch (11.81%). This is presumably because of higher lipid content (Moraes *et al.*, 2014). Literature shows that loss on drying of starches from corn and wheat, potato and tapioca can normally be up to 15, 16 and 20%, respectively (USP 30 / NF 25, 2007) confirming that NTB1S has preferably lower moisture content. This is favorable as it reduces chances of unintended gelatinization at high temperatures (Fellows, 2000).~~Loss on drying of starches from corn and wheat, potato and tapioca can normally be up to 15, 16 and 20%, respectively (USP 30 / NF 25, 2007), which shows that NTB1S has preferably lower moisture content.~~

3.1.2.2. Granule Sizes and Shapes

Particle sizes and shapes of excipient powders, especially starches for disintegrant effects, affect flow and hence tablet manufacturing. Moreover, these parameters may affect both rate and extent of disintegration maybe due to attainment of continuous hydrophilic network of disintegrants is better with bigger particles. As a result, dissolution and bioavailability of tablets are affected by the particle sizes and shapes of disintegrant starches (Swarbrick, 2007). For this concern, the laser light diffraction results of NTB1S and potato starch are shown in Fig. 3.2 and Table 3.2.

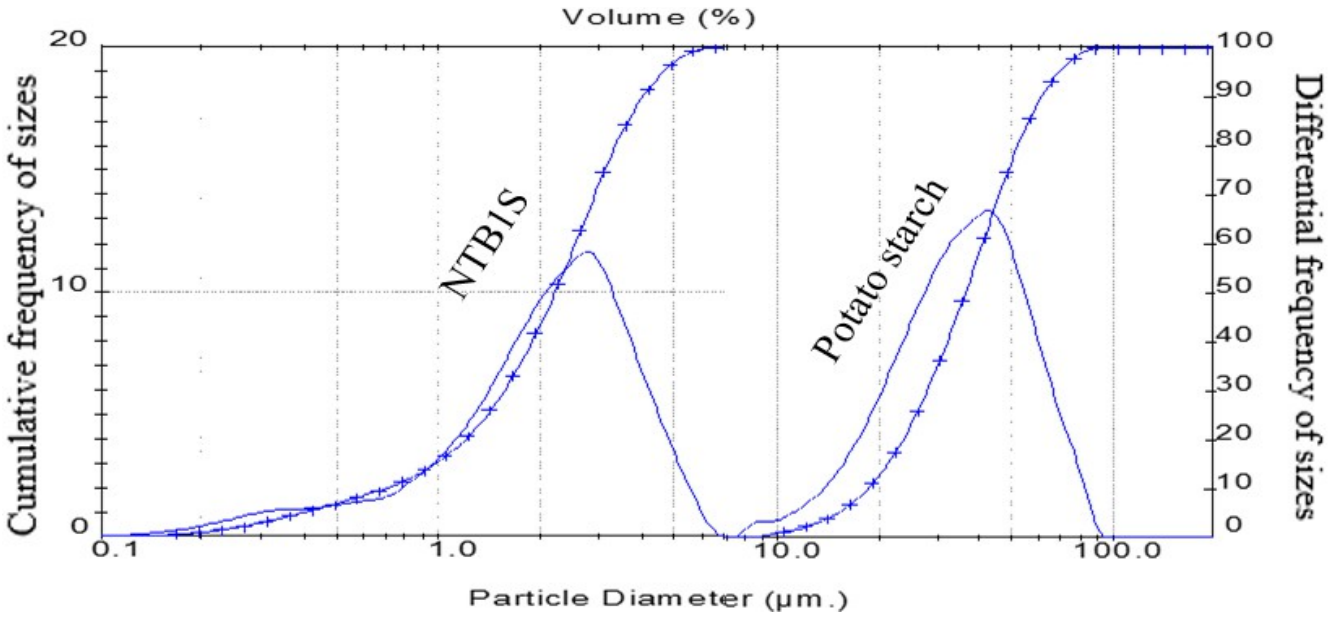

Fig. 3.4.Volume weighted size distributions of NTB1S and potato starch.

Table 3.7. Volume weighted size distribution of NTB1S and potato starch.

Parameters	NTB1S	Potato starch	Godare Starch*
Volume weighted mean (µm)	2.365 ± 0.05	38.025 ± 0.25	13.072*
Surface weighted mean (µm)	1.350 ± 0.01	29.615 ± 1.72	10.314*
Specific surface area (m^2/g)	2.879 ± 0.00	0.127 ± 0.00	0.582*
Uniformity	0.489 ± 0.05	0.398 ± 0.05	0.422*
$D_{10\%}$ (µm)	0.705 ± 0.01	16.305 ± 3.12	-
$D_{50\%}$ (µm)	2.225 ± 0.01	36.315 ± 0.16	-
$D_{90\%}$ (µm)	4.030 ± 0.01	62.710 ± 2.39	-
$D_{90\%}$ / $D_{10\%}$	5.716	3.846	

*Values adopted from the report by Adane *et al* (2006b).

Accordingly, NTB1S granules have smaller volume and surface weighted mean diameters than potato starch and Godare starch ($p < 0.05$) leading to higher specific surface area ~~(Adane *et al.*, 2006)~~. It has also higher uniformity of sizes. ~~which~~This can result in~~is~~ better ~~for~~ mixing quality (Shenoy *et al.*, 2015) ~~than potato and Godare starches~~. The volume weighted mean size distribution of the granules is unimodal like those of potato and Godare starches. All the granules of NTB1S were less than 6.63 ± 0.1 µm where as those of potato starch were bigger than 7.72 ± 0.2 µm (Fig. 3.2).

The scanning electron micrograph of taro Boloso one starch are shown in Fig. 3.3 which reveals the morphology of the starch granules.

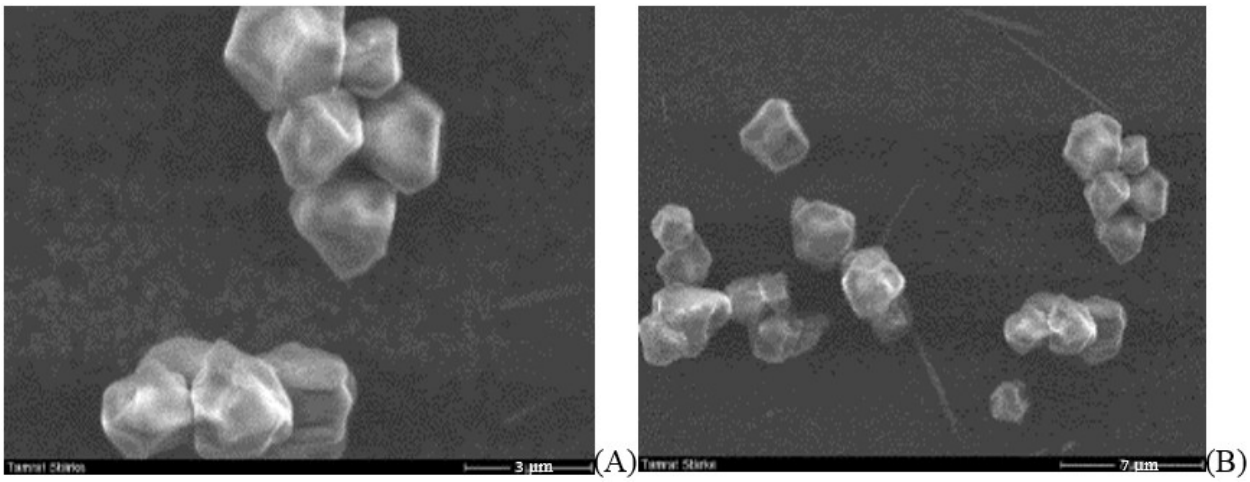

Fig. 3.5. Scanning electron micrographs of NTB1S; (A) (3µm scale bar); (B) (7µm scale bar).

Unlike ~~the~~ Godare starch which was described by Adane *et al* (2006) to be ~~is~~ spherical to polygonal with some cracks on surfaces ~~(Adane *et al.*, 2006)~~, the shape of Taro *Boloso-I* granules is more of polyhedral. ~~The tendency of granules to aggregate is also the same as that of rice starch (Elessandra *et al.*, 2010).~~ The aggregation of granules could have been avoided at a bit higher alkaline (NaOH) concentration but that was not done in order to avoid gelatinization by alkaline solution. Under the extraction condition, the effect of NaOH on clogging was ruled out as 0.03 N NaOH is by far lower for NaOH induced gelatinization which is claimed to occur ~~because the alkaline gelatinization is known to occur higher than~~at 0.24 N and higher NaOH. ~~which is by far above 0.03 N.~~ The starch was also dried at 40 ºC which was too low for heat induced gelatinization to take place. ~~.~~ Likewise~~On the other hand~~, ~~the~~ chance of aggregation to be caused by residual protein is very ~~low~~improbable (Ashogbon and Akintayo, 2012) ~~because~~as the total granule protein content was determined to be very ~~small~~low ~~, i.e.,~~ (0.23%). The tendency of granules to aggregate is the same as that of rice starch (Elessandra *et al.*, 2010). ~~(Ashogbon and Akintayo, 2012).~~

3.1.2.3. Fourier Transform Infrared Spectra (FTIR)

For identification of starch molecules in the samples, features of infrared spectra typically common to C-C, C-O-C, C–OH and C-H bonds of starches were observed on the sample spectra. The spectra were used to critically confirm the presence of pyranose ring, glucosyl groups and anhydroglucose ring C-O in NTB1S comparing it with potato starch (Fig. 3.4 and Fig. 3.5, respectively).

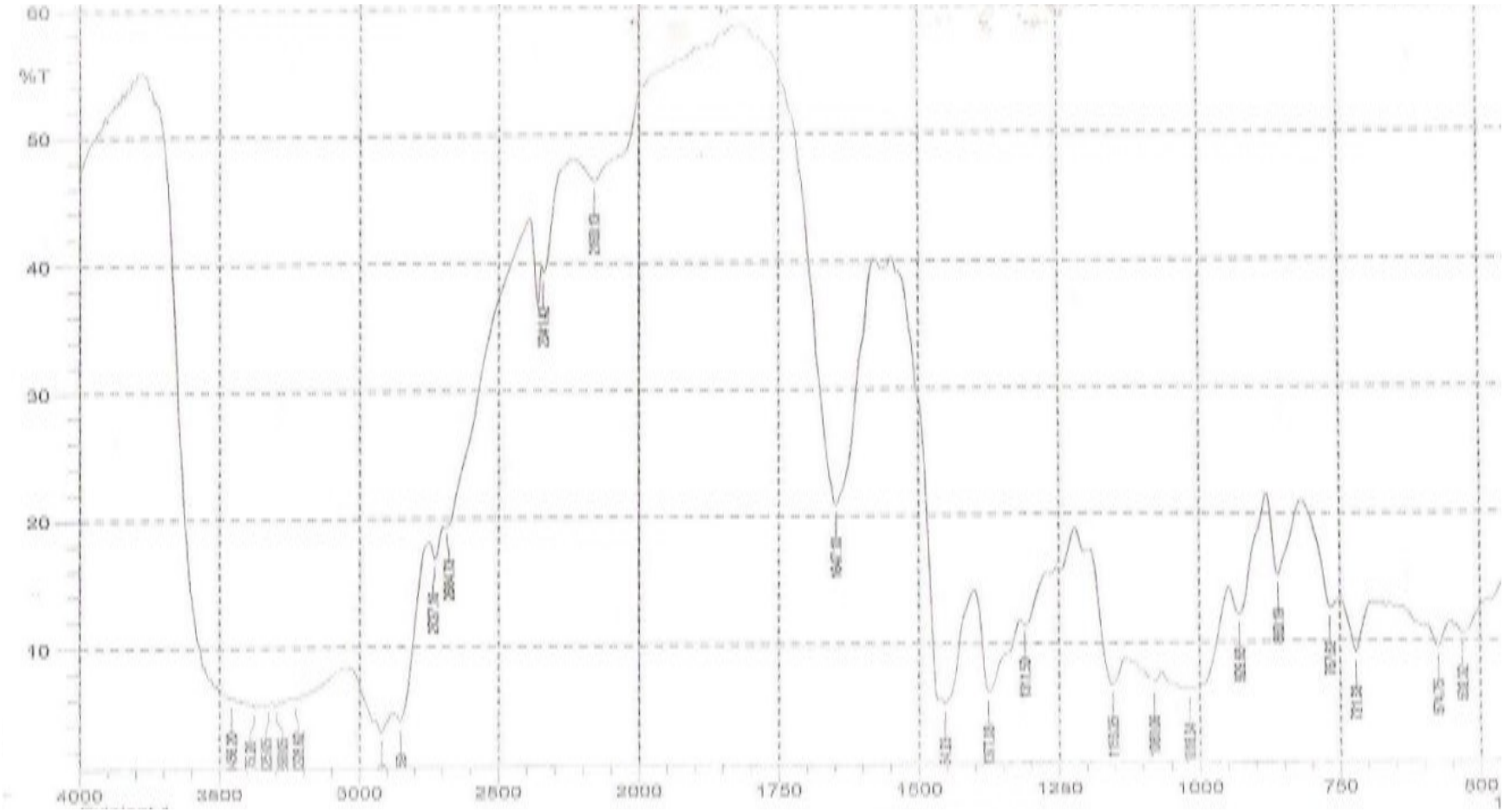

Fig. 3.6. FTIR spectra of NTB1S.

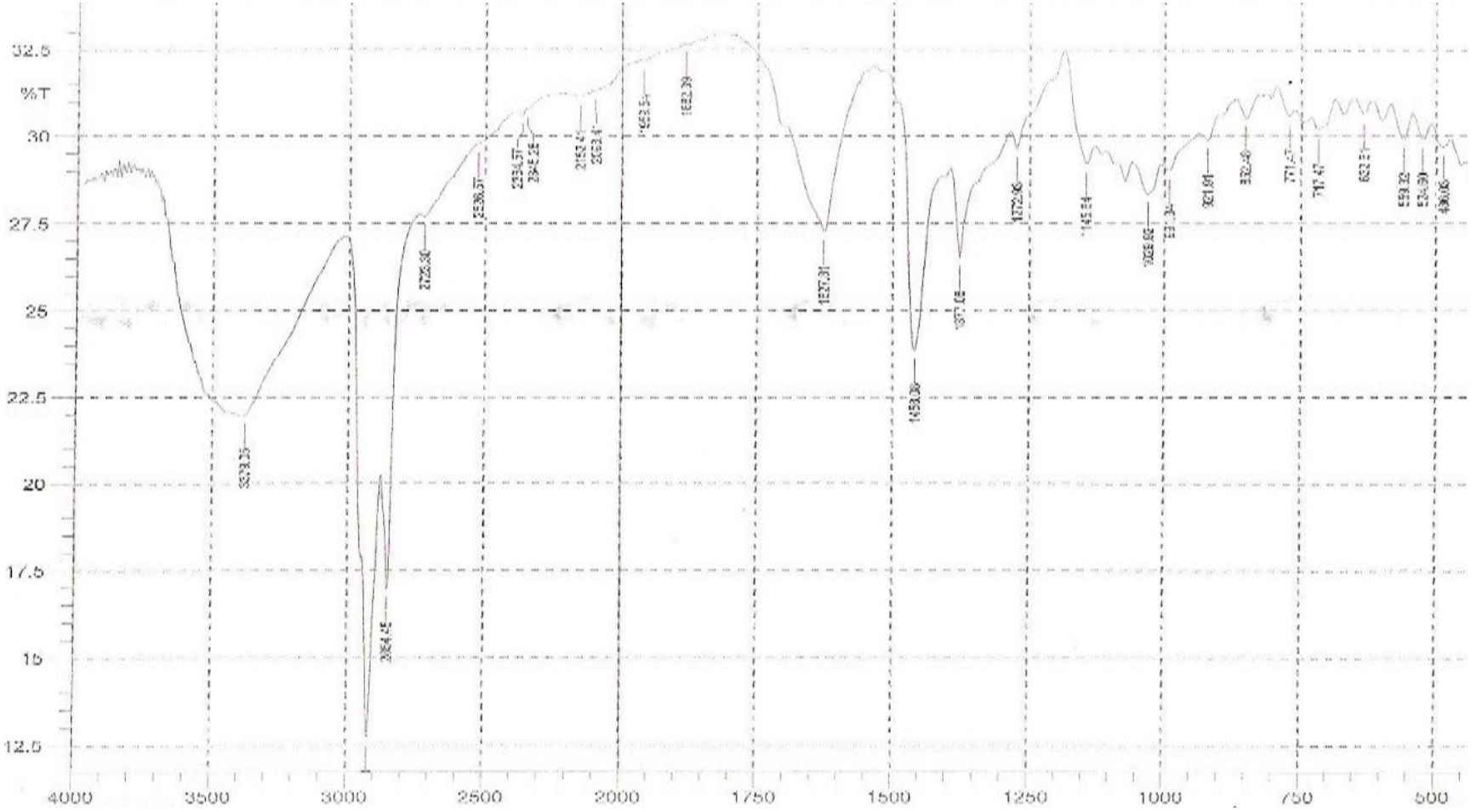

Fig. 3.7. FTIR spectra of potato starch.

~~Accordingly, there is a~~The broad and very strong peak between 3200 $cm^{-1}$and 3600 cm^{-1} which belongs likely to complex stretching vibrations of -OH. The ~~spectrum exhibits~~ two peaks at 721.33 cm^{-1} and 767.62 cm^{-1} ~~which~~ likely ~~belong~~ attributable to bending ~~vibrations~~ of ~~the~~ pyranose ring skeleton. The~~re are~~ peaks around 1078.13 to 1155.28 are ~~which are most~~ probably attribut~~ed~~able to C-O-C and C-OH bonds, respectively. ~~Likewise, t~~The peaks in between 990 cm^{-1} and 1250 cm^{-1} including 1018.30 cm^{-1}, 1045.35 cm^{-1}, 1078.13 cm^{-1}, 1155.28 cm^{-1} and 1205.43 cm^{-1} belong ~~most~~ likely to anhydroglucose ring C-O stretching ~~vibration~~. A typical peak at 1641.31 cm^{-1} is ~~most possibly~~ a feature of firmly bound water. The peaks around 2900 cm^{-1}~~re are absorbance peaks of~~belong to C-H stretching ~~around 2900 cm^{-1}~~. These arguments which were also true for ~~the~~the standard potato starch spectrum claim that the extract ~~exhibited~~had all the vibrational absorbance peaks ~~common to~~common to starches (John, 2000).

3.1.2.4. Crystallinity

C~~The c~~rystal phases of t~~T~~aro *Boloso-I* starch were defined by diffraction spacing and quantified by relative intensities of diffraction peaks of its X-ray diffractogram (XRD) in Fig. 3.6. That is why XRD diffractogram is taken as finger prints of starch structure in ~~starch~~ granules (Zeng *et al.,* 2011).

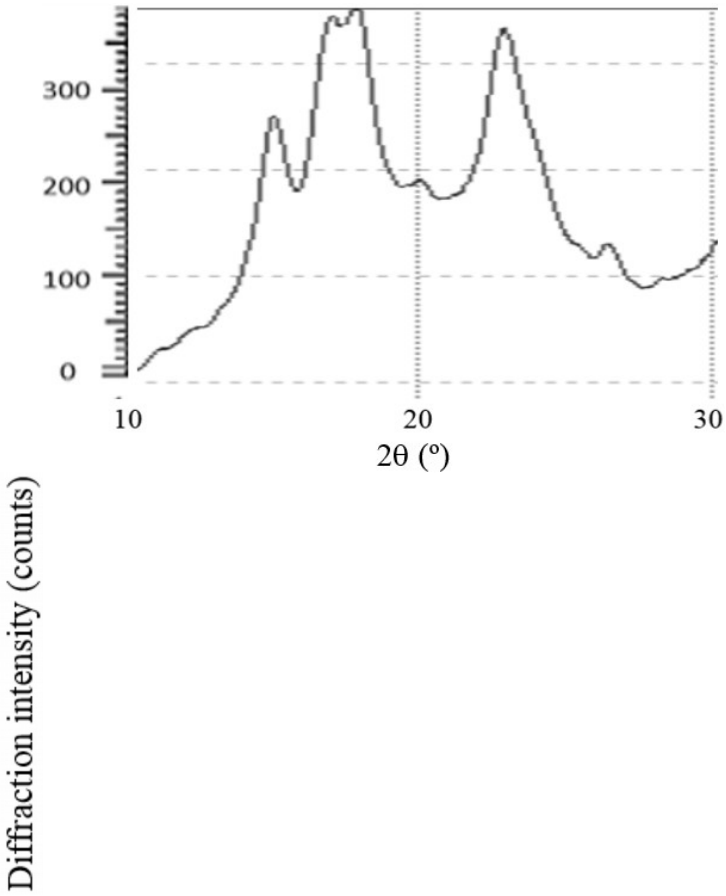

Fig. 3.8. The X-Ray diffractogram of NTB1S.

Accordingly, NTB1S has reflections at 2θ values of 15.02, 16.96, 17.9, 20.02, 23.08 and 26.48 °. The dominantly intense reflections at 2θ values of 15. 02 16.96, 17.9 and 23.08° suggest NTB1S is A-type polymorph revealing closely packed arrangement of the amylopectin molecules in the granules (Zenz *et al.,* 2011). This contradicts trends of most tuber starches exhibiting B-polymorphism including Godare starch (Adane *et al.,* 2006) but it is in line with reports on cassava starch (Paulos, *et al.,* 2009). The possible explanation of NTB1S is A-type polymorph rather than B-polymorph is ~~its~~ too low amylose content to have long ~~chain~~ molecules which permit lamellar formation (Yong-an *et al.,* 2012; Zhou et al., 2014).

3.1.2.5. Densities and Flow Properties

Knowledge of density is useful to avoid risk of segregation by avoiding mixing of powders ~~of significantly~~with differen~~ce~~t densities. D~~The d~~ensities and related properties of NTB1S and potato starch are shown in Table 3.3.

Table 3.8. The densities and related properties of taro *Boloso-I*, potato and Godare starches.

	Density in (g/ml)			**Compressibility index (%)**	Hausner Ratio
	Bulk	Tapped	True		
NTB1S	0.45 ± 0.01	0.59 ± 0.02	1.56 ± 0.02	23.1 ± 0.74	1.30 ± 0.01
Potato Starch	0.67 ± 0.01	0.77 ± 0.01	1.34 ± 0.02	13.3 ± 0.60	1.15 ± 0.04
Godare Starch	0.54 ± 0.01*	0.63 ± 0.03*	1.35 ± 0.02*	14.8*	1.170*

*Values adopted from the report by Adane *et al* (2006b)

Accordingly, NTB1S has lower bulk and tapped densities than potato starch and ~~also the values reported for~~ Godare starch~~, i.e., 0.54 ± 0.01 and 0.63 ± 0.03g/ml, respectively (Adane *et al.*, 2006b)~~. However, the reverse is true for true density, Hausner ratio and Carr's index compared to the values reported for Godare starch. Higher true density is expected for it is A-type polymorph that the molecules are closely packed (Gebre-mariam and Schmidt, 1996b; Adane *et al.,* 2006b~~; Pooja, *et al.*, 2015~~).

NTB1S powder was too cohesive to measure angle of repose and flow rate. Since Carr's index was > 23, Hausner ratio was > 1.25 (Table 3.3) and the powder failed to flow via the funnel, NTB1S is powder of poor flow property in contrast to potato starch and Godare starch. ~~The c~~Cohesiveness is expected as NTB1S granules are smaller ~~associated with~~so that ~~stronger~~ adhesive forces are strong enough to ~~which~~ hinder~~s~~ the ~~the~~ flow (USP 30 / NF 25, 2007).

3.1.2.6. Moisture Sorption Profile

Moisture sorption of starches can affect ~~the~~ physicochemical properties of solid dosage forms containing the starches. ~~Moreover, high moisture sorption might also induce swelling which tends to burst and break-up tablets in the way it does when the starch is used as disintegrant (James, 2007).~~ The moisture sorption profiles of NTB1S and potato starch are depicted in Fig. 3.7.

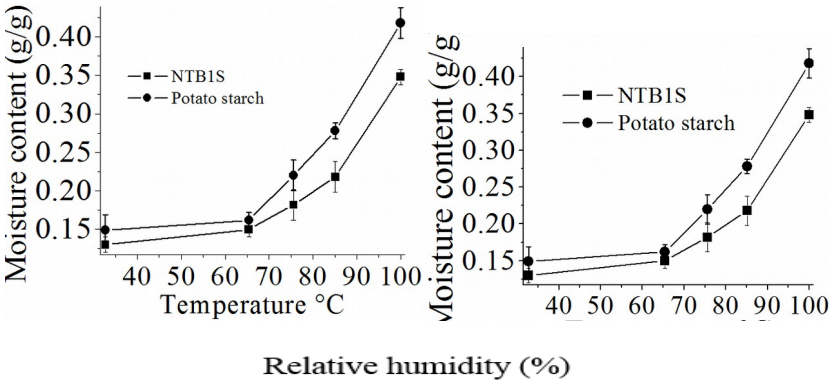

Fig. 3.9. Moisture sorption profile of various NTB1S and potato starch.

The results show that NTB1S was found to exhibit lower moisture sorption than potato starch may be for higher lipid content prohibits moisture sorption ~~(Belitz *et al.*, 2009)~~. Higher crystallinity (A-polymorphism) of NTB1S compared to potato starch (B polymorph) is another reason as moisture is absorbed throughout the amorphous region ~~(James, 2007)~~. The lower moisture sorption of NTB1S is desirable as~~since~~ it minimizes risk of loss of color or physical integrity of solid dosage forms, flow problems~~,~~, microbial growth ~~and stability problem~~ and stability problems ~~-~~associated with hydrogen bonding with –OH ~~of starch~~. Moreover, it avoids burst and break-up of tablets with a mechanism it is used as disintegrant ~~-~~(Aulton, 2002; Yoshioka and Stella, 2002; Swarbrick, 2007; Shayne, 2008).

3.1.2.7. Gelatinization Property

While gelatinization temperature of starch reveals the extent of ordered arrangement, its enthalpy (ΔH) reflects energy of disorganization of double helices of glucan chains and is linked to crystallite fusion. It is presumably affected by many aspects of ~~starch~~ granule gelatinization. It is ~~and it is~~ difficult to link ΔH to only one factor, e.g., amylose content or crystallinity ~~-~~(Zhou et al., 2014). Fig. 3. 8 and Table 3.4 show DSC ~~G~~gelatinization properties of NTB1S and potato starch at starch to water ratio of 1:2 (w/w)~~were compared with potato starch using DSC results at starch/water ratio of 1:2 (w/w) (~~Fig. 3. 8 and Table 3.4~~)~~.

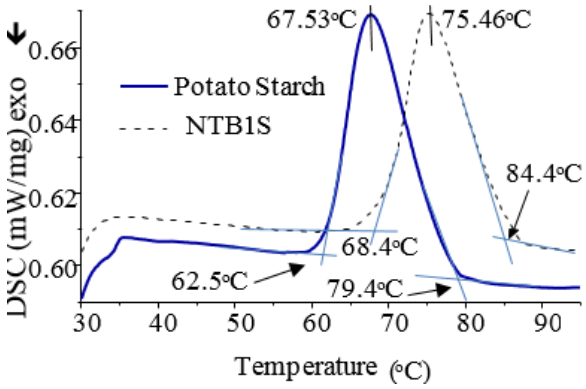

Fig. 3.10. Gelatinization DSC thermographs of NTB1S and potato starch.

Table 3.9. Gelatinization temperatures and enthalpies of NTB1S and potato starches.

Parameter	NTB1S	Potato starch
On set (T_O) (°C)	68.40	62.50
Peak (T_P) (°C)	75.46	67.53
End set (T_E) (°C)	84.40	79.40
Enthalpy (ΔT) (mJ/mg)	3.991	4.999
ΔT (T_E-T_O) (°C)	16.00	16.90

Accordingly, the ~~Accordingly, at starch/water ratio of 1:2 w/w, g~~gelatinization temperatures of NTB1S (T_O = 68.4, T_P = 75.46 and T_E = 84.4 °C) were higher than that of potato starch (62.50, 67.53 and 79.40 °C, respectively). Moreover, T_O, T_P and T_E of NTB1S were~~are~~ higher than those of Godare starch. Most likely, this is due to stronger, close and ordered packing of A-type polymorph granules (Dalonso and Petkowicz, 2014; Moraes *et al.*, 2014). ~~On the other hand~~However, ~~the~~ enthalpy of gelatinization of NTB1S (3.991 mJ/mg) was~~is~~ lower than that of potato starch (4.999 mJ/mg). This is expected as~~because~~ the higher granular lipid content ~~which~~ causes exothermic complex formation during gelatinization ~~(~~Eliasson and Wahlgren, 2004) presumably letting the completion of gelatinization with lower amount of energy ~~. As a result~~ once the peak ~~gelatinization~~ temperature has been reached~~, the granules require lower amount of energy than potato starch granules (Gebre-mariam and Schmidt, 1996b)~~.

3.1.2.8. Swelling Power and Solubility Index in Water

Force and extent of swelling of starch play great role in solid dosage forms, especially in disintegration (Alfonso, 2000) ~~, as it is one of the mechanisms of tablet disintegration~~ by bursting and bringing break-up of tablets into granules (Swarbrick, 2007). Solubility index of starches is affected by source

and swelling power (Paulos, *et al*, 2009). The swelling power and the solubility index of NTB1S and potato starch are illustrated in Fig. 3.9.

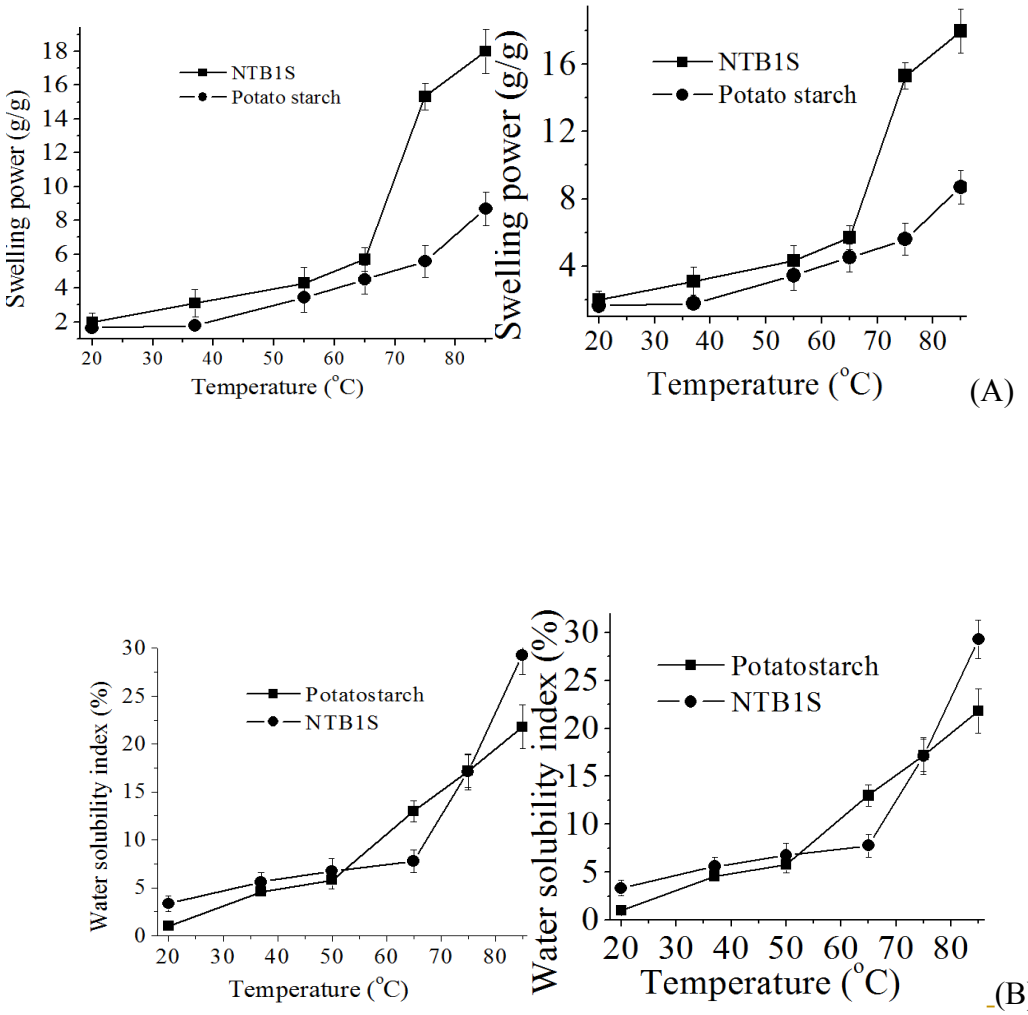

Fig. 3.11. Swelling power (A) and solubility index (B) of NTB1S and potato starch in water.

It is observable from the result that swelling power of NTB1S in water is higher ($p < 0.05$) at 20, 37, 50, 65, 75 and 85 °C than potato starch. The higher swelling power can be explained at lower temperature by larger surface area and at high temperature higher branching (Zhou et al., 2014) and lower protein content which means reduced stiff protein matrixes embedding the granules (Israkarn *et al.,* 2007; Wang *et al.,* 2014).

The s~~The s~~olubility index of NTB1S was higher at low temperatures (20, 37 and 50 °C) and 85 °C ($p < 0.05$), comparable at 75 °C ($p > 0.05$) but lower at 65 °C ($p < 0.05$) than potato starch. The likely reason for higher solubility index of NTB1S at lower temperatures is higher surface accessibility of NTB1S granules which are smaller than potato starch granules as particle size distribution also

determines starch behavior in moisture and moisture plus heat (Al-Rabadi *et al.,* 2012). At 65 °C, potato starch has higher solubility may be because potato starch has undergone significant gelatinization which increases solubility in contrast to NTB1S granules which has not yet started to gelatinize prior to 68.4 °C. Nevertheless, solubility was comparable at 75 °C which is about the peak gelatinization temperature for NTB1S (Swarbrick, 2007). At 85 °C ~~(higher than the endset temperatures of both NTB1S and potato starch)~~, solubility index of NTB1S was higher than that of potato starch may be for the higher content of amylopectin which has more exposure of –OH groups than the amylose.

3.1.3. Drug - Excipient Compatibility

In order to check the drug excipient compatibility, presence of characteristic vibrations of paracetamol including -NH-, -OH,-CO, -CH_3, benzene ring and phenyl-OH were considered. This was used by discerning the corresponding absorbance peaks in the spectra of mixtures of 1:1 drug to excipients ratio and critically comparing with the spectrum of paracetamol (Fig. 3.10, 3.11 and 3.12).

The sharp absorption bands around 3321.19 - 3325.05 cm^{-1} and at 1612.38 cm^{-1} are thought to be the symmetric stretching and out-of-plane (OOP) bending bands of –NH– bonds, respectively. The broad background absorption around 3450-3112.89 cm^{-1} (OH-stretches) and the presence of bands at 1600 cm^{-1} (likely OOP bends of aminophenol-OH bond) claims the presence of phenolic –OH group. The presence of aromatic ring was evidenced by the doublets (1558.38-1562.23 cm^{-1} and 1504.37 cm^{-1}), possible weak overtone and combination bands in between 2000 cm^{-1} and 1600 cm^{-1}. The presence of acetyl group was supported by the strong band at 2898.8 cm^{-1} (owing to stretching vibrations) and 1373.22 cm^{-1} (owing to bending/umbrella vibrations) of the methyl C-H bonds. It was reinforced by the presence of strong protruding band at 1650.95 cm^{-1} suggesting CO stretching vibration. The presence of the peaks at 1259.43 cm^{-1} and 1226.64 cm^{-1} are common to C-O/C-N stretching vibrations (John, 2000; Sakataa *et al.,* 2007). The presence of the vibrational absorbance bands which possibly qualify the structural groups of paracetamol states that it is unlikely that there will be interaction of paracetamol with NTB1S or PGTB1S (Chadha and Bhandari, 2014).

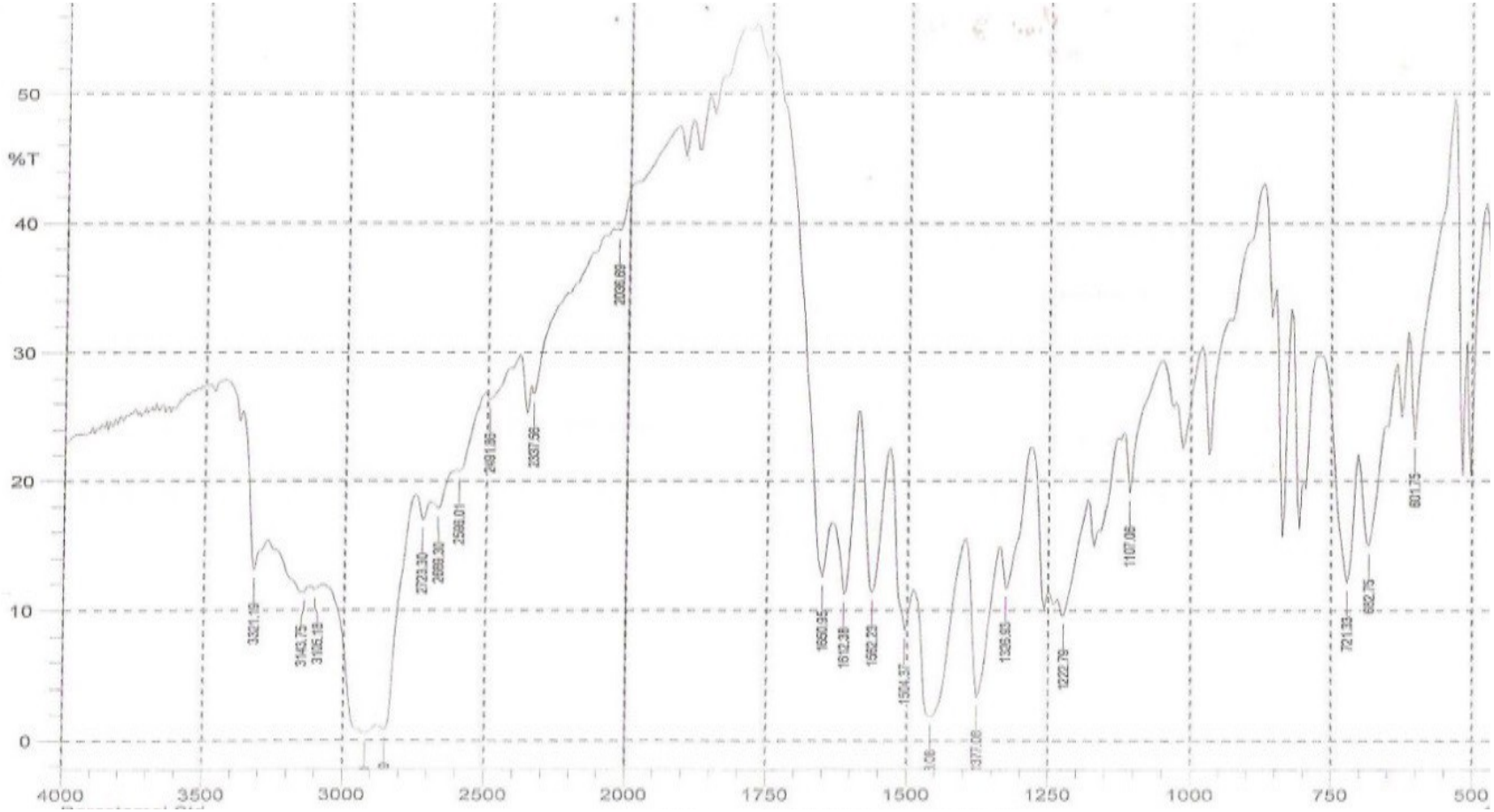

Fig. 3.12. FTIR of pure paracetamol.

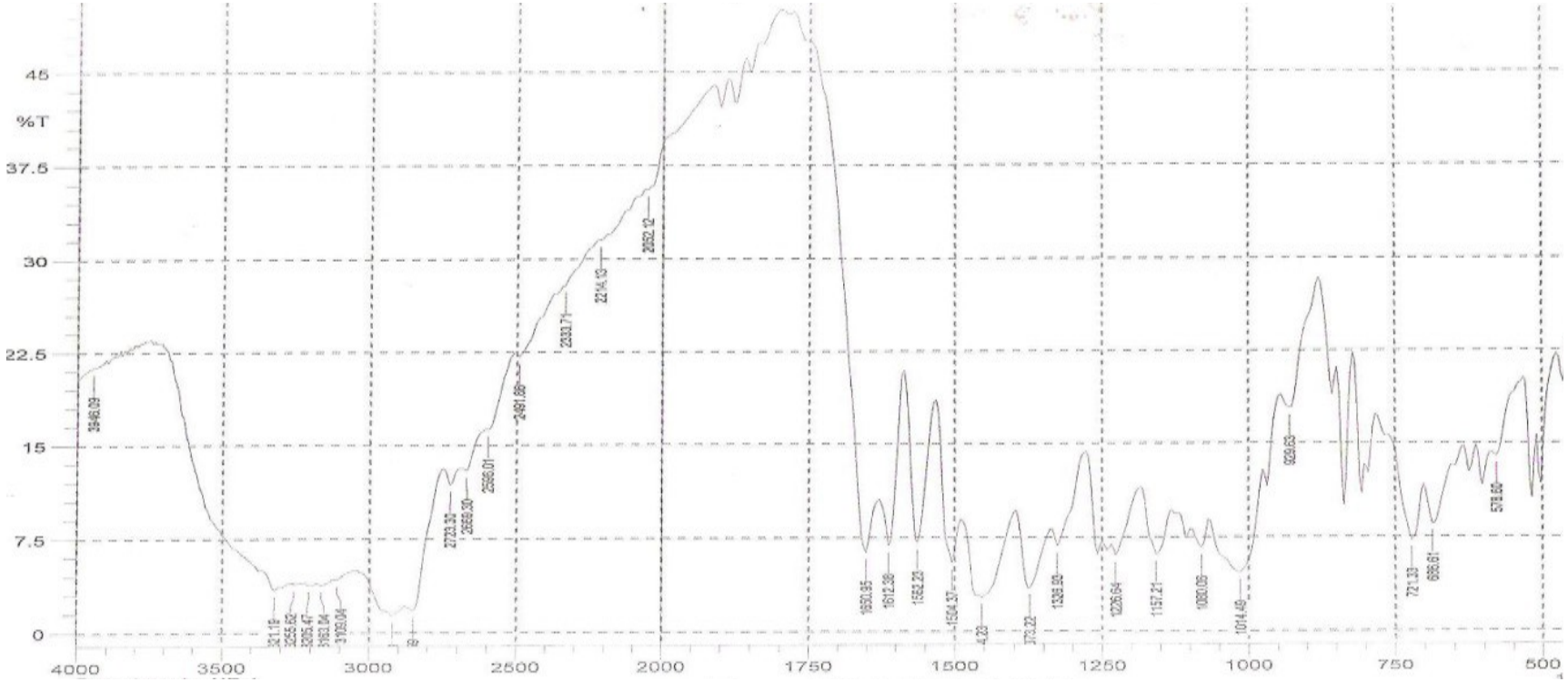

Fig. 3.13. FTIR spectra of pure paracetamol mixed with NTB1S (at 1:1 ratio).

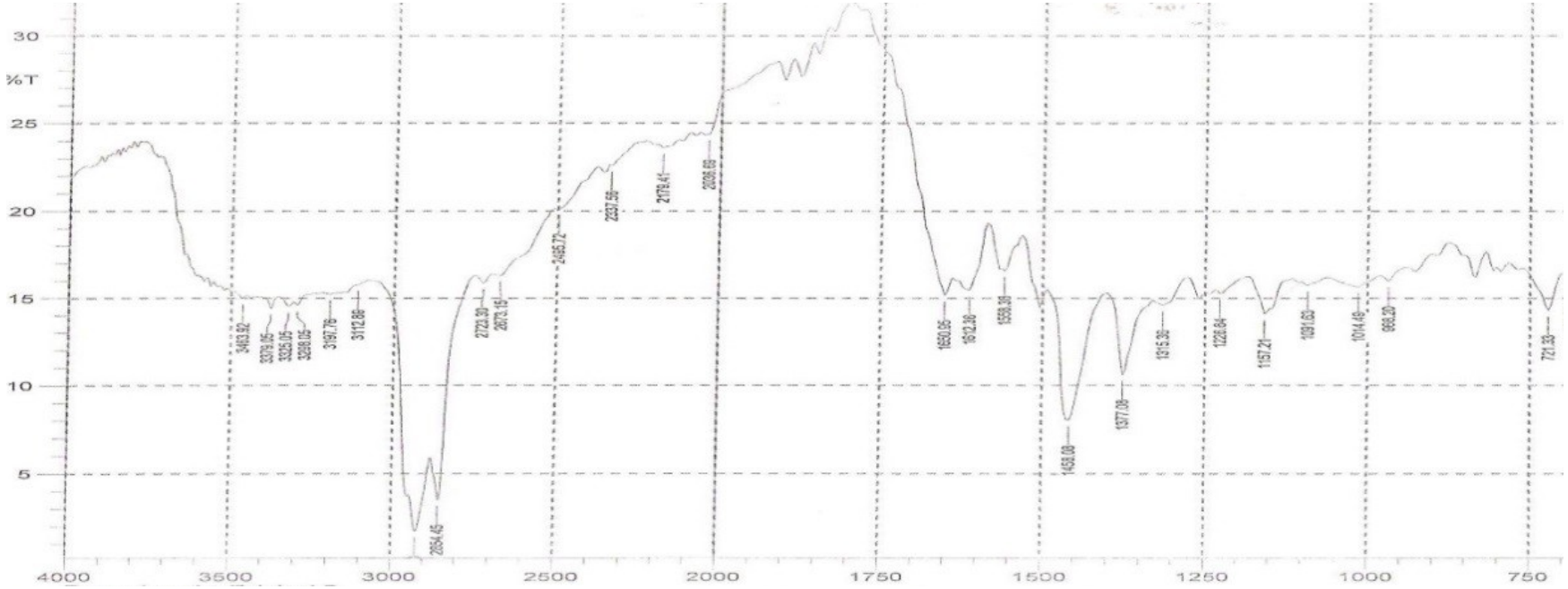

Fig. 3.14. FTIR spectra of pure paracetamol mixed with PGTB1S (at 1:1 ratio).

In order to confirm the absence of paracetamol-NTB1S incompatibility, the DSC curves of pure components and their 1:1 (w/w) physical mixtures were compared (Fig. 3.13).

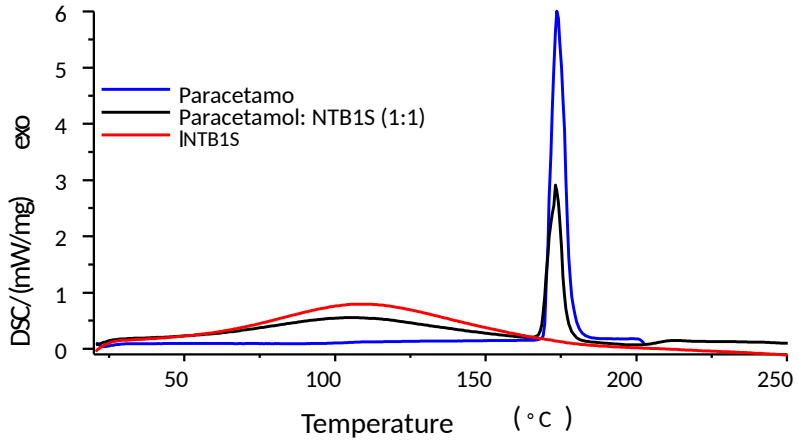

Fig. 3.15 DSC thermogram of drug-excipient compatibility study.

As per the DSC thermograms, there occurred neither appearance of strange peak nor disappearance of existing characteristic peaks up to 200 °C. Moreover, there is no significant shift of the existing peaks. These facts confirm that the interaction between paracetamol and NTB1S is highly unlikely to occur in the range of temperature investigated (Sakataa *et al.,* 2007; Chadha and Bhandari, 2014).

3.2. Tablet Disintegrating Properties of Native NTB1S

Preliminary study showed that incorporation of NTB1S as endo-disintegrant decreases its paracetamol tablet disintegrating efficiency in line with a report by Adedokun and Itiola (2011) on starches from trifoliate yams, rice and corn. Hence for this study, it was used only as exo-disintegrant. The appropriate ranges of concentration of NTB1S (NTB1SC) and compression force (CF) were determined.

3.2.1. Precompression Properties of Tablet Formulations

Before compression of tablet formulations, pre-compression parameters including granule size, size distribution and granule friability which would potentially indicate aptness of granule processing and formulation were measured. The size distributions of the paracetamol granules are shown in Fig. 3.14.

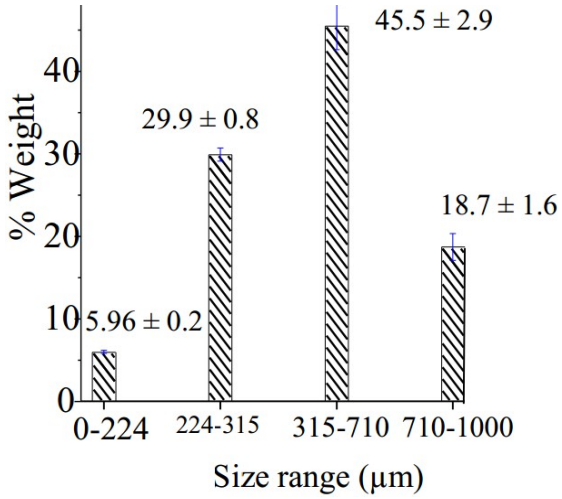

Fig. 3.16. Size distribution of paracetamol granules.

Table 3.10. Size distribution of paracetamol granules of study formulations.

Size range (µm)	Average size (µm)
0-224	112.0 ± 0.0
224-315	269.5 ± 0.0
315-710	512.5 ± 0.0
710-1000	855.0 ± 0.0
0-1000	480.3 ± 13.68

As shown in Fig. 3.14 and also Table 3.5, size distribution of the granules is reasonably close to normal distribution. This is because overall average size (480.3 ± 13.68 µm) of the granules was comparable with the corresponding midpoint of the size range (500 µm) with error of 3.94%.

Besides size distribution, ~~the~~ granule strength affects ~~the~~ compressibility of granules into cohesive tablets and hence quality of tablets. In this regard, granule friability was measured ~~in order~~ to estimate ~~the~~ relative magnitudes of attractive forces keeping the granules strong. The friability was found to be 0.63 ± 0.04% which is acceptable (< 1%) indicating that the equipment type and type and amount of granulating agent were appropriate for their intended uses.

After characterization of size, size distribution and friability of the paracetamol granules separately, disintegrant NTB1S was added as per the experimental plan ~~(13 design points)~~. Meanwhile, densities ~~of the mixtures~~ and flow properties which per se depend on the density were determined and analyzed. This was ~~for the reason that~~because density ~~profiles~~ of powders for solid dosage forms potentially affects die fill volume, compressibility and compaction properties. Besides it is ~~and also~~ used for derivation of compressibility ind~~ices~~exes and Hausner ratios (Table 3.6).

Table 3.11. Bulk density, tapped density, Carr's index and Hausner ratio of paracetamol granules.

	Bulk density (g/ml)	**Tapped density (g/ml)**	**Carr's index (%)**	Hausner ratio	**Angle of repose (°)**	**Flow rate (g/sec)**
F1	0.53 ± 0.06	0.57 ± 0.06	7.02 ± 0.71	1.18 ± 0.01	31.0 ± 2.8	6.65 ± 0.4
F2	0.53 ± 0.04	0.58 ± 0.05	9.48 ± 0.76	1.03 ± 0.01	26.6 ± 2.1	6.03 ± 0.6
F3	0.52 ± 0.05	0.56 ± 0.04	7.14 ± 0.66	1.14 ± 0.01	30.5 ± 2.9	6.65 ± 0.5
F4	0.52 ± 0.04	0.57 ± 0.03	9.65 ± 0.54	1.03 ± 0.01	26.6 ± 2.0	6.04 ± 0.2
F5	0.54 ± 0.04	0.59 ± 0.05	8.47 ± 0.79	1.14 ± 0.02	31.5 ± 2.9	6.66 ± 0.7
F6	0.53 ± 0.03	0.59 ± 0.02	10.2 ± 0.74	1.14 ± 0.01	27.0 ± 2.4	6.00 ± 0.8
F7	0.50 ± 0.05	0.55 ± 0.05	9.09 ± 0.67	1.02 ± 0.01	25.0 ± 2.0	8.05 ± 0.9
F8	0.50 ± 0.06	0.54 ± 0.03	7.41 ± 0.60	1.18 ± 0.00	23.9 ± 2.0	8.06 ± 0.0
F9	0.50 ± 0.04	0.55 ± 0.05	9.09 ± 0.78	1.09 ± 0.01	24.7 ± 2.3	8.04 ± 0.6
F10	0.51 ± 0.04	0.56 ± 0.06	8.93 ± 0.64	1.03 ± 0.01	21.2 ± 2.0	8.03 ± 0.7
F11	0.50 ± 0.05	0.55 ± 0.04	9.09 ± 0.69	1.02 ± 0.01	23.9 ± 1.7	8.03 ± 0.8
F12	0.51 ± 0.03	0.56 ± 0.05	8.65 ± 0.73	1.02 ± 0.01	24.8 ± 2.0	8.05 ± 0.9
F13	0.50 ± 0.04	0.55 ± 0.05	9.09 ± 0.65	1.03 ± 0.01	24.9 ± 2.0	8.04 ± 0.8

The Carr's indices of all formulations were below 10% except 10.2% of +1.414 (F6) containing 17.00 % of the disintegrant NTB1S. Similarly, Hausner ratios of the formulations were < 1.25. None of the formulations exhibited angle of repose above 31.5 ± 2.9 °. Accordingly, all the formulations have at least good flow property. Since the values of Carr's indices, Hausner ratio and angle of repose were lower than 15.00%, 1.25 and 35.0 °, respectively, the powder will not normally have flow problem impairing tablet manufacturability through content uniformity (USP 30 / NF 25, 2007).

3.2.2. Properties of Compressed Tablets

Since the formulations involved in the study are uncoated tablets containing more than 25 mg paracetamol, weight variation test was assumed to signify content uniformity (USP 30 / NF 25, 2007). The weights and thickness of the tablets are shown in Table 3.7.

Table 3.12. Characteristics of paracetamol tablets with NTB1S as disintegrant

	Weight (mg)	Thickness (mm)
F1	351.7 ± 3.5	3.96 ± 0.05
F2	350.3 ± 4.9	3.91 ± 0.04
F3	349.0 ± 3.8	3.94 ± 0.07
F4	349.5 ± 4.1	3.90 ± 0.04
F5	350.2 ± 2.9	3.95 ± 0.05
F6	349.8 ± 6.0	3.89 ± 0.04
F7	350.0 ± 3.0	3.94 ± 0.08
F8	350.1 ± 3.1	3.93 ± 0.06
F9	350.0 ± 2.8	3.93 ± 0.05
F10	351.8 ± 3.0	3.94 ± 0.06
F11	351.0 ± 4.5	3.93 ± 0.05
F12	350.5 ± 4.5	3.94 ± 0.06
F13	350.0 ± 3.0	3.93 ± 0.04

As per the results, tablet formulations of the study are all within ± 5% in terms of weight variation test which is acceptable for tablets weighing > 250 mg (BP, 2009). This reaffirms and appears to be due to good flow properties of the granules. The tablet thickness was found to decrease slightly with increasing CF probably because higher compression force brings the granules into more cohesive form and hence decreases the thickness and porosity (USP 30 / NF 25, 2007).

Similarly, the hardness, friability and disintegration time values of the tablets were determined and described in Table 3.8.

Table 3.13. Hardness, friability and ~~disintegration time~~DT values of paracetamol tablets.

	Hardness (N)	Friability (%)	DT (Min)
F1	97.30 ± 6.0	0.150 ± 0.10	14.10 ± 0.9
F2	131.00 ± 5.9	0.200 ± 0.02	2.65 ± 0.0
F3	110.75 ± 8.8	4.000 ± 0.60	43.00 ± 0.6
F4	161.32 ± 5.7	0.200 ± 0.02	3.00 ± 0.3
F5	107.00 ± 11.2	0.600 ± 0.17	42.50 ± 0.3
F6	153.43 ± 6.8	0.100 ± 0.02	2.08 ± 0.1
F7	99.20 ± 3.4	0.175 ± 0.08	3.02 ± 0.5
F8	143.00 ± 6.1	2.880 ± 0.47	10.20 ± 0.3
F9	141.50 ± 5.6	0.233 ± 0.01	6.40 ± 0.4
F10	138.25 ± 6.3	0.200 ± 0.04	6.30 ± 0.3
F11	141.50 ± 5.1	0.195 ± 0.03	6.30 ± 0.1
F12	138.00 ± 3.5	0.217 ± 0.04	2.40 ± 0.3
F13	137.10 ± 5.7	0.198 ± 0.03	2.60 ± 0.6

3.2.3. Mathematical Model

In order to graphically and mathematically demonstrate ~~the~~ trends of levels of the responses across ~~the~~ changing levels of the factors, ~~the~~ respective best fitting models had to be selected using the Design Expert Software version 8. To this end, the arithmetic means of the response values of the tablets that had been determined (Table 3.8) were fed into the mathematical software. Subsequently, as a result of Design Expert software output, available models including linear, two factor interaction (2FI), quadratic and cubic models were compared in terms of R^2, adjusted R^2, predicted R^2 and predicted residual sum of square (PRESS) values (Table 3.9) computed using the software for each of the responses.

Table 3.14. Fit summary of responses (hardness, friability and DT).

Response	Source	R^2	Adjusted R^2	Predicted R^2	PRESS
Hardness	Linear	0.8318	0.7981	0.7069	1482.22
	2FI	0.8458	0.7945	0.6251	1896.03
	Quadratic*	0.9797	0.9653	0.8749	632.92
	Cubic**	0.9965	0.9915	0.9866	67.90
Friability	Linear	0.6542	0.5850	0.2951	2.030
	2FI	0.8306	0.7741	0.6320	1.060
	Quadratic*	0.9941	0.9898	0.9661	0.098
	Cubic**	0.9981	0.9954	0.9697	0.087
DT	Linear	0.6640	0.5968	0.3477	1639.39
	2FI	0.7451	0.6601	0.3810	1555.61
	Quadratic*	0.9720	0.9520	0.8398	402.52
	Cubic**	0.9918	0.9802	0.9110	223.61

* Suggested model ** Aliased model

Accordingly, all the three responses best satisfy ~~the~~ quadratic polynomial model. This is because ~~the~~ quadratic polynomial model has R^2 values (0.9797, 0.9941 and 0.9720) larger, adjusted R^2 values (0.9653, 0.9898 and 0.9520) closer to 1, predicted residual sum of square (PRESS) values (632.92, 0.098 and 402.52) less and predicted R^2 values (0.8749, 0.9661 and 0. 0.8398) in more reasonable agreement with ~~the~~ adjusted R^2 than any other non-aliased model (Lewis *et al.,* 1999; Huang *et al.,* 2005). Adequacy of these models for predicting influences of the factors on the responses was verified by ANOVA at 95% CI (Table 3.10).

Table 3.15. Summary of ANOVA results for dependent variables from CCD.

Source		Sum of Squares	df	Mean square	F-value	p-value Prob > F
Hardness	Model	4955.14	5	991.03	67.67	< 0.0001*
	NTB1SC (X_1)	2809.95	1	2809.95	191.88	< 0.0001*
	CF (X_2)	1396.89	1	1396.89	95.39	< 0.0001*
	X_1^2	151.63	1	151.63	10.35	0.0147*
	X_2^2	592.16	1	592.16	40.44	0.0004*
	LOF	85.20	3	28.40	6.56	0.0503**
Friability	Model	2.860	5	0.57000	234.58	< 0.0001*
	NTB1SC (X_1)	0.650	1	0.65000	265.26	< 0.0001*
	CF (X_2)	1.240	1	1.24000	506.61	< 0.0001*
	X_1X_2	0.510	1	0.51000	208.14	< 0.0001*
	X_2^2	0.470	1	0.47000	192.82	< 0.0001*
	LOF	0.013	3	0.00427	3.97	0.1082**
DT	Model	2442.76	5	488.55	48.59	< 0.0001*
	NTB1SC (X_1)	1474.58	1	1474.58	146.65	< 0.0001*
	CF (X_2)	194.08	1	194.08	19.30	0.0032*
	X_1X_2	203.78	1	203.78	20.27	0.0028*
	X_1^2	570.31	1	570.31	56.72	0.0001*
	LOF	52.72	3	17.57	3.98	1.077**

* Significant ** Not significant

The model significance tests were significant ($p < 0.05$) and lack of fit tests (mean errors) were insignificant ($p > 0.05$) for all the three responses**.** In the same fashion, ~~the~~ signal to noise ratios (adequate precision values), 24.583 of hardness, 49.677 of friability and 19.881 of DT, show the signal is adequate and quadratic models are quite valid.

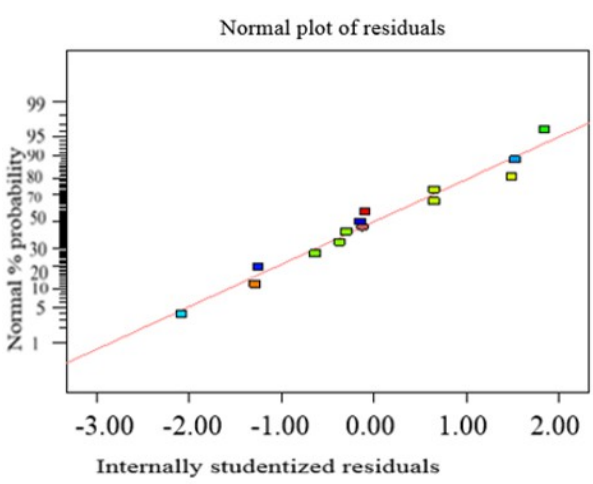

(A)

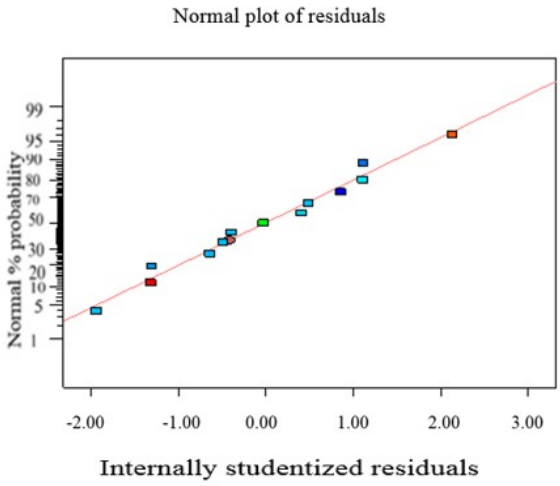

(B)

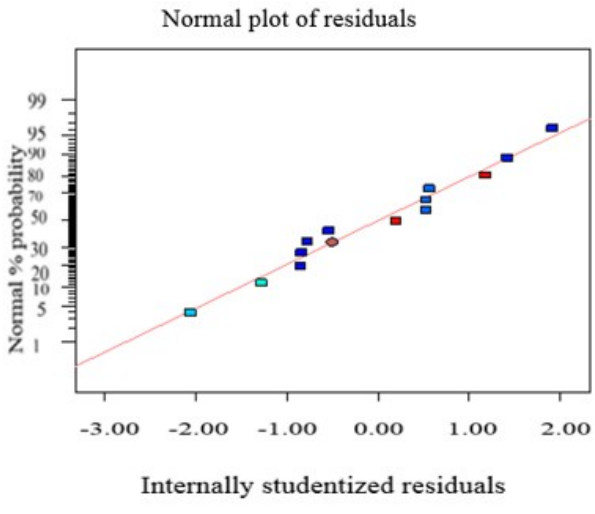

(C)

Fig. 3.17. Normal probability plot of residuals for tablet hardness (A), friability (B) and DT (C).

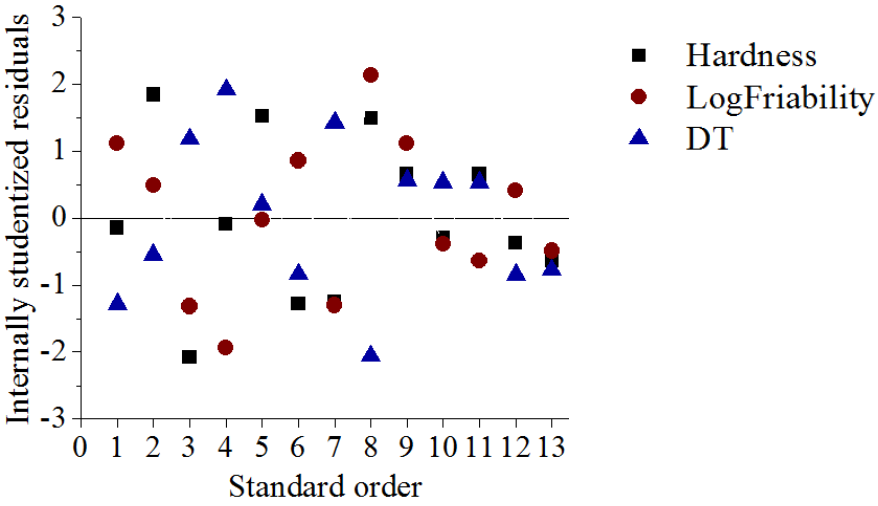

Fig. 3.18. Internally studentized residual of the hardness, friability and DT.

Furthermore, two extra tests proved the validity of the regression models. The first is that the normal probability plots of residuals versus predicted values reasonably approximated the normal plot of predicted values (Fig. 3.15). The second is that internally studentized residuals are < 3 units away from zero and also randomly scattered (Fig 3.16). Thus, the selected models are adequate enough to reveal the relationships existing between the variables within 95% CI and used to explain the types and trends of influences (Lewis et al., 1999).

3.2.4. **Trends of Responses with Changing Levels of Factors**

Having selected the models of best fits with statistically valid adequacy, equivalent mathematical equations were generated in order to summarize trends of hardness, friability and ~~disintegration time~~DT with changing levels of disintegrant concentration and compression force. Moreover, the

response surface and contour plots were constructed. Using these mathematical and diagrammatic approaches, the individual and interaction effects of the factors on the responses were revealed.

In this regard, eq. 3.3, Fig. 3.17A and B show trend of hardness of tablets with varying levels of concentration of NTB1S and compression force.

$$H = 139.27 + 18.74X_1 + 13.21X_2 - 4.67X_1^2 - 9.23X_2^2 \qquad \text{eq. 3.3}$$

Where; H, X_1 and X_2 stand for the levels of hardness, NTB1S concentration and the compression force, respectively.

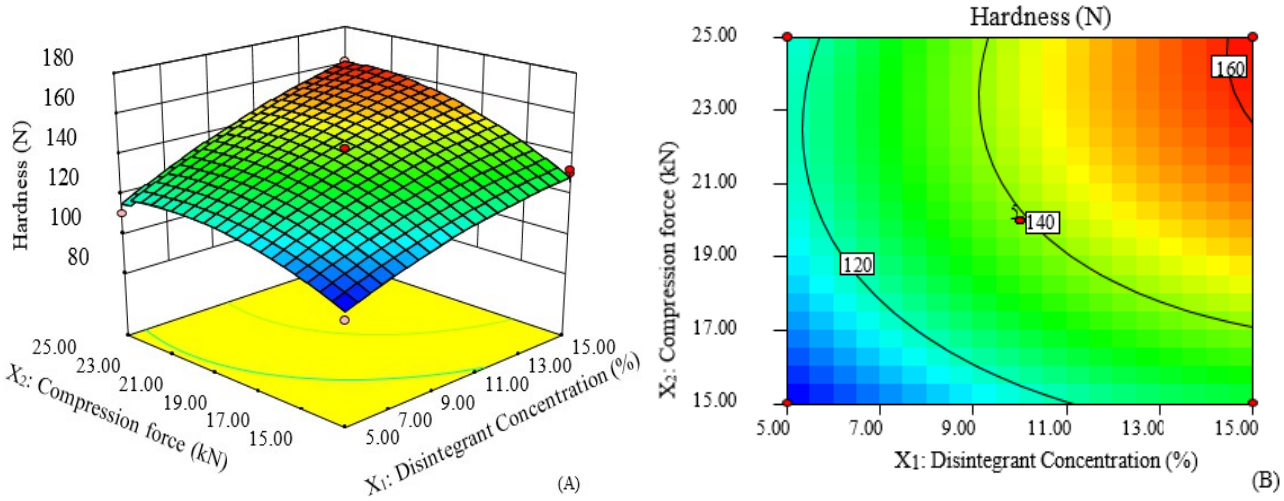

Fig. 3.19. Response surface (A) and contour plots (B) of hardness as a function of compression pressure and NTB1SC.

The illustrations show that hardness of the tablets increases with increase in the disintegrant starch concentration (coefficient = 18.74, $p < 0.0001$) and also compression force (coefficient = 13.21, $p < 0.0001$). The reason for increasing of hardness with compression force is maybe NTB1S has good compactibility presumably due to fine particle sizes. This is because the finer the particle size of the powder, the stronger the influence of adhesive forces on the powder bulk. Consequently, when the particles are compressed, the adhesive force between the particles increases thereby large stresses prevail (locally) at the particles' contact points, due to very small contact points. In this way, occurrence of plastic deformation of the particles in contact area and increment of contact area with the particles approaching each other is expected (Swarbrick, 2007). It is discernible that both NTB1SC and compression force have convex (negative) quadratic effect on the hardness of the tablet with coefficients of -4.67 ($p < 0.0147$) and -9.23 ($p < 0.001$), respectively. The presumed reason for the negative quadratic effect of compression force on the tablet hardness is that paracetamol pure is a

powder of poor compressibility and bonding leading to high tendency for capping at higher CFs. The NTB1SC has stronger positive influence on tablet hardness than CF as the term X_1 has larger coefficient (18.74) than that of X_2 (13.21).

Similarly, trend of friability of tablets with varying levels of concentration of NTB1S and compression force is shown in eq. 3.4, Fig. 3.18A and B.

$$\log Fr = -0.68 - 0.28X_1 + 0.39X_2 - 0.36X_1X_2 + 0.26X_2 \qquad \text{eq. 3.4}$$

Where; logFr, X_1 and X_2 stand for the levels of log transformed friability, NTB1S concentration and the compression force, respectively.

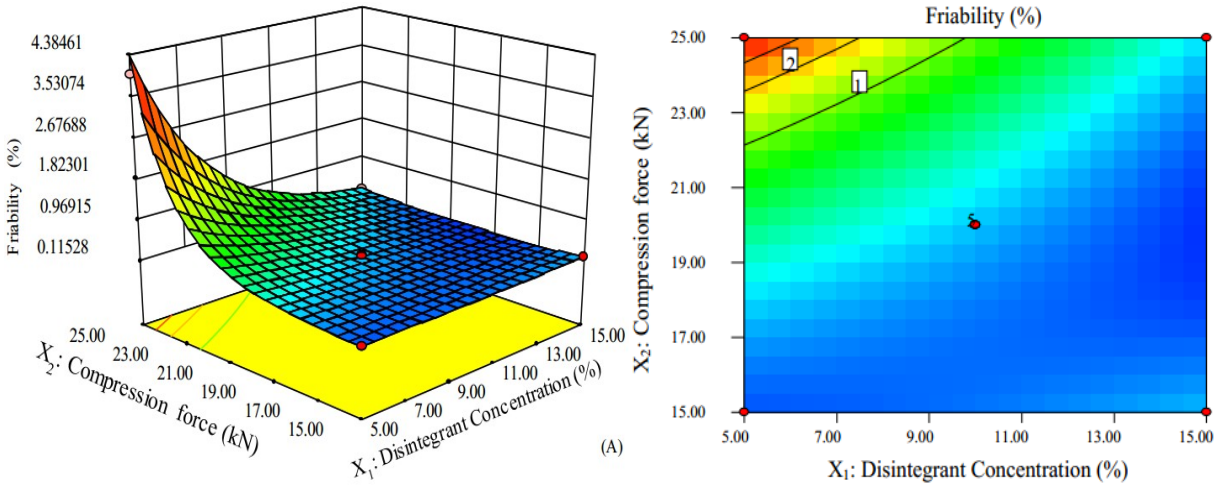

Fig. 3.20. Surface response (A) and contour plot (B) of friability as a function of compression pressure and NTB1SC.

The equation and diagrams suggest that friability of the tablets decreases with increase in disintegrant concentration (coefficient = -0.28, $p < 0.0001$). Perhaps the reason for positive and negative effects of the starch concentration on hardness and friability, respectively, is increase in availability of particles in closer contact which brings about more interparticular bonding (Adedokun and Itiola, 2011). On high and fast compression, this smaller size of NTB1S granules might experience interparticular adhesive forces to increase and transmit axial pressure better. The subsequent stronger stresses at particles contact points, which are small enough result in plastic increment of contact area and let the particles approach each other forming stronger compacts (Abdel-Hamid *et al.,* 2011). Another point of view for this is that rice starch which has similar morphology with that of NTB1S is claimed to be the most compressible native starch. The reason for strong compactibility can also be mechanical

interlocking of aggregates of granules (Kittipongpatana and Kittipongpatana, 2012). On the other hand, compression force (coefficient = 0.39, $p < 0.0001$) has increasing effect on the friability. The interaction of the NTB1SC and CF antagonises log friability of tablet (coefficient = -0.36, $p < 0.0001$). CF has positive quadratic effect on log transformed friability of the tablets with coefficient of 0.26 ($p < 0.0001$).

In the same way, eq. 3.5, Fig. 3.19A and B show trend of ~~disintegration time~~DT of tablets with varying levels of concentration of NTB1S and compression force.

$$DT = 4.8 - 13.58x_1 + 4.93x_2 - 7.14x_1x_2 + 9.05{x_1}^2 \qquad \text{eq. 3.5}$$

Where; DT, X_1 and X_2 stand for the levels of ~~disintegration time~~DT, NTB1S concentration and the compression force, respectively.

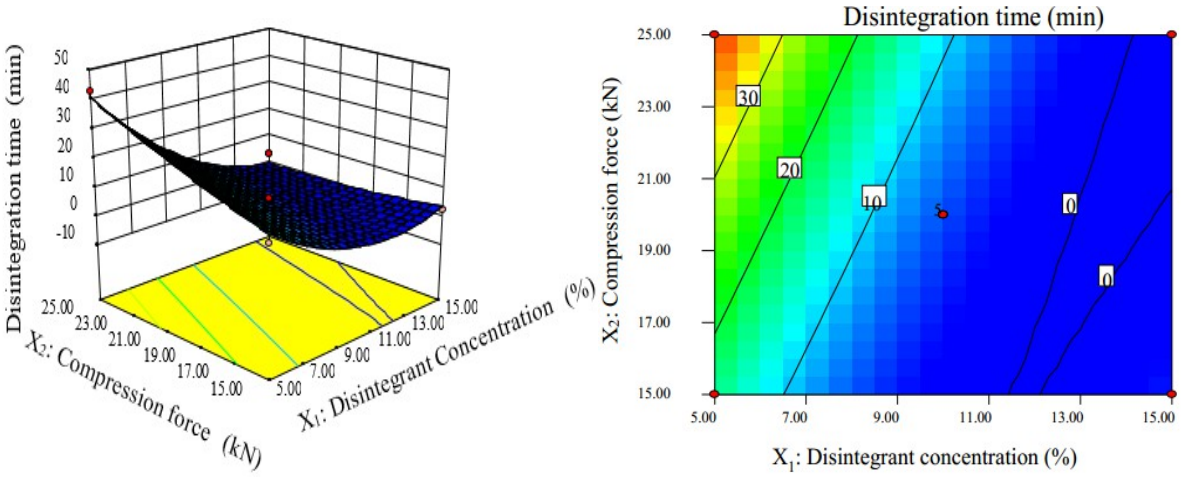

Fig. 3.21. Surface response (A) and contour plot (B) of ~~disintegration time~~DT as a function of compression pressure and NTB1SC.

The equation and plots show that DT of the tablets is negatively affected by the concentration of the disintegrant starch (coefficient = -13.58, $p < 0.0001$) but positively affected by compression force (coefficient = 4.93, $p = 0.0032$). Depending on the mechanism of disintegrant action the reason for decreasing effect of NTB1S on the disintegration may be different but feasibly it perhaps increases the porosity and hence penetration of the liquid into the tablet and facilitates swelling. Conceivably, the reason for increment of the DT with increasing compression force is higher compaction decreases the porosity and hence liquid permeation resulting in lower swelling (Riippia *et al.,* 1998). The interaction of the NTB1SC and compression force antagonises DT of the tablets as shown by the sign of the term X_1X_2 eq. 3.5, -7.14 ($p = 0.0028$). It is observable that the NTB1SC has positive (concave) quadratic

effect on the DT of the tablet with coefficient of 9.05 (p = 0.0001). NTB1SC has stronger negative influence on tablet DT than the positive influence of CF as the magnitude of coefficient of X_1 (-13.58) is greater than that of X_2 (4.93). Hence, the hardness and DT of tablets are affected more by concentration of NTB1S than compression force whereas friability is affected more by compression force.

3.2.5. Optimization and Validation

To optimize the factors into the response limits of equal importance (Fig. 3.20A), numerical (desirability based) optimization method described in Fig. 3.20B and graphical (overlaying or superimposing contours) optimization method described in Fig. 3.21 were used (Lewis *et al.,* 1999).

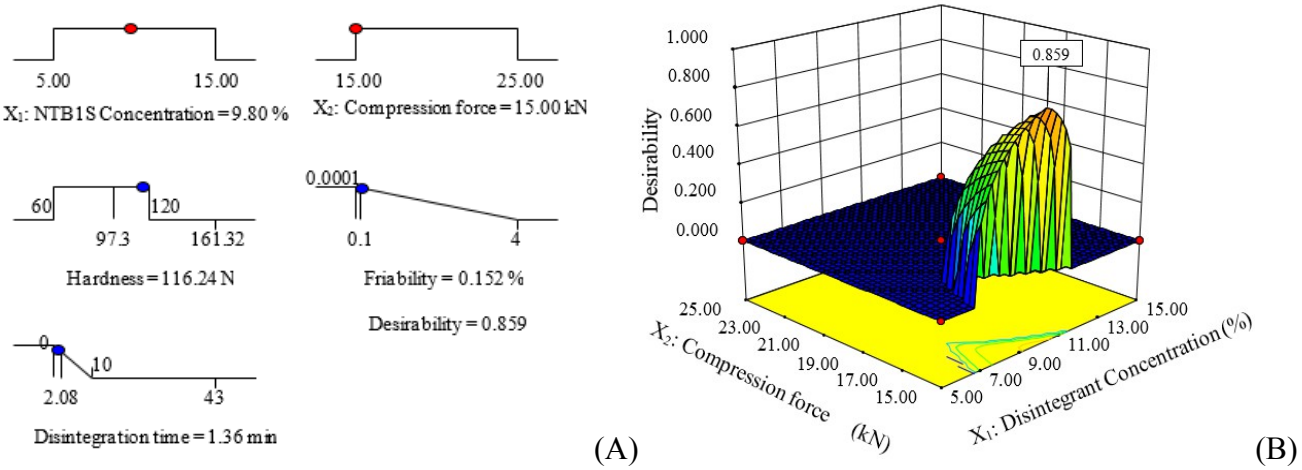

Fig. 3.22. The ramps of optimization (A) and the overall desirability function (B).

As a result, optimum starch concentration is 9.80% while compression force is 15 kN resulting in values of hardness, friability and DT of 116.24 N, 0.152% and 1.36 min, respectively, with desirability 0.859.

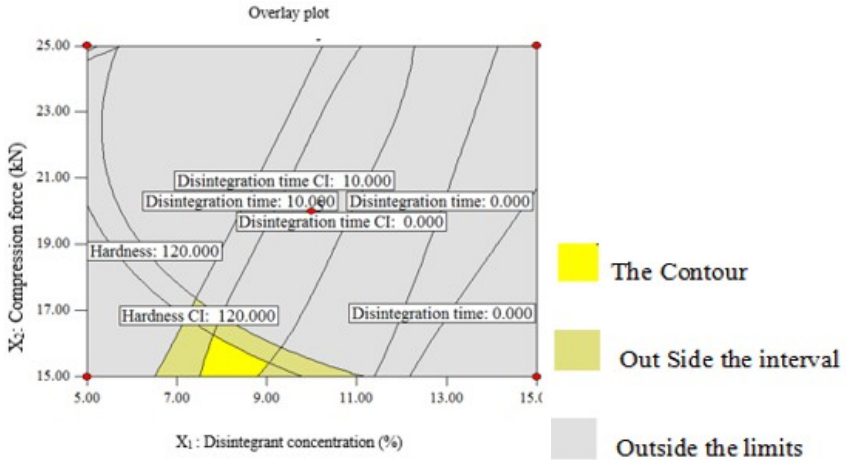

Fig. 3.23. Superimposed contour plots of the responses of the tablets as a function of the factors.

~~As a result the optimum starch concentration is 9.80%, compression force of 15 kN resulting in optimum values of hardness, friability and disintegration time of 116.24 N, 0.152% and 1.36 min, respectively, with desirability 0.859.~~

In order to validate the tool, process and results of optimization, paracetamol tablets were prepared at three points (9% NTB1S versus compression force 19 kN, 10.5% of NTB1S versus compression force of 15.5 kN and 11% of NTB1S versus compression force of 16 kN). All the three response values of the resulting tablets were determined experimentally. Then, relative errors between the predicted and experimental values were computed as shown in Table 3.11.

Table 3.16. Responses of validation formulations.

NTBS1C (%)		9	10.5	11
CF (kN)		19	15.5	16
Hardness (N)	Observed	137.16 ± 5.6	126.4 ± 7.8	122.8 ± 9.2
	Predicted	132.52	121.2	125.7
	Error	-3.50	-4.32	2.31
Friability (%)	Observed	0.206 ± 0.02	0.150 ± 0.01	0.145 ± 0.01
	Predicted	0.198	0.152	0.149
	Error	-4.05	1.22	2.69
DT (Min)	Observed	6.97 ± 0.46	0.756 ± 0.09	0.430 ± 0.6
	Predicted	6.67	0.724	0.414
	Error	-4.51	-4.35	-3.8

The relative errors between the predicted values and the observed values were within ± 5% as per the selected data points. This indicates validity of the tool, process and results of optimization and effectiveness of optimized levels of responses.

3.2.6. Properties of Optimized Paracetamol Tablet Formulations

3.2.6.1. Precompression Properties of the Optimum Tablet Formulations

Flow properties of the granules of the optimized formulations ~~the~~(NTB1S of 9.80%) was determined (Table 3.12).

Table 3.17. Properties of optimized formulation paracetamol tablet granules.

Parameters	NTB1S	Potato starch
Angle of repose (°)	26.37 ± 0.65	28.37 ± 0.65
Flow rate (g/s)	6.59 ± 0.07	5.68 ± 0.10
Bulk density (g/ml)	0.52 ± 0.07	0.55 ± 0.08
Tapped density (g/ml)	0.60 ± 0.01	0.61 ± 0.03
Carr's index (%)	13.32 ± 1.2	9.25 ± 0.91
Hausner ratio	1.17 ± 0.02	0.25 ± 0.02

As it is obvious from the results, the powder/granule mixture exhibited angle of repose < 30 °, Carr's index < 15% and Hausner ratio < 1.25. This indicates that use of 9.80% of NTB1S as disintegrant in paracetamol granules yields a compaction mixture of acceptable flow properties.

3.2.6.2. Evaluation of Optimized Tablets

There are different methods of tablet evaluations stated. Tablet hardness ~~,~~is the most common method of measuring mechanical strength (Swarbrick, 2007). Similarly, friability reveals poor cohesion of tablet ingredients. For tablets to be acceptable, a maximum mean weight loss from three samples of not more than 1% is considered (USP30-NP25, 2007; Puttewar *et al.,* 2010). The tablet properties of the paracetamol tablets prepared with the optimum levels of the factors, *i.e.,* using 9.80% ~~concentration~~ of NTB1S as disintegrant ~~of 9.80%~~ and compression force of 15 kN and those of potato starch, were determined (Table 3.13).

Table 3.18. The properties of the optimized paracetamol tablets, with NTB1S as disintegrant.

	Weight (mg)	**Hardness (N)**	**Friability (%)**	Thickness (mm)	∈ (%)	**DT (Min)**	H/F/D
B1	350.0± 8	112.0 ± 6.0	0.19	4.0	9.1	1.31	475
B2	350.0 ± 4	122.0 ± 7.0	0.13	3.9	7.0	1.35	631
B3	351.0 ± 7	116.0 ± 6.0	0.15	4.0	9.8	1.39	602
μ ± SD	350.0 ± 7	116.7 ± 5.0	0.157 ±0.03	4.0	8.6 ±1.5	1.35	569 ± 83
PV	350.0	116.2	0.152	-	-	1.36	-
ε	0	0.367	3.07	-	-	-0.74	-
B1	349.8 ±11	58.5 ± 6.0	0.96	4.1	10.0	1.20	50.8
B2	351.0 ± 8	50.4 ± 5.8	1.08	4.0	8.1	1.23	45.5
B3	350.5 ± 3	55.4 ± 4.8	1.0	4.0	9.2	1.3	42.8
μ ± SD	350.4 ± 3	54.8 ± 5.6	1.0 ± 0.0	4.0	9.1 ± 0.9	1.24 ± 0.05	46.4 ± 4

*B, H/F/D, ∈, PV, ε stand for batch number, hardness to friability to DT ratio, porosity, predicted value and percent error, respectively.

The tablets ~~of optimum formulations are of~~showed acceptable average hardness (116.7 ± 5 N) for the three batches, *i.e.*, in between 50 N and 150 N, and reasonably agree with the predicted value (116.2 N) (Table 3.13). Similarly, average friability value of the three batches was 0.157 ± 0.03% which is far below 1% sensibly agreeing with the predicted value (0.152) and hence acceptable. The equivalent tablets prepared with the same concentration of potato starch compressed at the same compression force did not show acceptable mechanical strength (54.8 ± 5.6 N hardness and 1.0 % friability). The findings ~~tend to~~ suggest the tablets prepared at the optimum levels of the factors, *i.e.*, 9.8% of disintegrant NTB1S and 15 kN of compression force, maintain better mechanical strength than the report by Adane *et al* (1996a) ~~the cases using~~about the case of Godare starch with corresponding optimum levels ~~of these fa~~of these factors (7% *Godare starch* and 19 kN of compression force) ~~according to Adane *et al* (1996a)~~. This is because, according to Adane *et al* (2006a), the friability values of the three batches of paracetamol tablets had 0.76, 0.96 and 0.87 % which means 0.86 ± 0.1% which is higher than 0.157 ± 0.03% ($p < 0.05$) of NTB1S settings.

Disintegration is an essential quality of oral tablets unless for chewable and some of extended release tablets. Disintegration test fixes the time in which disintegration comes about, apt for the tablets in hand (Flickinger and Drew, 1999). Porosity plays key role on the disintegration property of tablets and its value for the three batches of the optimized paracetamol tablets using NTB1S were found to be 9.101, 6.975 and 9.846%. The mean ~~disintegration time~~DT of the optimum tablets (1.35 ± 0.04 min)

was comparable with predicted value (1.36 min) ($p > 0.05$) and acceptable. The disintegration time of the tablets prepared with the same concentration of potato starch and compression force was about 1.24 ± 0.05 min. As per the results of this study about NTB1S and the report by Adane *et al* (2006a) about Godare starch, ~~I~~if the respective optimum concentrations of the starches and compression forces are used as disintegrant, paracetamol tablets using NTB1S would disintegrate faster (1.35 ± 0.04 min) than Godare starch (3.18 ± 0.13 min in the report) ~~(Adane *et al.*, 2006a)~~. The tablets with NTB1S fulfill the criteria of fast dissolving tablets according to European Pharmacopeia (PhEur, 2005).

It is worth to concurrently study the mechanical properties of tablets together with the DT using the H/Fr/DT ratio which is a good indicator of tablet quality. This is because hardness of tablet is a role of physical nature of granules like hardness and deformation under load, binders and above all the compression force and the hardness per se influences disintegration (Alebiowu and Itiola, 2003; Puttewar *et al.,* 2010). The ratio of hardness to friability to DT correlates DT with hardness and friability hence weighing the cumulative impacts of strength and weakness of tablets simultaneously on the DT. In this regard, it qualifies the tablet better than either each of hardness and friability or the hardness to friability ratio experiences. The average H/Fr/DT of the optimum formulations was higher (569 ± 83 $NMin^{-1}\%^{-1}$) than that of the tablets in which the potato starch was used (46.4 ± 4 $NMin^{-1}\%^{-1}$) and it indicates better balance between binding and disintegration for the tablets formulated (Alebiowu and Adeagbo, 2009; Adedokun and Itiola, 2011).

3.2.6.3. Calibration Curve and Dissolution Test

Dissolution rate is the absorption rate limiting step in many cases (Swarbrick, 2007) and hence potentially correlated with bioavailability. In such cases, it is more resonant quality attribute than disintegration (USP30-NP25, 2007). For determination of the dissolution rate of the optimum formulation in this study, the absorbance versus concentration plot fitting eq. 3.6 was obtained (Fig. 3.22), in phosphate buffer (pH = 5.8). Its correlation coefficient (R^2) is ~~=~~ 0.999 (USP 30 / NF 25, 2007). The percent drug dissolved versus time curve (Fig. 3.23), based on the calibration curve, was created for the optimum tablets in 3 batches.

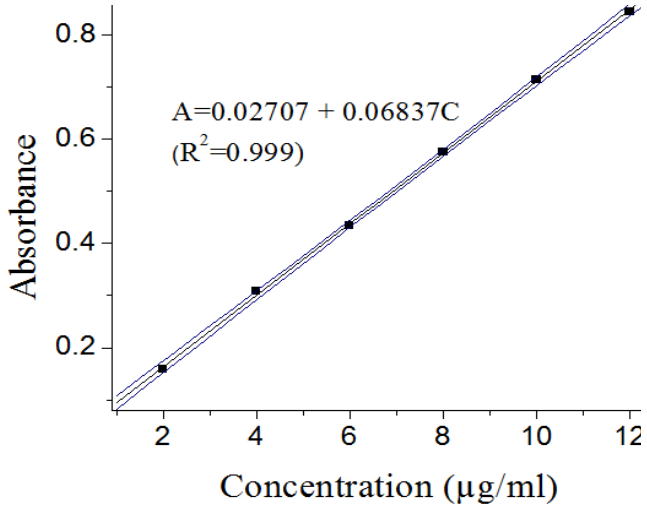

Fig. 3.24. Calibration curve of paracetamol with phosphate buffer (pH = 5.8) at 243 nm.

$$A = 0.02707 + 0.0683C \qquad \text{eq. 3.6}$$

Where A is the absorbance and C is the concentration in µg/ml

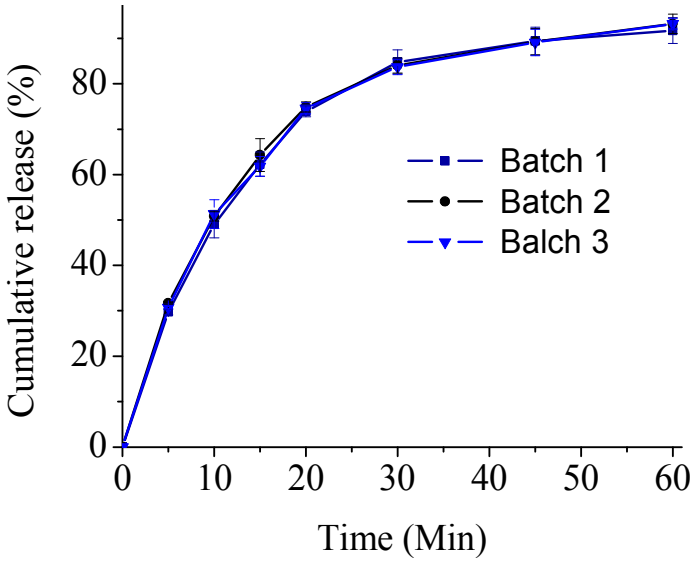

Fig. 3.25. The dissolution profile of optimized paracetamol tablets.

All the three batches of paracetamol tablets of optimum formulations released more than 80% within 30 min in phosphate buffer at 37 °C. This indicates that paracetamol tablets prepared by using native NTB1S release their content and are acceptable (USP 30 / NF 25, 2007).

3.3. Direct Compression Properties of Pregelatinized TB1S

Preliminary study showed that the flow and compressibility profiles of NTB1S are better when a 15% (w/v) suspension of NTB1S in water was used for pre/gelatinization. Hence for this study, 15% (w/v) of NTB1S was consistently used for pre/gelatinization. The appropriate ranges of temperature and time of pre/gelatinization were also selected based on literature and preliminary studies.

3.3.1. Densities and Flow Properties

Density values are related to total, inter-particle and intra-particle porosities which in turn indicate properties of excipients like tablet disintegrating potential –(Swarbrick, 2007). The bulk, tapped and true densities of PGTB1S are presented in Table 3.14.

Table 3.19. Bulk, tapped and true densities of the 13 pregelatinized starches (in standard order).

	Temperature (ºC)	**Time (min)**	Bulk density	Tapped density	True density
1	65	20	0.6233 ± 0.05	0.751 ±0.02	1.52000 ± 0.12
2	85	20	0.6767 ± 0.01	0.794 ± 0.01	1.44540 ± 0.01
3	65	60	0.6867 ± 0.02	0.844 ± 0.01	1.49817 ± 0.08
4	85	60	0.6667 ± 0.03	0.827 ± 0.02	1.43870 ± 0.02
5	61	40	0.5100 ± 0.01	0.657 ± 0.01	1.55000 ± 0.02
6	89	40	0.6633 ± 0.01	0.810 ± 0.01	1.43030 ± 0.25
7	75	12	0.6867 ± 0.03	0.776 ± 0.01	1.44763 ± 0.08

8	75	68	0.6967 ± 0.04	0.830 ± 0.00	1.44880 ± 0.07
9	75	40	0.6833 ± 0.02	0.833 ± 0.01	1.47811 ± 0.10
10	75	40	0.7033 ± 0.02	0.858 ± 0.01	1.47100 ± 0.07
11	75	40	0.7000 ± 0.02	0.838 ± 0.01	1.48746 ± 0.03
12	75	40	0.6600 ± 0.00	0.800 ± 0.01	1.46030 ± 0.02
13	75	40	0.6600 ± 0.01	0.790 ± 0.01	1.45939 ± 0.07

Pre/gelatinization at all the 13 levels of temperature versus time increased bulk and tapped densities but decreased true density. The most probable reason for decrease in true density is hydrothermal disruption of the granules through break-up of hydrogen bonds loosening the closely packed molecules leading to diffusion of amylose molecules out of granules (Belitz *et al.,* 2009). These effects were highest at 89 ºC for 40 min and lowest at 61 ºC for 40 min.

For acceptable weight (content) uniformity of tablets, powder mixture should have better fluidity as poor flow badly affects scale up and scale down of unit operations (Chaudhuri *et al.,* 2006). Carr's index and Hausner ratio (Kojima and Eliott, 2012), flow rate, direct observation and angle of repose are used to characterize powder flowability. Since no single powder flow method can satisfactorily or completely characterize the wide range of flow properties practiced in the industry, in this study, flow rate, angle of repose, Hausner's ratio, and Carr's indices of the powders were investigated. The results of the experimental values of these parameters at 13 different design points are shown in Table 3.15.

Table 3.20. Flow properties of the 13 pregelatinized starches (in standard order).

	Temperature (ºC)	**Time (min)**	**Carr's index (%)**	Hausner ratio	**Angle of repose (º)**	Flow rate (gm/s)
1	65	20	17.0 ± 2.2	1.20 ± 0.08	**30.8 ± 1.5**	0.00 ± 0.00
2	85	20	14.8 ± 0.2	1.17 ± 0.01	18.9 ± 1.6	5.81 ± 0.10
3	65	60	18.6 ± 1.0	1.23 ± 0.02	24.6 ± 1.4	2.50 ± 0.31
4	85	60	18.1 ± 2.2	1.22 ± 0.08	15.6 ± 0.8	4.82 ± 0.92
5	61	40	22.3 ± 1.0	1.29 ± 0.03	**33.0 ± 0.5**	0.00 ± 0.00
6	89	40	18.1 ± 1.7	1.22 ± 0.01	16.1 ± 3.5	6.06 ± 0.52
7	75	12	11.5 ± 1.2	1.13 ± 0.06	21.2 ± 1.5	5.67 ± 0.84
8	75	68	16.1 ± 0.7	1.19 ± 0.05	17.5 ± 1.6	5.48 ± 0.73
9	75	40	18.0 ± 2.0	1.22 ± 0.02	20.7 ± 0.4	5.58 ± 0.69
10	75	40	18.0 ± 2.4	1.22 ± 0.03	21.6 ± 0.8	5.65 ± 0.98
11	75	40	16.5 ± 2.8	1.20 ± 0.04	20.9 ± 0.9	6.08 ± 0.75
12	75	40	17.5 ± 1.0	1.21 ± 0.02	21.0 ± 0.4	6.06 ± 0.55
13	75	40	16.5 ± 0.6	1.20 ± 0.02	21.8 ± 0.0	6.39 ± 0.71

At all the temperature and time levels of heating, Hausner ratios and Carr's indices of the starch were decreased. Lower Hausner ratio indicates that there are lower interparticular interactions. The lower

value of Carr's index indicates that the powder volume reduces to a lesser extent during compression. Low value of both Carr's index and Hausner ratio is the sign of good flow property. Besides, the pre/gelatinization also changed the angles of repose and flow rates of the NTB1S. Generally, except for the modifications at 61 ºC for 40 min and 65 ºC for 20 min, the modification improved the flow property of the starch which is consistent with published literature elsewhere (Odeku and Picker-Freyer, 2010).

3.3.2. Compressibility: Kawakita and Heckel Plots

The higher compressible the powder particles are the closer the particles to each other generating more contact points and resulting in higher number of bonding and stronger compacts (Santl *et al.,* 2011; ElShaer *et al.,* 2013). In other words, compressibility implies compactibility which per se leads to tabletability. Accordingly, compressibility levels of the pre/gelatinized starches were tested by applied tapping - densification and applied pressure - densification relationships using Kawakita and Heckel models, respectively. Since the Kawakita and Heckel plots exhibit linearity at low and high pressures, respectively, both of these models were used combined expecting more comprehensive information than using either one alone (Bakre and Ayodele, 2013). The slopes and related properties of Kawakita plots are used to draw measurable information regarding powder compressibility. This is because the inverse of constant 'a' of Kawakita plot is equal to minimum porosity of the material before compression and constant 'b' which is called coefficient of compression is related to the plasticity of the material (Bakre and Ayodele, 2013). Kawakita plots of the 13 powder samples were constructed and superimposed as shown in Fig. 3.24 for comparison.

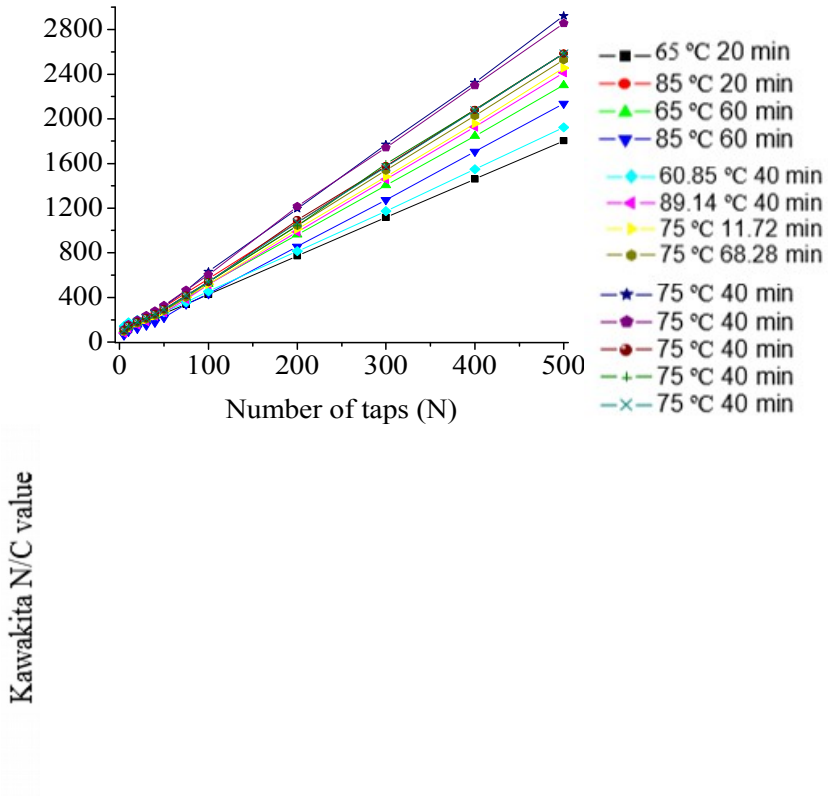

Fig. 3.26. Kawakita plots of NTB1S pregelatinized at different conditions

In order to derive the aforementioned information from the plots regarding the compressibility behaviors of the sample powders between the bulk and tapped density states, Kawakita constants 'a' and '1/b' were calculated and described in Table 3.16.

Table 3.21. Kawakita parameters of different pregelatinized at different conditions

Standard Order	**Temperature °C)**	**Time (min)**	**a**	**1/b**	**R^2**
1	65	20	0.2901	23.7	0.9999
2	85	20	0.1982	12.5	0.9999
3	65	60	0.2261	18.1	0.9998
4	85	60	0.2382	6.0	0.9998
5	61	40	0.2780	29.9	0.9996
6	89	40	0.2124	10.1	0.9999
7	75	12	0.2101	12.6	0.9999
8	75	68	0.2028	11.3	0.9998
9	75	40	0.1757	10.7	0.9998

10	75	40	0.1796	12.9	0.9998
11	75	40	0.1986	12.7	0.9997
12	75	40	0.1977	11.0	0.9997
13	75	40	0.1987	12.1	0.9998

The highest value of Kawakita compressibility (a = 0.2901), showing highest compressibility, was observed for the modification at 65 ºC for 20 min. The explanation is that the powder at this point attained highest volume reduction before compression, *i.e.*, the most fluidy than the others. The next point was at 61 ºC for 40 min. This is clearly observed from the steepness of respective plot in Fig. 3.24. On the other hand, the lowest values for Kawakita cohesiveness (1/b = 6.0) was observed for the modification at 85 ºC for 60 min. The interpretation is that half the maximum degree of volume reduction by tapping was attained with the first 6 taps implying that it is the least cohesive powder. Conversely, the powder at 61 ºC for 40 min was observed to be the most cohesive (1/b = 29.9) which corresponds to the least coefficient of compression (Swarbrick, 2007; Bakre and Ayodele, 2013; Widodo and Hassan, 2015).

In order to construct Heckel plots, NTB1S modified at the 13 experimental design points were compressed at compression pressures in the range 38.22 - 305.58 MPa corresponding to 3 - 24 kN of compression forces. Since the design space of the present study encompasses data points (65 ºC for 20 min, 65 ºC for 60 min and 60.85 ºC for 40 min) where the powder samples are poor in flow, careful manual weighing and filling was used at these points. There was no significant difference in weight variations in between the tablets of these points and the rest compressed automatically. Fig. 3.25 shows Heckel plots of the modified powders.

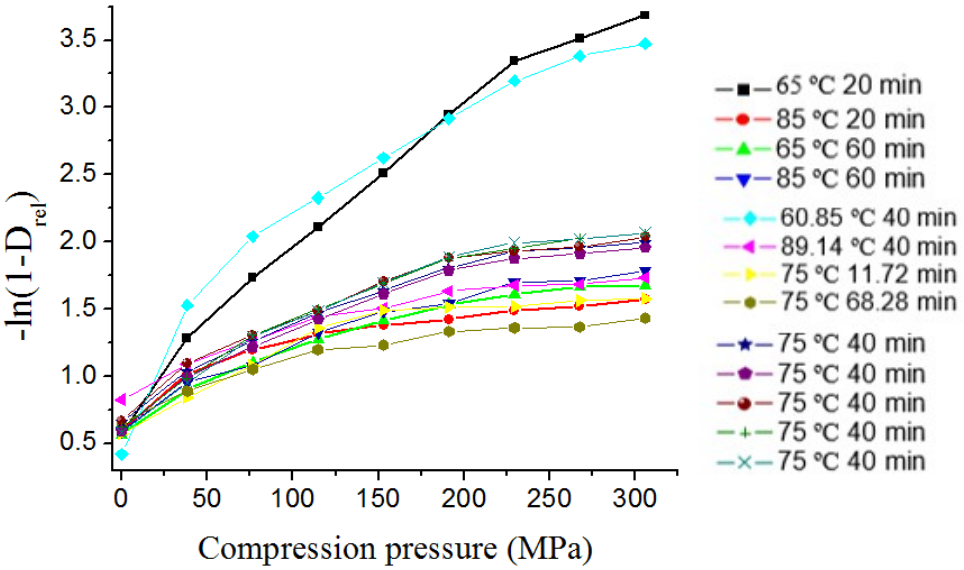

Fig. 3.27. Heckel plots of NTB1S pregelatinized at different conditions.

As it is visible on the diagram, all the plots start with non-linear portions notifying that the initial densification is dominantly due to rearrangement. The reason for the non-linearity in the early region is that the powder particles behave individually than as a coherent mass following the absence of inter particular bonding. The next segment for all of the plots is linear suggesting that it is a region of plastic deformation. In other words, ~~i.e.,~~ all the 13 powder samples have a region where dominant mechanism of densification is plastic deformation. The straight lines are followed by a second non-linear phase where ~~. These are the 3 regions where d~~the dominant mechanism~~s~~ of densification is ~~are rearrangement, plastic deformation and~~ elastic deformation~~, respectively~~. The relevant parameters of the initial non-linear and linear regions including spans of pressure are described in Table 3.17. The plots of powders of design points 68 ºC for 40 min and 85 ºC for 60 min were observed to have ups and downs. This is a sign of brittle fracture as a mechanism of deformation explained by ~~the~~ secondary rearrangement phases of particles~~.~~ (Mitrevej *et al.* 1996; Kelevan *et al.* 2009). The changes can be attributable to annealing effect of the starch at the point 68 ºC for 40 min and full gelatinization in the case of that at 85 ºC for 60 min. ~~because a~~Annealing occurs at temperatures below gelatinization temperature and it improves crystallinity which is associated with higher brittleness (Shirestha and Halley, 2014).

Table 3.22. Heckel parameters of NTB1S pregelatinized at different conditions.

Temperature (ºC)	**Time (min)**	Initial non-linear region (MPa)	Linear region		
			Range (MPa)	Length (MPa)	R^2
65	20	0-76.43	76.43-229.30	152.87	0.9997
85	20	0-38.22	38.22-114.65	76.43	0.9925
65	60	0-76.43	76.43-191.08	114.65	0.9962
85	60	0-76.43	76.43-152.87	76.44	0.9905
61	40	0-76.43	76.43-229.30	152.87	0.9999
89	40	0-76.43	76.43-152.87	76.44	0.9988
75	12	0-38.22	38.22-152.87	114.65	0.9910
75	68	0-38.22	38.22-114.65	76.43	0.9994
75	40	0-76.43	76.43-191.08	114.65	0.9984
75	40	0-76.43	76.43-191.08	114.65	0.9995
75	40	0-76.43	76.43-191.08	114.65	0.9990

75	40	0-76.43	76.43-191.08	114.65	0.9999
75	40	0-76.43	76.43-191.08	114.65	0.9999

The results indicate that the starch modified at 85 ºC for 20 min, 75 ºC for 12 min and 75 ºC for 68 min attain maximum densification accountable to rearrangement (relative density D_b) within 0-38.22 MPa span of compression pressure. At 38.22 MPa onwards, the particles of these powders start to deform and possibly form bonding. All the rest of points including 5 replica at 75 ºC for 40 min start particulate deformation beyond this pressure, observed at the point 76.43 MPa onwards. Likewise, plastic deformation of the powder extends highest (229.30 MPa) for the modification at 65 ºC for 20 min and 61 ºC for 20 min followed by all the 5 central replica (191.08 MPa). The maximum pressure for the plastic deformation was least (114.65 MPa) for the starches modified at 85 ºC for 20 min and 75 ºC for 68 min followed by 85 ºC for 60 min, 89 ºC for 40 min and 75 ºC for 12 min which are plastic up to 152.87 MPa. The largest region (152.87 MPa) of plastic deformation was observed at 65 ºC for 20 min and 61 ºC for 40 min.

The quantitative information on ~~the~~ influence of pressure on the powder is related to slope~~s~~ (k) and the extrapolated intercept~~s~~ (A) of the linear segment. With this consideration, the plastic volume reduction per applied pressure was determined from the mean yield pressure (P_y) which equals the inverse of slope (1/k) of linear portions. The constant 'A' is believed to be related to particle rearrangement and die filling just before deformation and the bonding of discrete particles. It was used to calculate the total densification hitherto (D_A). The phase of densification at low pressure (D_b) was calculated from the values of the D_A and the value of densification due to die filling (D_0) (Table 3.18).

Table 3.23. The yield pressure and different phases of densification of powders.

Temperature (ºC)	**Time (min)**	**A_0**	**P_y**	A	**D_A**	**D_0**	**D_b**
65	20	0.5725	94.34	0.9086	0.5969	0.4359	0.1610
85	20	0.5944	256.41	0.8750	0.5831	0.4481	0.1350
65	60	0.5654	277.78	0.8682	0.5803	0.4319	0.1484
85	60	0.5891	188.68	0.6842	0.4955	0.4452	0.0503
61	40	0.4190	131.58	1.4600	0.7678	0.3423	0.4255
89	40	0.8259	238.10	0.8486	0.5720	0.5622	0.0098
75	12	0.5751	172.41	0.6330	0.4690	0.4374	0.0317
75	68	0.6485	243.90	0.7346	0.5203	0.4772	0.0431
75	40	0.6563	212.77	0.9109	0.5978	0.4812	0.1166
75	40	0.5942	200.00	0.8477	0.5716	0.4480	0.1236
75	40	0.6658	196.08	0.9129	0.5986	0.4861	0.1125
75	40	0.6190	200.00	0.9258	0.6038	0.4615	0.1423

75	40	0.5798	192.31	0.8891	0.5890	0.4400	0.1490

Accordingly, the modification at 65 ºC for 20 min had the smallest yield pressure (P_y = 94.34 MPa) indicating an onset of plastic deformation at lowest pressure, *i.e.*, modification at this point results in the most compressible powder. This can possibly explain that low temperature has not yet significantly changed the native nature of the starch which has fine enough particles to be compressible (Swarbrick, 2007; Abdel-Hamid *et al.,* 2011). The second most compressible powder was observed at 61 ºC for 40 min (131.58 MPa). On the other hand, the least compressible powder (P_y = 277.78 MPa) was observed at 65:00 ºC for 60 min followed by 256.41 MPa at 85:00 ºC for 20 min.

The constant A is related to the particle rearrangement and die filling before deformation (Widodo and Hassan, 2015). According to the results, the powder at 61 ºC for 40 min showed highest value for A (1.4600) the least being 0.6330 observed at 75 ºC for 12 min. The corresponding relative density (D_A) values were observed to be 0.7678 and 0.4690 implying the powders to be the most and the least compressible, respectively. The phase of densification at low pressure (D_b) was also used to show further densification due to particle rearrangement/fragmentation. In this regard, the powder at 61 ºC for 40 min showed the largest D_b (0.4255) due to rearrangement/fragmentation phase, the least (D_b = 0.0098) being observed at 89 ºC for 40 min. The next largest was at the point 60 ºC for 20 min.

Both the Kawakita and Heckel plots agree that the starch modified at 65 ºC for 20 min and 61 ºC for 40 min attain the maximum volume reduction before compression (plasticity), with exertion of the least load compared to the other samples. On the other hand, while Kawakita model claims the sample at 61 ºC for 40 min is the most difficult to attain its maximum volume reduction before compression, Heckel plot implies this powder attains the largest densification before particulate deformation and the second most compressible next to 65 ºC for 20 min.

3.3.3. Compactibilities

Tablet hardness is the most common method of measuring mechanical strength of compacts ~~, in order~~ to compare compactibility of the powder samples. Friability ~~measures~~ reveals poor cohesion of tablet ingredients and supplements hardness test (Swarbrick, 2007; Puttewar, *et al.*, 2010). In order to investigate and compare the influence of temperature and time on these properties of ~~the~~ compacts~~powder samples~~, the powder ~~sampless~~ were compressed at the pressure 152.80 MPa where the densification of most of the samples was observed to be plastic (Section 3.3.2). Table 3.19 shows the hardness and friability values of the compacts.

Table 3.24. Hardness and friability of the compacts of compacts of the PGTB1S.

Standard order	**Temperature (ºC)**	**Time (min)**	**Hardness (N)**	Friability
1	65	20	145.3 ± 7	0.2 ± 0.0
2	85	20	32.7 ± 4	Friable
3	65	60	48.3 ± 3	Friable
4	85	60	0.0 ± 0	Friable
5	60	40	17.0 ± 2	Friable
6	89	40	24.4 ± 2	Friable
7	75	12	59.4 ± 5	0.6 ± 0.0
8	75	68	0.0 ± 0	Friable
9	75	40	70.6 ± 5	0.6 ± 0.0
10	75	40	73.0 ± 5	0.5 ± 0.0
11	75	40	78.6 ± 6	0.4 ± 0.0
12	75	40	77.0 ± 7	0.6 ± 0.0
13	75	40	86.2 ± 6	0.5 ± 0.0

The highest value of hardness was observed at 65 ºC for 20 min followed by the central replica. The modifications at 75 ºC for 12 min, 65 ºC for 20 min and 75 ºC for 40 min had friability < 1%. The weakest tablets (hardness = 0 N and friable) were observed at 85 for 60 min and 75 ºC for 68 min.

3.3.4. Mathematical Model

Adequate flow, compressibility/compactibility are vital for a direct compression diluent. To select the point of NTB1S pre/gelatinization where the powder optimally best satisfies these requirements, further knowledge on the influences of temperature and time of pre/gelatinization on flow, compressibility and compactibility profiles of the NTB1S w~~er~~as~~e~~ critical. To this end, Central composite design~~,~~ (CCD)~~,~~, a very efficient design tool for fitting second order models, was used. For easier computation, ~~the~~ average values of the responses consisting of angle of repose, Hausner ratio, ~~tablet hardness,~~ Kawakita compressibility (a) ~~and,~~ yield pressure (inverse of Heckel number) and tablet hardness of the 13 design points were entered into the Design Expert Software. Subsequently, linear, two factor interaction (2FI), quadratic and cubic models were compared in terms of R^2, adjusted R^2 and predicted R^2 and predicted residual sum of square (PRESS) values for each of the responses (Table 3.20) computed using the software.

Table 3.25. Model fit summary of responses of pre/gelatinization of starch.

Response	Source	R^2	Adjusted R^2	Predicted R^2	PRESS	Remark
Angle of repose	Linear	0.8821	0.8586	0.7491	79.0650	
	2FI	0.8888	0.8517	0.7274	85.9168	
	Quadratic	0.9846	0.9736	0.9064	29.5147	Suggested
	Cubic	0.9954	0.9890	0.8836	36.6862	Aliased
Hausner ratio	Linear	0.3355	0.2026	-0.4387	0.0215	
	2FI	0.3450	0.1267	-0.4650	0.0219	
	Quadratic	0.9458	0.9071	0.7634	0.0035	Suggested
	Cubic	0.9731	0.9354	0.9507	0.0007	Aliased
Kawakita compressibility	Linear	0.2698	0.1237	-0.3346	0.0192	
	2FI	0.4580	0.2774	-0.3926	0.02	
	Quadratic	0.9392	0.8958	0.7699	0.0033	Suggested
	Cubic	0.9423	0.8615	-0.419	0.0204	Aliased
Mean yield pressure	Linear	0.4167	0.3001	-0.2795	38151.38	
	2FI	0.9406	0.9208	0.8241	5245.148	Suggested
	Quadratic	0.9610	0.9332	0.7658	6983.062	
	Cubic	0.9890	0.9736	0.7799	6563.805	Aliased
Hardness	Linear	0.7454	0.6945	0.5045	91.1771	
	2FI	0.7460	0.6613	0.4161	107.4565	
	Quadratic	0.9949	0.9913	0.9778	4.0906	Suggested
	Cubic	0.9966	0.9919	0.9380	11.4010	Aliased

As per the fit summary results, all the responses best satisfy the quadratic polynomial model except yield pressure in which case 2FI satisfies the best fit. This is because these respective models have least PRESS values (29.5147, 0.0035, 0.0033, 5245.148 and 4.0906), largest R^2 values (0.9846, 0.9458, 0.9392, 0.9406 and 0.9949), adjusted R^2 values (0.9736, 0.9071, 0.8958, 0.9208 and 0.9933) closest to 1 and predicted R^2 values (0.9063, 0.7634, 0.7699, 0.8241, and 0.9778) in most reasonable agreement with the adjusted R^2 of all otherwise aliased models –(Lewis *et al.,* 1999; Huang *et al.,* 2005). Validity of these models was verified by ANOVA at 95% CI (Table 3.21).

Table 3.26. Summary of ANOVA results for responses from CCD for pregelatinization of starch.

Source		Sum of Squares	df	Mean square	F-value	p-value Prob > F
Inverse of angle of repose	Model	310.31030	5	62.06206	89.52326	< 0.0001*
	X_1	250.88230	1	250.88230	361.89260	< 0.0001*
	X_2	27.13120	1	27.13115	39.13613	0.0004*
	X_1^2	22.69590	1	22.69592	32.73841	0.0007*
	X_2^2	4.38288	1	4.38288	6.32221	0.0401*
	Lack of Fit	3.95276	3	1.31759	5.85593	0.0604**

Hausner ratio	Model	0.01412	5	0.002823	24.43765	0.0003*
	X_1	0.00231	1	0.002310	19.99642	0.0029*
	X_2	0.00270	1	0.002696	23.34169	0.0019*
	X_1^2	0.00359	1	0.003588	31.05750	0.0008*
	X_2^2	0.00421	1	0.004212	36.46342	0.0005*
	Lack of Fit	0.00041	3	0.000136	1.36212	0.3742**
Kawakita compressibility	Model	0.01349	5	0.002698	21.63145	0.0004*
	X_1	0.00377	1	0.003727	29.88516	0.0009*
	X_1 X_2	0.00270	1	0.002704	21.68100	0.0023*
	X_1^2	0.00654	1	0.006536	52.40361	0.0002*
	Lack of Fit	0.00035	3	0.000117	0.89148	0.5183**
Yield pressure	Model	28046.740	3	9348.913	47.49110	< 0.0001*
	X_1	6040.736	1	6040.736	30.68605	0.0004*
	X_2	6385.836	1	6385.836	32.43911	0.0003*
	X_1 X_2	15620.170	1	15620.170	79.34816	< 0.0001*
	Lack of Fit	1540.970	5	308.194	5.342828	0.0648**
Square root of Hardness	Model	183.08730	5	36.61746	275.4957	< 0.0001*
	X_1	78.20693	1	78.20693	588.3989	< 0.0001*
	X_2	58.96907	1	58.96907	443.6606	< 0.0001*
	X_2^2	44.61150	1	44.61150	335.6398	< 0.0001*
	Lack of Fit	0.47523	3	0.158408	1.392056	0.3671**

Where, X_1 and X_2 stand for temperature and time respectively.*Significant **Not significant

The model significance tests ($p < 0.05$) and lack of fit tests ($p > 0.05$) show errors are insignificant. Moreover, the adequate precision values, 36.86, 20.032, 12.564, 23.306 and 54.469 of angle of repose, Hausner ratio, Kawakita compressibility, yield pressure and hardness, respectively, show the signals are adequate and the respective models are quite valid.

Furthermore, the validity of the models was checked by normal probability plot of residuals versus predicted values which reasonably approximated the normal plot of predicted values line (Fig. 3.26).

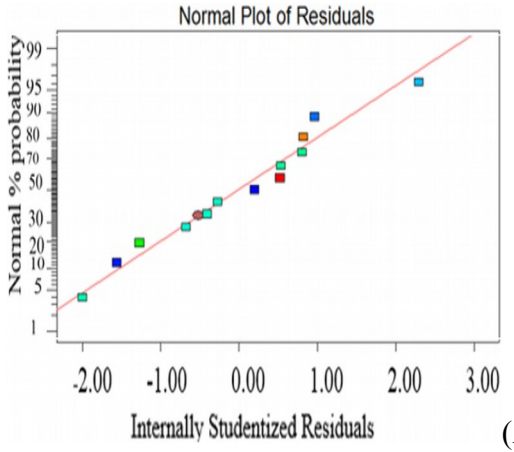

(A)

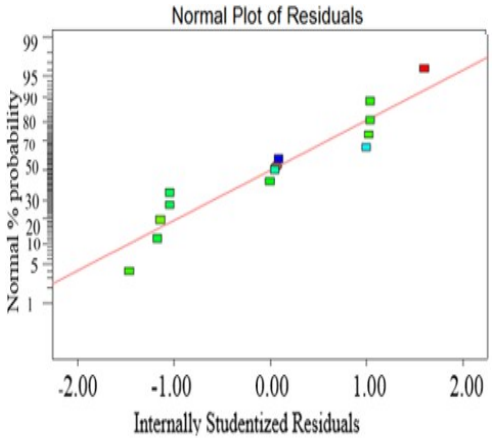

(B)

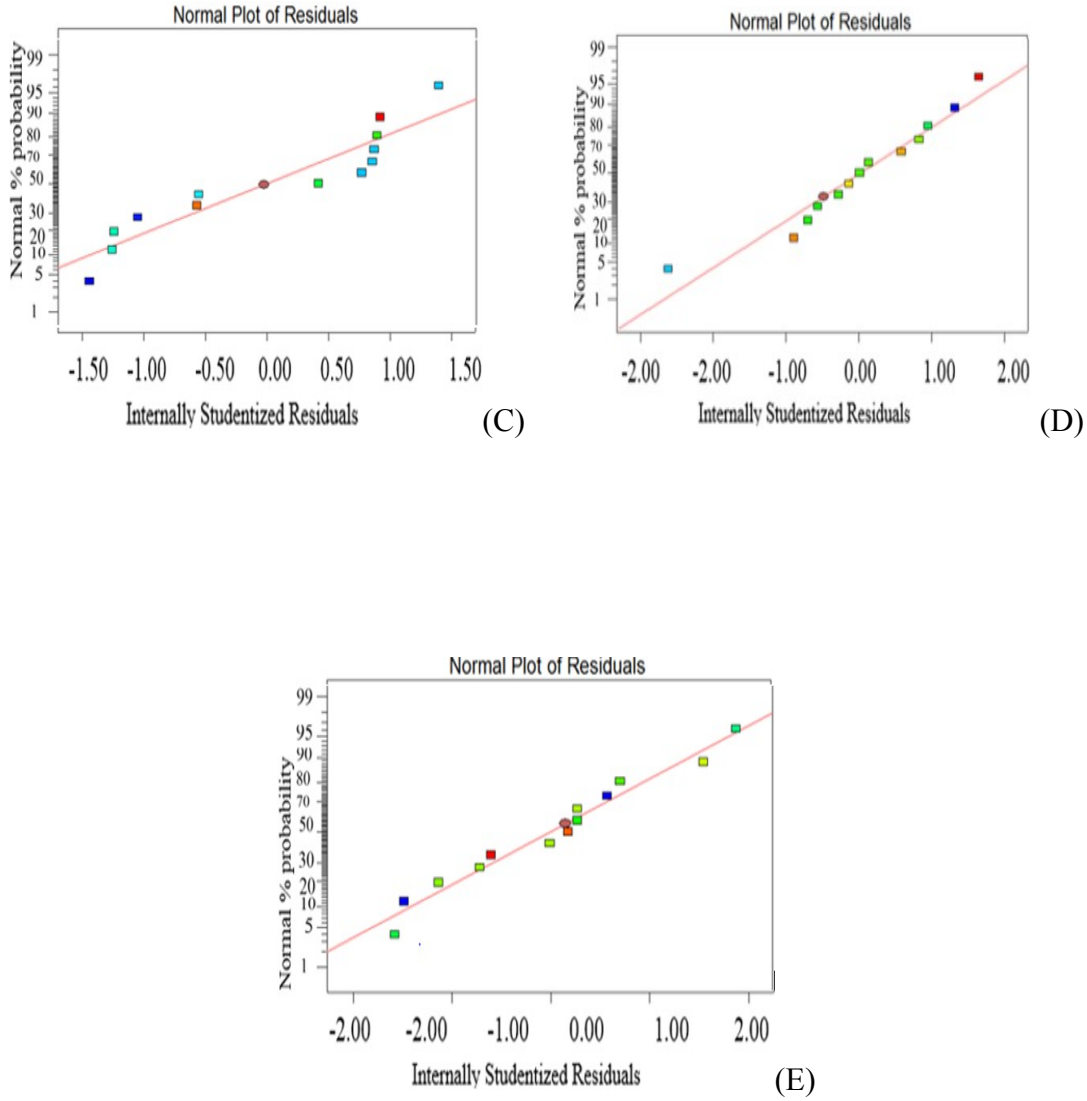

Fig. 3.28. Normal probability plot of residuals for the study responses of A. angle of repose, B. Hausner ratio, C. Kawakita compressibility index, D. Yield pressure and E. hardness for pregelatinized starch.

Secondly, internally studentized residuals which are randomly scattered less than 3 units away from zero (Fig. 3.27) further verified the validity of the models (Lewis *et al.,* 1999).

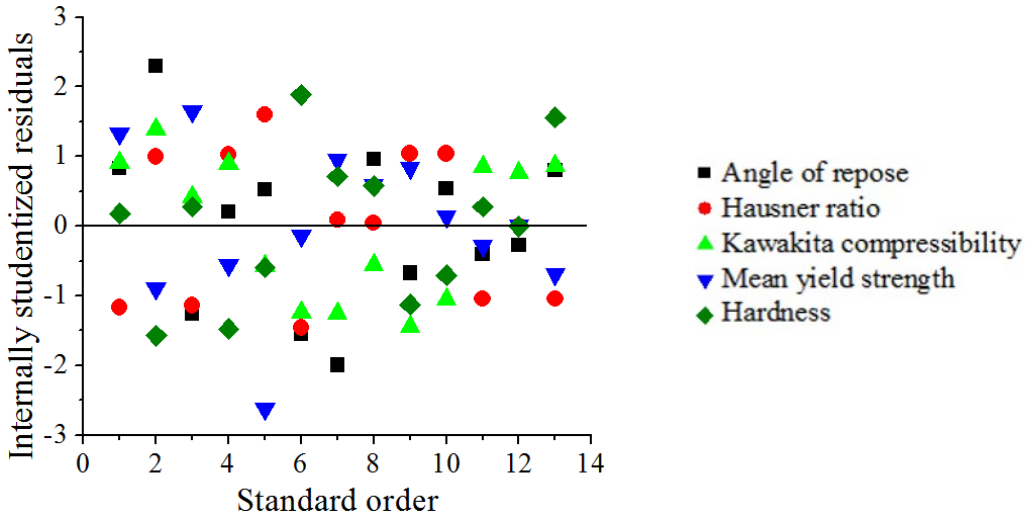

Fig. 3.29. Plot of internally studentized residuals at each of design points.

Thus, the selected models are adequate enough to reveal the relationships existing between the variables within 95% CI and used to explain the types and trends of influences (Lewis *et al.,* 1999).

3.3.5. Factor - Response Relationships

Having selected the models of best fits with statistically valid adequacy, equivalent mathematical equations were generated in order to summarize the trends of levels of angle of repose, Hausner ratio, Kawakita compressibility, mean yield pressure and Hardness with changing levels of temperature and time of pre/gelatinization. Moreover, the response surface and contour plots of these responses were constructed. Using these mathematical and diagrammatic approaches, the individual and interaction effects of the factors on the responses were revealed. With this concern, eq. 3.7 and Fig. 3.28 show trend of angle of repose of pre/gelatinized NTB1S with varying levels of temperature and time.

$$\frac{1}{\text{Angle of repose}} = 0.047 + 0.011X_1 + 0.004185X_2 - 0.002072{X_2}^2 \qquad \text{eq. 3.7}$$

Where; X_1, X_2 and values of temperature and time, respectively

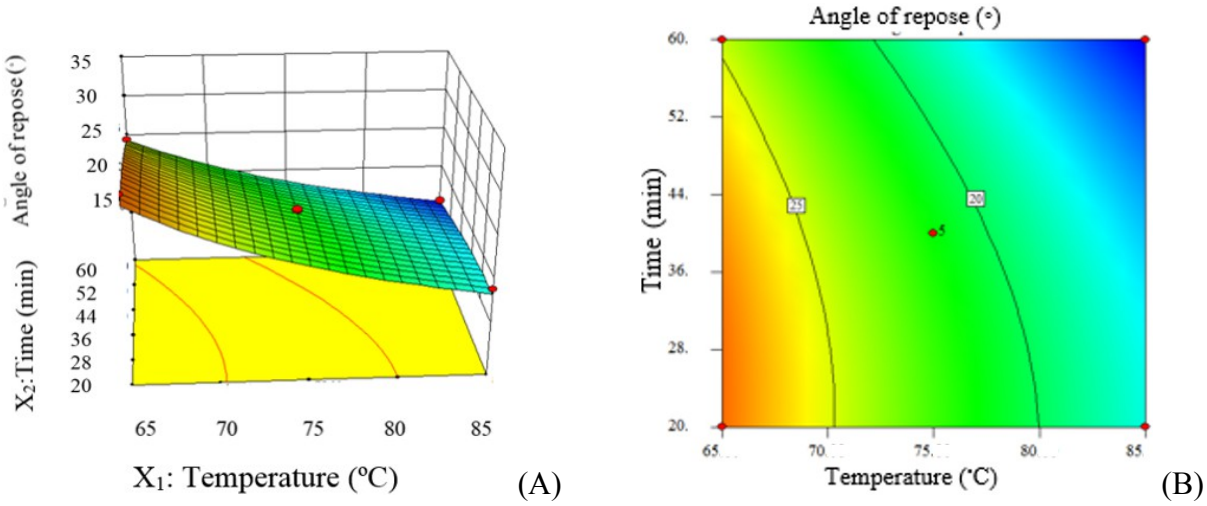

Fig. 3.30. Surface response (A) and contour plot (B) of angle of repose versus the factors.

Obviously, increase in both temperature and time increases the inverse of angle of repose ($p < 0.0001$) indicating it improves flow property suppported by published report elsewhere about effect of the modification by Adedokun and Itiola (2011). Increase in time of pre/gelatinization also increases inverse of angle of repose ($p = 0.0004$) which means it enhances flow property which can possibly be explained by extension of temperature effect. Heating time has negative (convex) quadratic effect on the angle of repose ($p = 0.0401$).

The influence of temperature and time of pre/gelatinization on the Hausner ratio is depicted in eq. 3.8 and Fig. 3.29, mathematically and diagrammatically, respectively.

$$\text{Hausner ratio} = 1.21 - 0.017X_1 + 0.018X_2 + 0.023X_1^2 - 0.025X \quad \text{eq. 3.8}$$

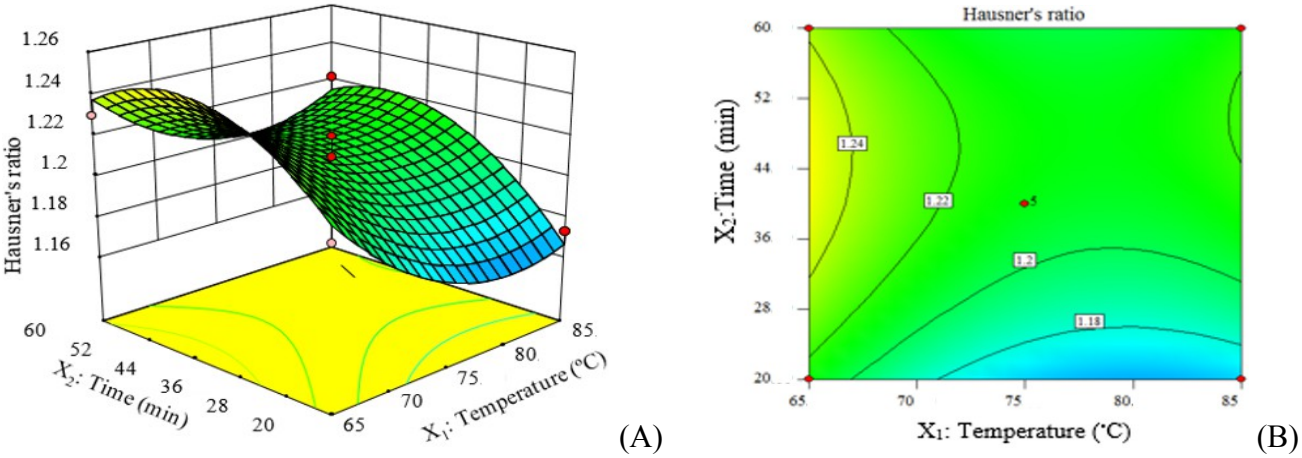

Fig. 3.31. Surface response (A) and contour plot (B) of Hausner ratio versus the factors.

The illustrations show that increase in temperature decreases Hausner ratio as indicated by sign of the term X_1 in the eq. 3.8. Increase in time of pre/gelatinization increases the Hausner ratio evidenced by the signs of the term X_2. Positive and negative quadratic effects, with coefficients of 0.023 ($p = 0.0008$) and -0.025 ($p = 0.0005$) of temperature and time of pre/gelatinization on the Hausner ratio were also observed, respectively.

Similarly, eq. 3.9 and Fig. 3.30 show the trend of Kawakita compressibility (a) with changing levels of temperature and time of pre/gelatinization.

$$a = 0.19 - 0.022X_1 + 0.026X_1X_2 + 0.031X_1^2 \qquad \text{eq. 3.9}$$

Where a represents Kawakita compressibility constant

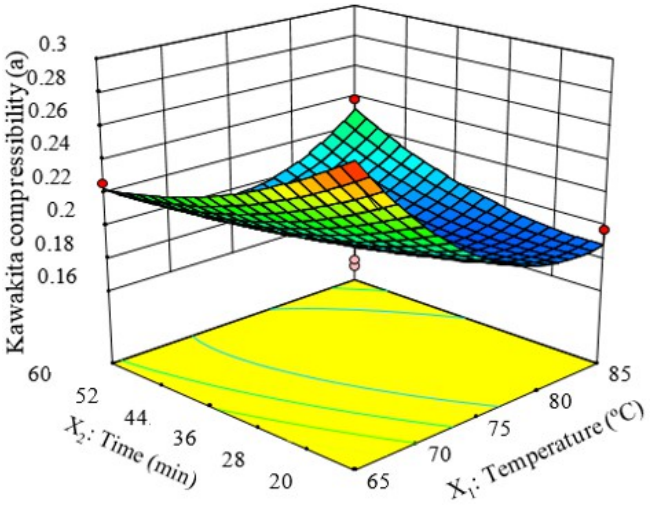

(A)

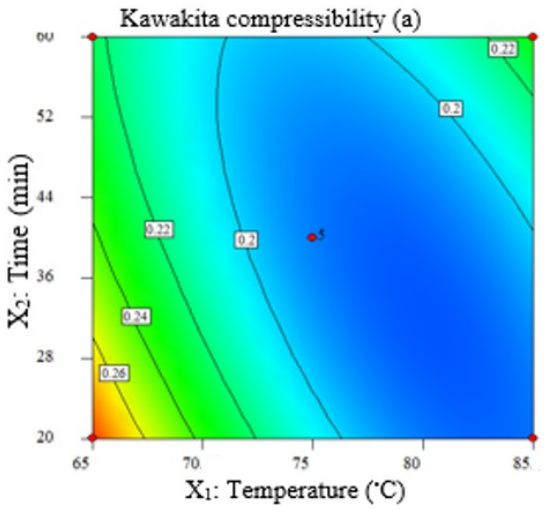

(B)

Fig. 3.32. Surface response (A) and contour plot (B) of Kawakita compressibility versus the factors.

Temperature has negative effect on Kawakita compressibility (a) with coefficient of -0.022 ($p = 0.0009$). The interaction of the two factors has synergistic effect on Kawakita constant 'a' with a factor of 0.031 ($p = 0.0023$).

Eq. 3.10 presents the dependence of the mean yield strength of the pre/gelatinized starches on the temperature and time of pre/gelatinization which is also illustrated in both three and two dimensional plots in Fig. 3.31, respectively.

$$P_y = 200.21 + 27.47X_1 + 20.20X_2 - 27.31X_1X_2 \qquad \text{eq. 3.10}$$

Where yield P_y stands for yield pressure.

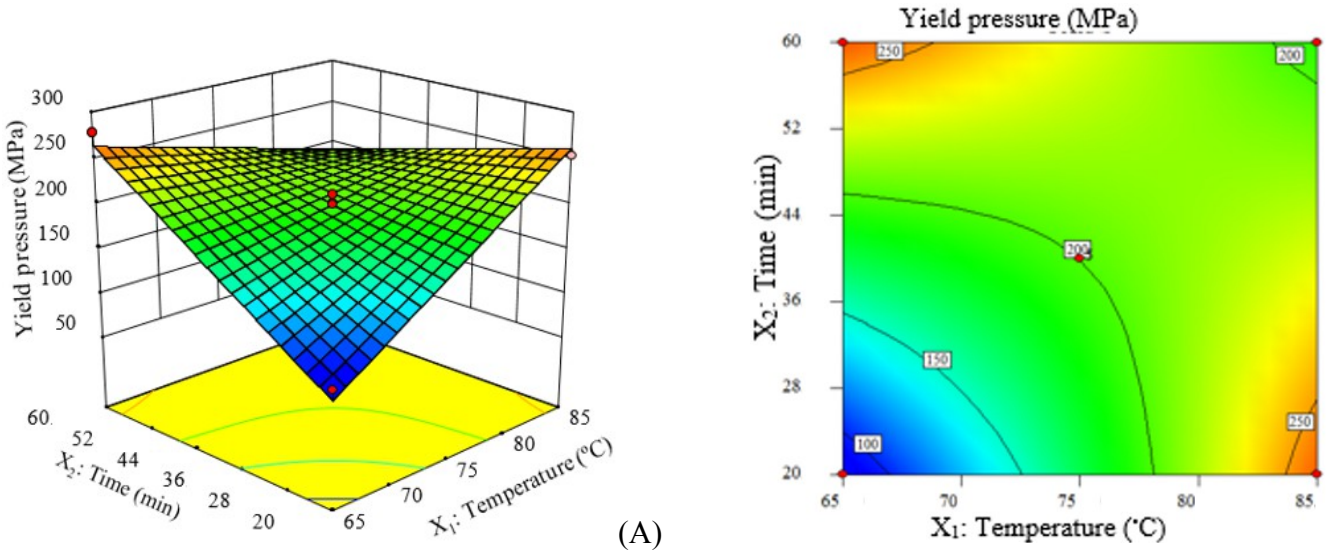

(A) (B)

Fig. 3.33. Surface response (A) and contour plot (B) of yield pressure versus the factors.

The mean yield pressure calculated from the Heckel plot was observed to increase with increasing levels of both temperature (coefficient of 27.47, p = 0.0004) and time (coefficient of 28.26, p = 0.0003). The interaction of the two factors antagonized the yield pressure with a factor of -62.51 (p < 0.0001).

In the same fashion, the compactibility property with changing levels of the factors in the design space was described in terms of hardness as shown in eq. 3.11 and Fig 3.32 A and B.

$$sqrtH = 8.77 - 3.13X_1 - 2.71X_2 - 2.53X_2^2 \qquad \text{eq. 3.11}$$

Where: sqrtH stands square root of hardness, respectively.

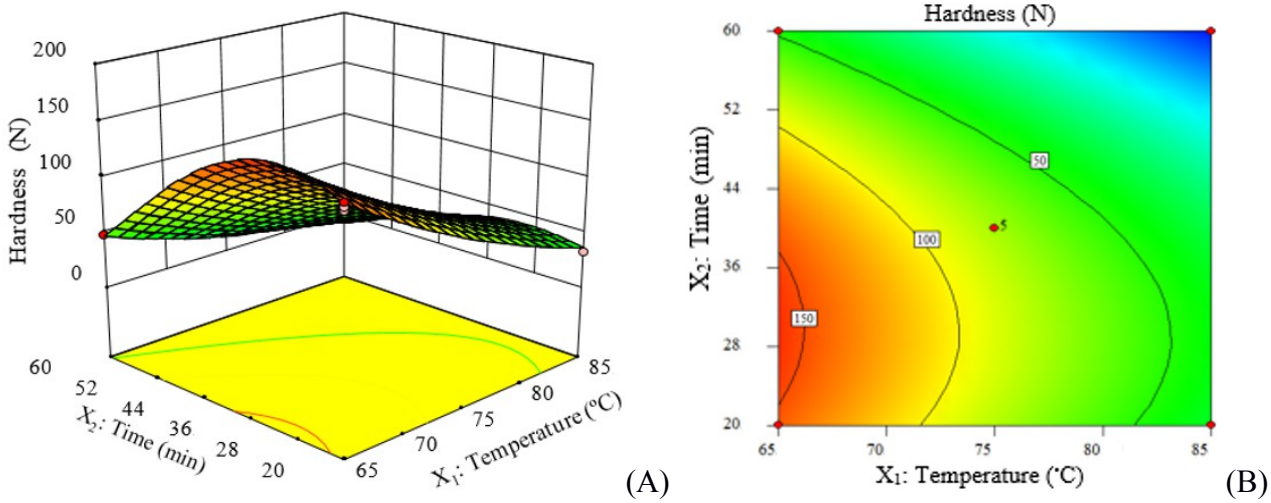

(A) (B)

Fig. 3.34. Surface response (A) and contour plot (B) of hardness versus the factors.

Both temperature and time of pre/gelatinization exhibited decreasing effect on the square root of hardness with coefficients of -3.13 ($p < 0.0001$) and 2.71 ($p < 0.0001$), respectively. Time of pre/gelatinization was observed to have convex quadratic effect on the square root of hardness with coefficient of -2.53 ($p < 0.0001$).

In this study, the trends of hardness didn't universally parallel that of neither Kawakita compressibility nor mean yield pressure and this is inline with the report by Murakami *et al* (2001) showing that densification (plastic deformation) alone doesn't necessarily represent compactibility (Khomane and Bansal, 2012).

3.3.6. Optimization and Validation

To optimize the factors towards the response targets, the numerical (desirability based) (Fig. 3. 33 and Fig. 3.34A) and graphical (overlaying or superimposing the contours, Fig. 3.34 B) methods of optimization were used (Lewis *et al.,* 1999).

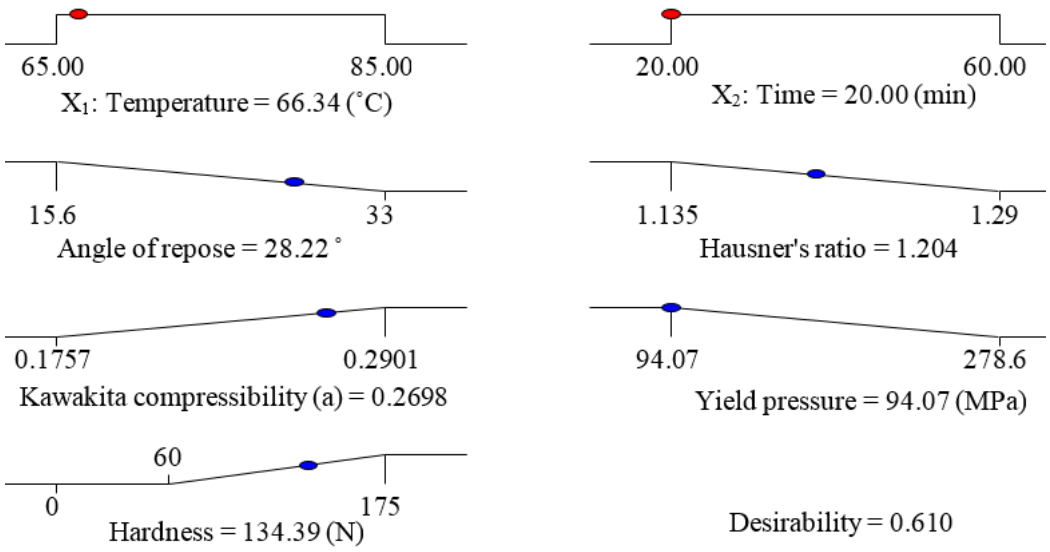

Fig. 3.35. The ramps of optimum responses and factors from numerical optimization.

As a result, the optimum condition of pregelatinization is 66.34 ˚C for 20 min resulting in the angle of repose of 28.22˚, HR of 1.204, Kawakita constant 'a' of 0.26976, yield pressure of 94.07 MPa and hardness of the tablet of 134.39 N with the desirability of 0.610.

As a result, the optimum condition of pregelatinization is 66.34 ˚C for 20 min resulting in the angle of repose of 28.22˚, HR of 1.204, Kawakita a of 0.26976, yield pressure of 94.07 MPa and hardness of the tablet of 134.39 N with the desirability of 0.610.

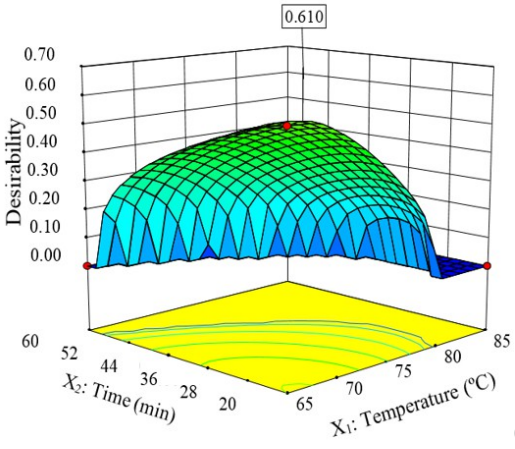

(A)

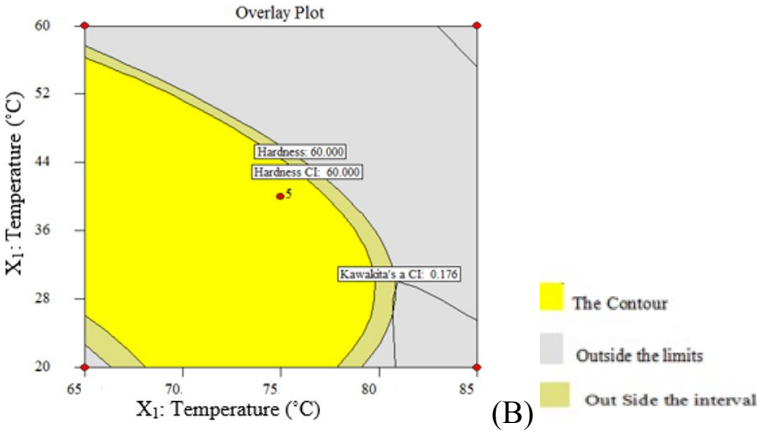

(B)

Fig. 3.36. The overall desirability function RSM (A) and the overlay plot of responses (B).

In order to validate the tool of optimization, NTB1S was pre/gelatinized at three points other than the experimental design points (72.00 ˚C for 37.00 min, 70.00 ˚C for 42.00 min and 65 ˚C for 30 min) and levels of responses were determined experimentally. Then, relative errors between the predicted and experimental values were computed as shown in Table 3.22.

Table 3.27. Validation of the optimization.

Temperature (ºC)		72	70	65
Time (Min)		37	42	30
Angle of repose (º)	Observed	23.8	24.05	28.64
	Predicted	23.13	23.9	29.43
	Error	-2.897	-0.628	2.684
Hausner ratio	Observed	1.224	1.236	1.226
	Predicted	1.214	1.226	1.237
	Error	-0.824	-0.816	0.889
Kawakita compressibility	Observed	0.201	0.112	0.249
	Predicted	0.201	0.107	0.26
	Error	0	-4.673	4.231
Yield pressure (MPa)	Observed	184.17	191.18	122.53
	Predicted	184.9	192.4	127.35
	Error	0.395	0.634	3.785
Tablet hardness (N)	Observed	102.32	103.11	153.42
	Predicted	101.28	101.4	159.56
	Error	-1.027	-1.686	3.848

As the results witness, none of the responses in the selected data points showed as high as ± 5% error with respect to the predicted value. The scenario suggests that process and results of optimization have acceptable validity. This verifies that the use of 66.34 ºC for 20 min is optimum point of pre/gelatinization of 15% (w/v) NTB1S. The optimum levels of angle of repose, Hausner ratio, Kawakita compressibility, mean yield strength and hardness are 28.22˚, 1.204, 0.26976, 94.07 MPa and 134.39 N, respectively.

3.3.7. Relevant Properties of the Pregelatinized Starch

3.3.7.1. Amylose to Amylopectin Ratio

The amylose and amylopectin contents of pregelatinized Taro *Boloso-I* starch (PGTB1S), NTB1S and the Starch 1500® are displayed in the Table 3.23.

Table 3.28. Amylose and amylopectin contents of the starches.

	NTB1S	PGTB1S	**Starch 1500®**
Amylose	20.7 ± 1.7	20.6 ± 2.02	27.5 ± 2.6
Amylopectin	77.3 ± 4.6	77.6 ± 6.13	72.07 ± 6.5

As the results show, PGTB1S has significantly lower amount of amylose than Starch 1500®. Moreover, the process of pre/gelatinization didn't affect the amylose to amylopectin ratio as it is a physical modification (Zobel, 1984).

3.3.7.2. Fourier Transform Infrared Spectra

For the assessment of functional groups that define starch, Fourier transform infra-red spectra of NTB1S and PGTB1S were compared (Fig. 3.35 and 3.36).

Accordingly, there is a broad peak between 3200 cm^{-1} and 3600 cm^{-1} which belongs likely to complex vibrational stretching vibration of -OH. Below 800 cm^{-1}, the spectrum exhibits two visible peaks at 721.33 cm^{-1} and 767.62 cm^{-1} which likely belong to the vibrations of the pyranose ring. In between 800-1500 cm^{-1}, the finger print region; there are peaks around 1078.13 to 1155.28 which are most probable to belong to C-O-C bond C-OH bond, respectively. Likewise, there are peaks in between 990 cm^{-1}-1250 cm^{-1} including 1018.30 cm^{-1}, 1045.35 cm^{-1}, 1078.13 cm^{-1}, 1155.28 cm^{-1} and 1205.43 cm^{-1} represent the anhydroglucose ring C-O stretch. A typical peak at 1641.31 cm^{-1} is most likely a feature of firmly bound water. There are absorbance peaks of C-H stretching around 2900 cm^{-1}.

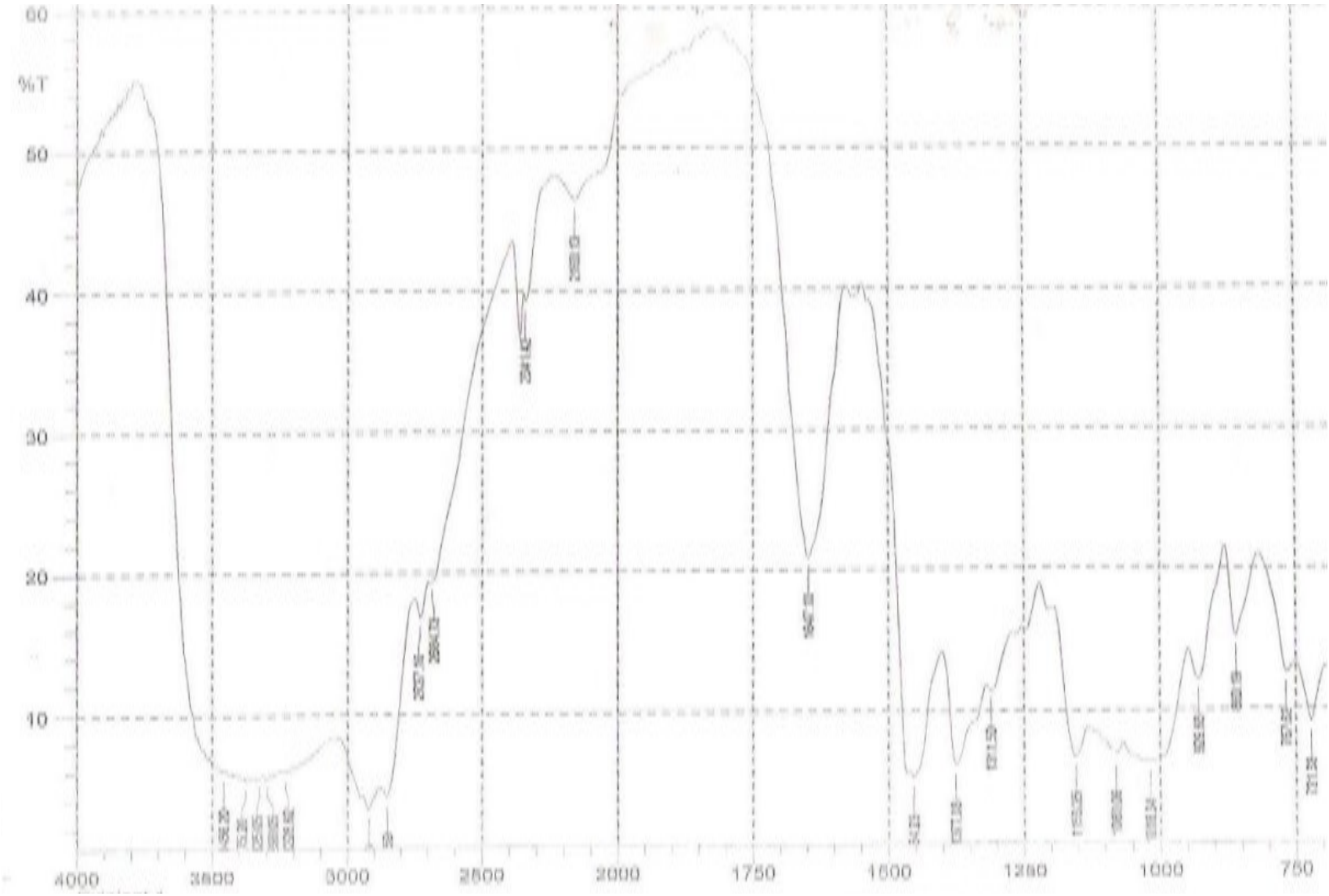

Fig. 3.37. FTIR spectra of NTB1S

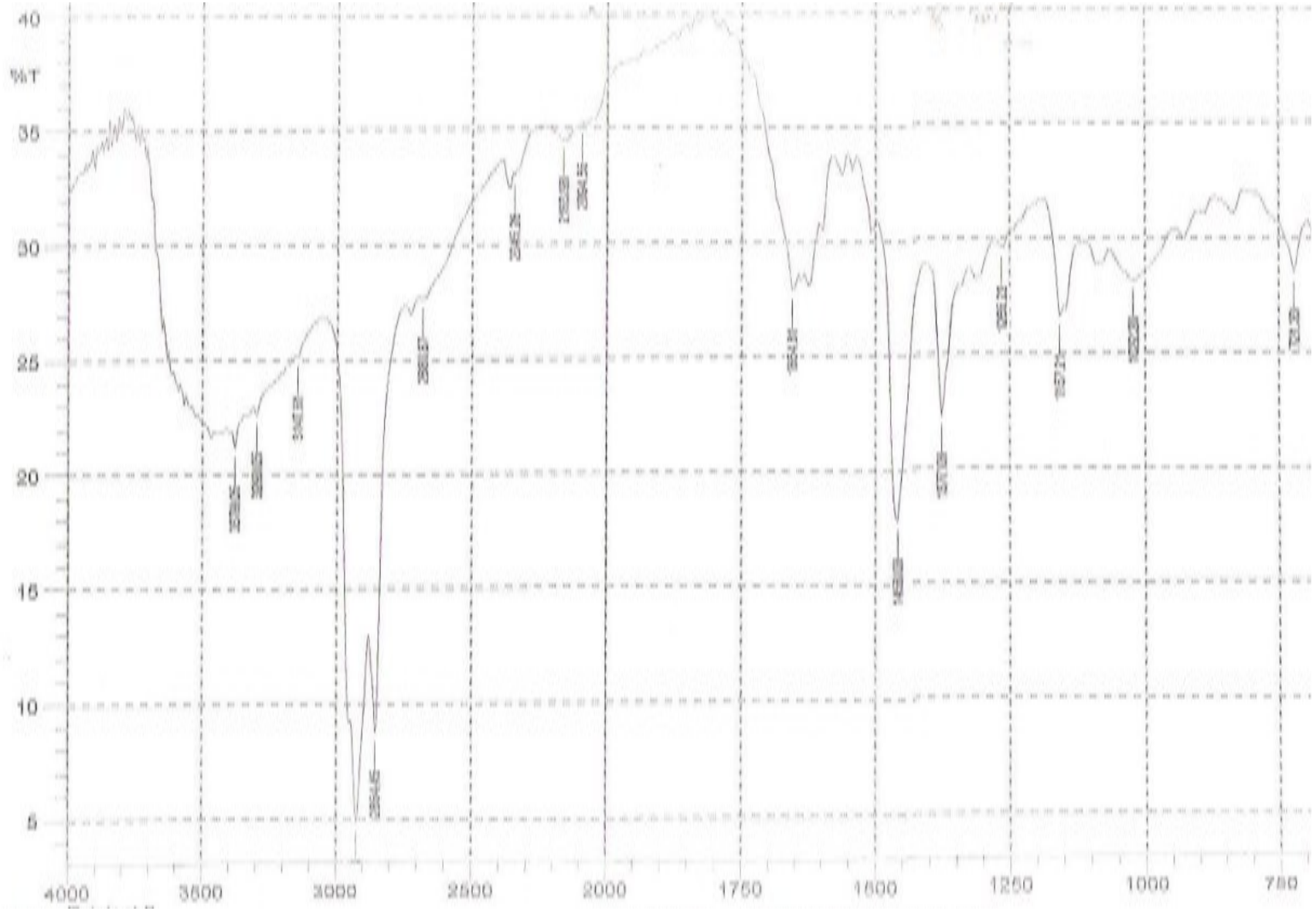

Fig. 3.38 FTIR spectra of PGTB1S.

These arguments which were true also for the NTB1S spectrum claim that the modified starch has all the functional groups common to starches. In the FTIR spectra of the pregelatinized PGTB1S (Fig. 3.36), all the major absorbance peaks are maintained indicating absence of chemical modifications on the starch molecules (John, 2000).

3.3.7.3. Swelling Power and Water Solubility Index

The swelling and solubility trends of PGTB1S, Starch 1500® and NTB1S across 20 ºC - 85 ºC are depicted in the Fig. 3.37.

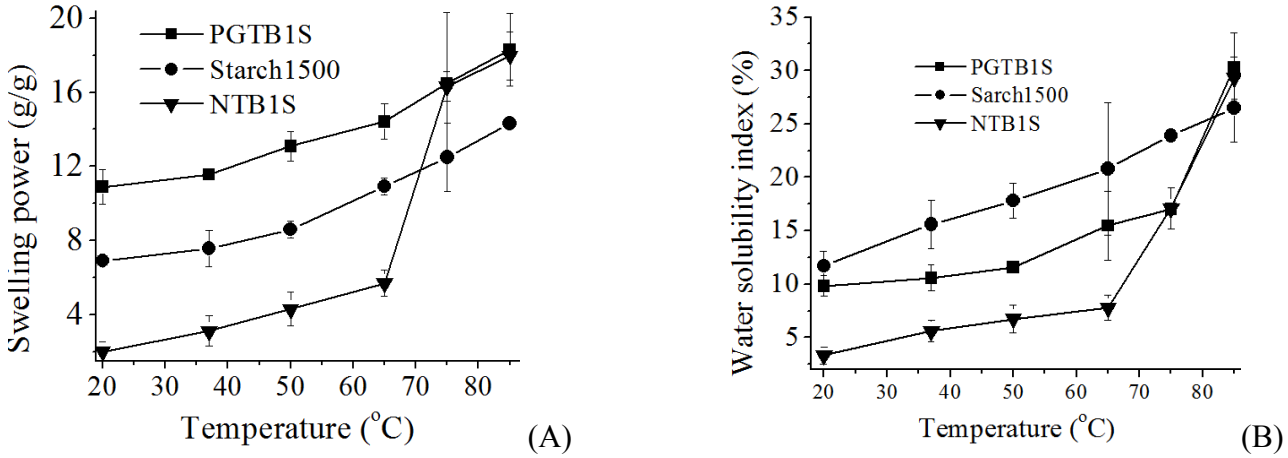

Fig. 3.39. Swelling power and water solubility indices of PGTB1S, Starch 1500® and NTB1S

The swelling power of the three starches follows the order: PGTB1S > Starch 1500® > NTB1S at 20, 37, 50 and 65 ºC. This indicates that pregelatinization increased the solubility index of the starch probably due to amylose leaching (Klein *et al.,* 2013). The same was reported elsewhere, for example rice and corn starches (Adedokun and Itiola, 2011). A possible explanation for the increase in the swelling power of PGTB1S than the NTB1S is that thermal disruption of crystal phases set the starch molecules free to absorb more water molecules than the amorphous intercluster lamellae (Costas, 2009). At 75 and 85 ºC, NTB1S and PGTB1S were observed to have comparable swelling power and solubility index.

3.3.7.4. Bulk Powder Properties

3.3.7.4.1. Particle Morphology

The technological importance of particle morphology has been discussed in the Section 3.1.2.2. The scanning electron micrographs (SEM) of PGTB1S is shown in Fig. 3.38.

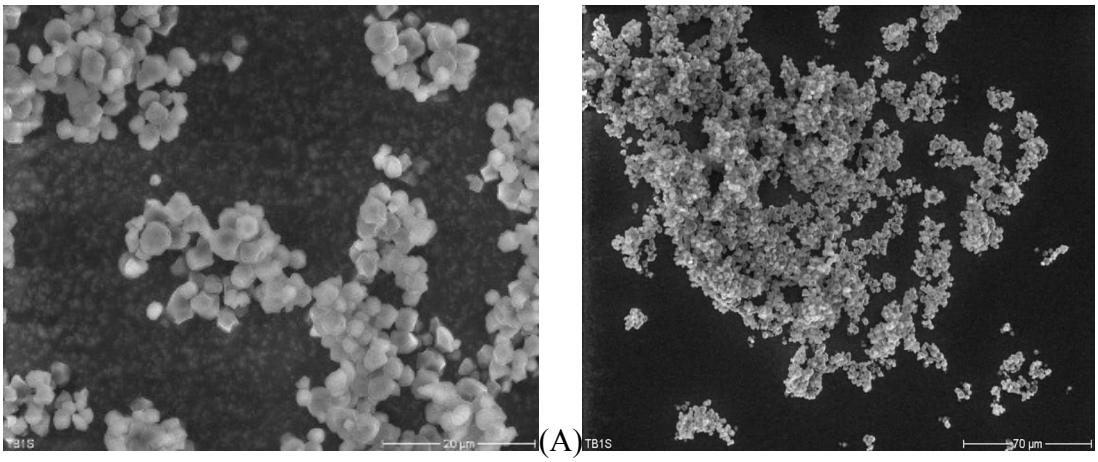

(A) (B)

Fig. 3.40. Scanning electron micrographs of PGTB1S: 20 µm scale bar (A) and 70 µm scale bar (B).

As it is clear from the Fig. 3.38, the optimum pregelatinized starch particles have slightly smoother polygonal shapes compared to the native granules (described in Fig. 3.3 in the Section 3.1.2.2). The morphological change may be for partial pre-gelatinization might have taken place as can be suspected from the granules more aggregated, having less physical integrity compared to the NTB1S. More spherical shape, aggregation and loss of physical integrity makes the changes similar to that of heat moisture treated low amylose rice starches published elsewhere (Elessandra *et al.*, 2010; Bakre *et al.*, 2014).

3.3.7.4.2. Moisture Content

Commonly, dry starch contains 6-16% moisture. Moisture content, if high, can result in microbial deterioration of the product (Moorthy, 2002). The optimized PTB1S has the least moisture content (9.11 ± 0.25%) followed by Starch 1500® (9.49 ± 0.39%), highest (10.43 ± 0.42%) belonging to NTB1S ($p < 0.05$). This implies that pregelatinization of NTB1S decreased the moisture content, enhancing its stability concerns.

3.3.7.4.3. Moisture Sorption Profile

Moisture sorption of starches can affect the physicochemical properties of solid dosage forms containing starches. The moisture sorption profiles of NTB1S, PGTB1S and Starch 1500® are shown in Fig. 3.39.

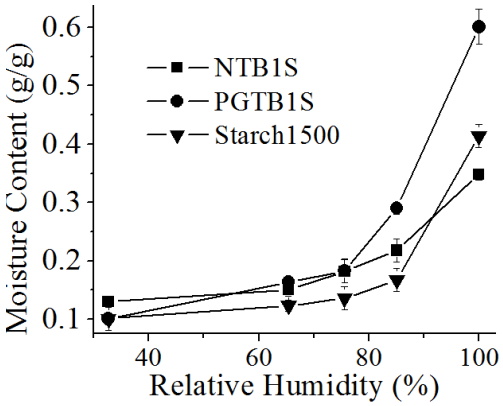

Fig. 3.41. Moisture sorption isotherm of NTB1S, PGTB1S and Starch 1500®.

Accordingly, the moisture sorption profile of the PGTB1S is higher than the corresponding values of NTB1S ($p < 0.05$). The likely reason for the increased moisture sorption of PGTB1S is decrement of crystal phases due to hydrothermal disruption accompanied by pregelatinization (Swarbrick, 2007) and it is expected for pregelatinized starches (Raymond, 2003). This property of pregelatinized starches is useful for scavenging moisture from solid dosage forms of moisture sensitive drugs.

3.3.7.4.4. Density and Flow Properties

Density values are related to total, inter-particle and intra-particle porosities which in turn indicate properties of excipients like tablet disintegrating potential (Swarbrick, 2007). The bulk, tapped and true densities of NTB1S, PGTB1S and Starch 1500® are presented in Fig. 3.40.

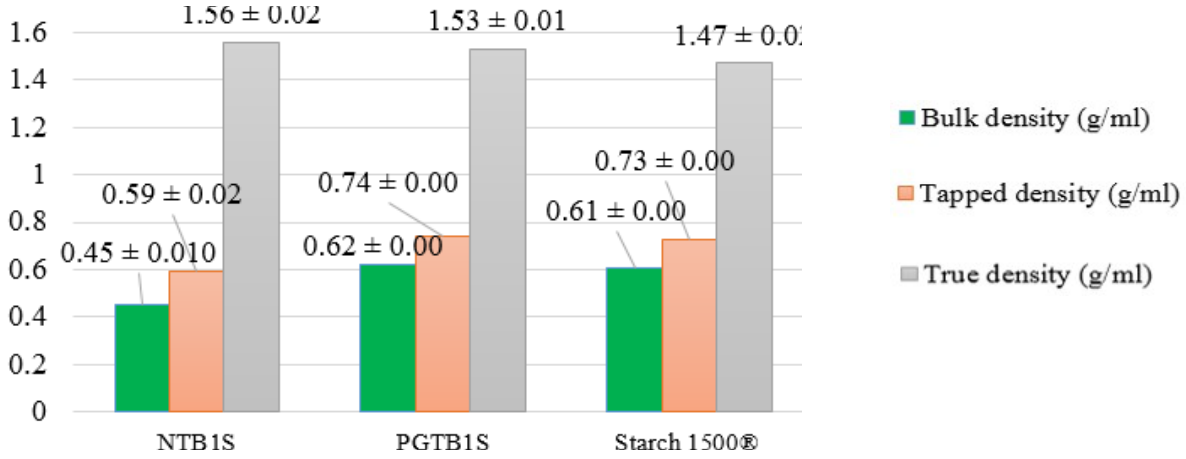

Fig. 3.42. The densities and related properties of NTB1S, PGTB1S and Starch 1500®.

Both bulk density (0.62 ± 0.005 g/ml) and tapped density (0.74 ± 0.001 g/ml) ($p < 0.05$) of PGTB1S were higher than NTB1S may be due to changes in particle sizes and shapes (Johansson and

Alderborn, 2001). Higher bulk density is advantageous in the fill volume reduction during tableting. Even though the pregelatinization decreased the true density from 1.56 ± 0.02 g/ml to 1.53 ± 0.01 g/ml, potentially owing to hydrothermal disruption of crystal structure and diffusion of amylose molecules out of the granules (Belitz *et al.,* 2009). However, it was denser than Starch 1500® (1.47 ± 0.02 g/ml) ($p < 0.05$).

Flow property can be characterized by using the values of Carr's index, Hausner ratio and angle of repose. In this regard, the values of these parameters for NTB1S, PGTB1S and Starch 1500® are presented in Table 3.24.

Table 3.29. Flow properties of NTB1S, PGTB1S and Starch 1500®.

	Carr's index (%)	Hausner Ratio	Angle of repose	Flow rate (g/s)
NTB1S	23.1 ± 0.7	1.30 ± 0.01	-	-
PGTB1S	10.2 ± 0.2	1.20 ± 0.02	29.56 ± 0.8	5.83 ± 0.7
Starch 1500®	10.4 ± 0.3	1.21 ± 0.03	26.59 ± 0.4	5.50 ± 0.6

The PGTB1S has lower Hausner ratio and Carr's index but higher angle of repose which suggest PGTB1S to be more cohesive. The reasons for its lower Hausner ratio and Carr's indexes are its slightly higher bulk, tapped and true densities and low porosity (Ahmada *et al.,* 2012). In terms of its Hausner's ratio, Carr's index and flow rate, PGTB1S exhibited flow property comparable to that of Starch 1500®.

3.3.7.4.5. Compressibility: Kawakita and Heckel Plots

Kawakita equation is one of the commonest methods to relate the degree of powder volume reduction with low pressure or taps. The Kawakita plots with slopes (1/a), Kawakita cohesiveness (1/b) and correlation coefficients (R^2) of PGTB1S and Starch 1500® are shown in Fig. 3.41.

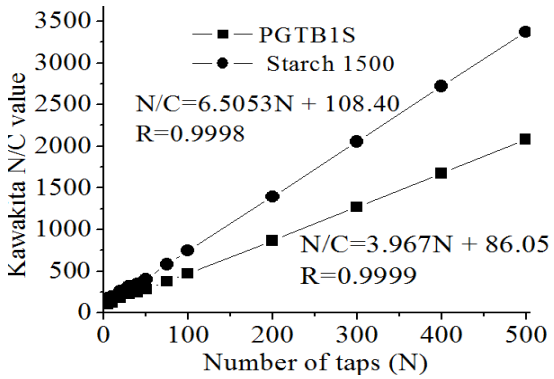

Fig. 3.43. Kawakita plots of PGTB1S and Starch 1500®

The results show that PGTB1S has higher values of Kawakita indices of compressibility (a = 0.2521) and cohesiveness (1/b = 21.69) than those of Starch 1500® (a = 0.1537 and 1/b = 16.66). This implies that maximum volume reduction of PGTB1S before compression was higher than that of Starch 1500® and PGTB1S is more cohesive than Starch 1500® (Bakre and Ayodele, 2013; Widodo and Hassan, 2015).

In addition to Kawakita plots, shape of Heckel plot and parameters from its linear segment (slope, k, and intercept, A) are used for exploration of mechanisms of deformation, extent of plastic deformation and influence of rearrangement or fragmentation on densification of powders. Accordingly, Heckel plot of PGTB1S was constructed and shown in Fig. 3.42.

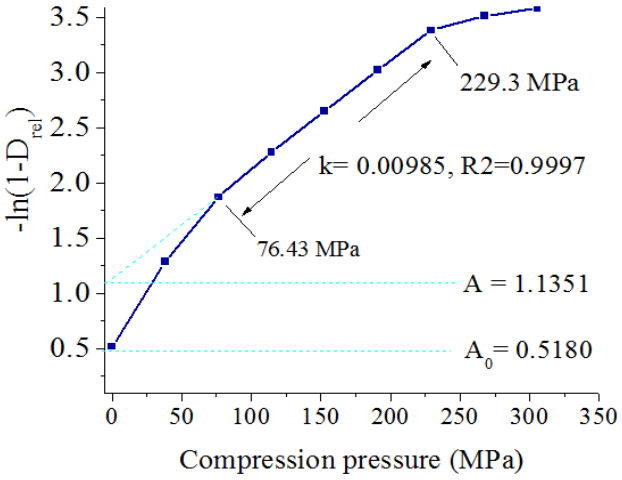

Fig. 3.44. Heckel plot of PGTB1S

Initial densification of PGTB1S gives the impression that it is due to rearrangement or fragmentation of the powder revealed by the initial non-linear region of the Heckel plot. In the linear segment of the plot (R^2 = 0.9997), 76.43-229.30 MPa, it suggests that the granules deform plastically showing a yield pressure (P_y) = 101.5 MPa (inverse of k = 0.00985 MPa^{-1}). In addition, the results show that PGTB1S particles deform plastically within 76.43 - 229.30 MPa. Moreover, the Heckel constant 'A' shows that the total densification of the powder bed before deformation was until –ln ($1-D_{rel}$) equals 1.1351 corresponding to D_A = ~~0~~= 0.6786. Phase of densification by rearrangement before the particles of powder start individual deformation and possible bonding was found to be, D_b = 0.2743. Besides the Kawakita and Heckel analysis, the compressibility behavior of PGTB1S was evidenced by low values of compressibility (Carr's) index (Table 3.24). The order of magnitudes of Carr's index for PGTB1S,

NTB1S and Starch 1500® follows PGTB1S ≈ Starch 1500® < NTB1S. The reason for low Carr's index is low interparticular interaction and it favors compressibility.

3.3.7.5. Compactibility and Lubricant Sensitivity

Mechanical properties of unlubricated PGTB1S were investigated to reveal the compactibility profiles. Moreover, since the presence of lubricants, e.g., magnesium (Mg) stearate, decreases the mechanical strength of tablets starting at a typical level (Aulton, 2002), hardness, friability, radial tensile strength and disintegration values of tablets of these starches [both unlubricated and lubricated (0.25 - 2.00% w/w)] were performed (Table 3.25).

Table 3.30. The properties of tablets PGTB1S containing magnesium stearate (0-2%).

Magnesium stearate (%)	Hardness (N)	Friability (%)	DT (min)	Tensile Strength (N/cm^2)	Weight (mg)	Thickness (mm)
0.00	138.0 ± 5.3	0.27 ± 0.01	3.2 ± 0.2	303.1 ± 8	301 ± 7	2.90 ± 0.0
0.25	92.4 ± 4.9	0.39 ± 0.01	4.0 ± 0.0	196 ± 10	302 ± 5	3.01 ± 0.1
0.5	75.9 ± 5.2	0.56 ± 0.01	6.2 ± 0.3	155 ± 9	303 ± 6	3.12 ± 0.2
0.75	56.8 ± 3.9	1.09 ± 0.04	6.9 ± 0.3	116 ± 9	302 ± 5	3.12 ± 0.1
1	53.2 ± 3.7	1.12 ± 0.01	7.8 ± 0.4	109 ± 9	302 ± 4	3.12 ± 0.1
1.5	35.1 ± 5.9	4.70 ± 0.20	9.6 ± 0.5	71 ± 12	302 ± 3	3.14 ± 0.1
2	16.6 ± 4.7	8.75 ± 1.2	11.9 ± 0.5	34 ± 10	299 ± 3	3.15 ± 0.1

The results show that the hardness and friability decrease and increase with increasing concentration of the lubricant, respectively ($p < 0.05$). This is likely due to increasing bond inhibition (Morin, 2012). Its tablets are acceptably hard (> 60 N) up to 0.5% of magnesium stearate concentration (BP, 2009). On the other hand, the hardness of NTB1S tablets was acceptable (≥ 60 N) at all levels of magnesium stearate. Besides, the friability of tablets of NTB1S was lower than PGTB1S. The NTB1S tolerated magnesium stearate (friability < 1%) through 0.00 - 2.00% (w/w) (Aulton, 2002; BP, 2009). The increase in concentration of magnesium stearate increased DT of the tablets of maybe due to the impaired wetting due to hydrophobic film production around the particles by magnesium stearate (Preethi *et al.,* 2013). However, NTB1S tablets had the slowest disintegrating tablet in the absence of magnesium stearate, presumably because of the gel forming property of the native starch in water which likely gets impeded in the presence of magnesium stearate. In the presence of magnesium stearate, the tablets of NTB1S disintegrated below 1 min which is faster than the tablets of PGTB1S up to 1.5% of magnesium stearate ($p < 0.05$). On the other hand, all the tablets of both of the starches

disintegrated within acceptable time for tablets except for the tablets of the unlubricated NTB1S (BP, 2009).

3.3.7.6. Dilution Potential

Dilution potential of PGTB1S was tested in paracetamol tablets compressed at 17 kN compression force at drug concentration of 20, 30, 40 and 50% w/w. Tablets of same compaction were repeated substituting PGTB1S with NTB1S and Starch 1500® as comparators. The properties of these tablets were determined and shown in Table 3.26.

Table 3.31. Properties of tablets compressed at 17 kN of various paracetamol concentrations.

Drug (%)	Starch type	**Hardness (N)**	**Friability (%)**	**DT (min)**	**Tensile Strength (N/cm^2)**	**Weight (mg)**	**Thickness (mm)**
20	PGTB1S	77.4 ± 6.1	0.61 ± 0.01	2.0 ± 0.1	156 ± 10	302 ± 3	3.17 ± 0.1
	Starch 1500®	64.7 ± 4.4	0.79 ± 0.02	5.7 ± 0.1	127 ± 8	300 ± 3	3.24 ± 0.0
	NTB1S	87.1 ± 5.9	0.32 ± 0.01	4.2 ± 0.9	184 ± 12	301 ± 2	3.01 ± 0.0
30	PGTB1S	69.9 ± 4.2	0.80 ± 0.02	1.0 ± 0.1	137 ± 8	300 ± 3	3.24 ± 0.0
	Starch 1500®	51.5 ± 2.4	1.11 ± 0.05	4.3 ± 0.2	101 ± 5	302 ± 3	3.26 ± 0.0
	NTB1S	74.3 ± 5.1	0.40 ± 0.02	1.5 ± 0.1	152 ± 10	300 ± 3	3.11 ± 0.0
40	PGTB1S	56.6 ± 4.1	1.60 ± 0.06	0.8 ± 0.0	110 ± 8	303 ± 4	3.28 ± 0.0
	Starch 1500®	43.4 ± 2.4	3.00 ± 0.09	3.5 ± 0.1	84 ± 5	301 ± 5	3.28 ± 0.0
	NTB1S	63.2 ± 4.5	0.80 ± 0.02	1.0 ± 0.0	125 ± 9	303 ± 3	3.22 ± 0.0
50	PGTB1S	16.1 ± 3.2	Friable	0.5 ± 0.0	29 ± 5	301 ± 6	3.50 ± 0.1
	Starch 1500®	15.1 ± 2.1	Friable	3.0 ± 0.0	29 ± 4	301 ± 6	3.30 ± 0.0
	NTB1S	54.7 ± 6.1	0.90 ± 0.03	0.7 ± 0.0	106 ± 11	301 ± 3	3.28 ± 0.0

The hardness of ~~the~~ paracetamol tablets decreased with increasing concentration of the drug for all the three starches. Up to 30% (w/w) dilution of PGTB1S with paracetamol, the tablets retained the quality requirements, experiencing higher dilution potential than Starch 1500®, 20% (w/w). Beyond these respective concentrations, the poor compressibility and elastic recovery of paracetamol assumed dominance and resulted in too friable and low tensile strength tablets. The equivalent tablets of NTB1S were acceptably hard (> 60 N) up to 40% (w/w) of paracetamol and attrition resistant up to 50 % (w/w) of the drug cargo.

3.3.7.7. Properties of PGTB1S-Paracetamol Directly Compressed Tablets

The average thickness of ~~the~~ tablets slightly increased with the presence and increasing concentration of paracetamol (Table 3.26). The weight uniformity of PGTB1S containing paracetamol tablets

satisfies the compendial requirements, *i.e.*, within ± 5% of the mean. The increases in a starch proportion increased hardness of paracetamol tablets reasonably. The tablets of the PGTB1S paracetamol tablets were acceptable up to 30% of drug. In contrast, Starch 1500® equivalent was hard and attrition resistant enough up to only 20% (w/w). At all the paracetamol levels, the tablets of the PGTB1S had higher mechanical strength than those of the Starch 1500®**.** The paracetamol tablets of both PGTB1S and Starch 1500® beyond the respective paracetamol concentration of 30% and 20% (w/w), had low tensile strength, higher friability (> 1%) or capping and lamination. At all the paracetamol levels, the tablets of native starch had acceptable friability (*i.e.*, < 1%) (BP, 2009).

The DTs of ~~the~~ paracetamol tablets in the study decreased with increasing concentration of the drug. At all levels of the drug, PGTB1S containing tablets disintegrated fastest followed by NTB1S and Starch 1500® which is the slowest. Moreover, the tablets of PGTB1S fulfilled the requirements of fast dissolving tablets. By any means, the tablets had acceptable DT (< 15 min), at all levels of the drug cargo for all the three types of starches. Similarly, the dissolution profile of the tablets formulated is described in the Fig. 3.43.

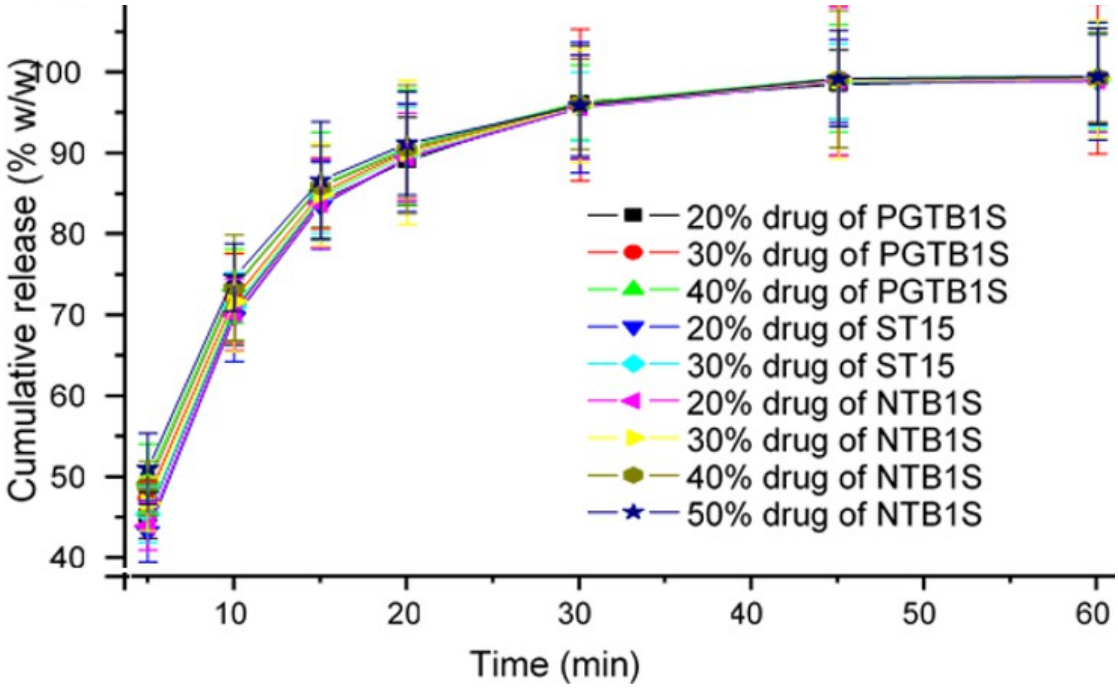

Fig. 3.45. Dissolution profile of the directly compressed paracetamol tablets

The dissolution profiles of tablets at paracetamol contents of 20, 30, 40 and 50% (w/w) prepared using the 3 starches as disintegrants was such that all the tablets released more than 90% within 30 min. For the first 20 min, the dissolution was faster with increasing concentration of the drug for all the three

starches. At and beyond 30 min, the dissolution rate was comparable for all the tablets of all the starches perhaps for the complete disintegration and dissolution of the tablets.

4. CONCLUSIONS

In this study, the isolation, physicochemical characterization, evaluation of the native as tablet disintegrant and pregelatinized starch from Taro Boloso-I as diluent of direct compression were investigated successfully. Accordingly, the chemical constituents of Native Taro *Boloso-I* starch (NTB1S), the major component of Taro *Boloso-I* yielding 83.5% ± 1.6% (w/w on dry basis), can be a potential source of industrial starch. The amylose to amylopectin ratio of NTB1S is 20.7 ± 1.8% to 77.3 ± 2.1% (w/w). Its granules are polyhedral/angular and have average size of 2.365 ± 0.05 µm exhibiting an A-type polymorphism. It has lower moisture content and sorption but higher swelling power than potato starch at 20, 37, 65, 75 and 85°C. It has also higher onset, peak or endset of gelatinization temperatures (68.4, 75.46 and 84.4°C) when compared with the values of potato starch ~~showing,~~ *i.e.*, 62.5, 67.53 and 84.4°C, respectively. Starch from Taro *Boloso-I* has significant differences from the Godare starch. As per the FTIR and DSC analyses, NTB1S undergoes no significant interaction with paracetamol.

The native NTB1S showed that it can be used as alternative disintegrant in tablets as demonstrated. It can result in acceptable hardness, friability and also fast dissolving paracetamol tablets. The reason is that, at its optimum concentration (9.80%) and compression force (15 kN), use of NTB1S as disintegrant resulted in acceptable tablets with hardness (117.1 ± 4.93 N), friability (0.159 ± 0.02%) and ~~disintegration time~~DT (1.31 ± 0.02 min) fulfilling the ~~disintegration time~~DT requirement of fast dissolving tablets, *i.e.*, < 3 min. Moreover, NTB1S resulted in tablets of high balance between binding and disintegration effects as indicated by (H/Fr)/DT (569 ± 83 $kN\%^{-1}Min^{-1}$).

Increasing flow property, optimum pregelatinization decreased the compressibility and compactibility of the NTB1S. At the optimum pregelatinization point (*i.e.*, 66.34 ˚C for 20 min), sufficient flow property (angle of repose of 28.22 ˚, Hausner ratio of 1.204) was achieved with good compressibility (Kawakita compressibility of 0.2697, yield pressure of 101.5 MPa and hardness of the tablet of 128 N when compressed at 15 kN). The optimum pregelatinization showed to have no effect on the amylose to amylopectin ratio and IR spectra. As per this finding, PGTB1S can be taken as alternative direct compression excipient tolerating 0.5% of magnesium stearate. Its dilution potential (30%) was also observed to be higher than that of Starch 1500®.

5. SUGGESTIONS FOR FURTHER WORKS

The findings of this study serve as the baselines for the following further investigations;

- The stability study of the products formulated using NTB1S and PGTB1S as an excipient
- Further applicability of NTB1S in pharmaceutical industries
- Physical and chemical modifications to enhance its application as pharmaceutical excipient

REFERENCES

Abdel-Hamid S, Alshihabi F, Betz G (2011). Investigating the effect of particle size and shape on high speed tableting through radial die-wall pressure monitoring. *Int J Pharm* 413: 29-35.

Adane M, Abdel-Mohsen M G, Gebre-mariam T (2006a). Evaluation and optimization of Godare starch as a binder and disintegrant in tablet formulation. *Ethiop Pharm J* 24: 106-115.

Adane M, Endale A, Bultosa G, Gemal M, Gebre-Mariam T (2006b). Isolation and physicochemical characterization of Godare (*Colocasia esculenta)* starch from Ethiopia. *Ethiop Pharm J* 24: 13-22.

Adane T, Shimelis A, Negussie R, Tilahun B, Haki G (2013). Effect of processing method on the proximate composition, mineral content and antinutritional factors of taro (C*olocosia esculenta*~~,~~ ~~l~~) grown in Ethiopia. *AJFAND* 13: 7383-7398.

Adedokun M O, Itiola O A (2011). Disintegrant activities of natural and pregelatinized trifoliate yams, rice and corn starches in paracetamol tablets. *JAPS* 1: 200-206.

Ahmad M Z, Akhter S, Anwar M, Rahman M, Siddiquib M A, Ahmad F J (2012). Compactibility and compressibility studies of Assam Borarice starch. *Powder Technol* 224: 281-286.

Alebiowu G, Adeagbo AA (2009). Disintegrant properties of a paracetamol tablet formulation lubricated with co - processed lubricants. *FARMACIA* 57: 500-510.

Alebiowu G, Itiola O A (2003). Effects of starches on the mechanical properties of paracetamol tablet formulations. II. Sorghum and plantain starches as disintegrants. ***Acta Pharm.* 53:** ~~xx-xx~~231-237**.**

Alfonso R (2000). Remington: The science and practice of pharmacy, 21st edition. USA, Lippincott Williams and Wilkins.

Al-Rabadi GJ, Torley PJ, Williams BA, Bryden WI, Gidley MJ (2012). Particle size heterogeneity in milled barley and sorghum grains: Effects on physico-chemical properties and starch digestibility. *J Ceral Sci* 56: 396-403.

Ashogbon AO; Akintayo ET (2012). Morphological, functional and pasting properties of starches separated from rice cultivars grown in Nigeria. *Int Food Res J* 19: 665-671.

Association of Official Analytical Chemists, AOAC, (2000). Official methods of analysis, 16th Edition. The association Arlington, New York: 15-37.

Aulton M E (2002). Pharmaceutics: The science of dosage form design, Churchil Livengstone.

Bakre LG, Ayodele D (2013). Compression characteristics of *Piper Guineense* Fruit. *Indonesian J. Pharm* 24 186-292

Bakre LG, Ogun O, Alayo MA (2014). Influence of pregelatinizatin on the physicochemical and compressional characteristics of starches obtained from two local varities of *Diascorea rotundata*. IOSR J. Pharm 4 24-32.

Belitz H D, Grosch W, Schieberle P (2009). Food chemistry 4th edition. Springer, Berlin.

Bello-Pérez LA, Contreras-Ramos SM, Jìmenez-Aparicio A, Predes-Lopez O (2000). Acetylation and characterization of banana (*Musa paradisiaca)* starch.

BP (2009). British Pharmacopeia: The Pharmaceutical Press, Her Majesty's Stationary Office, London, Vol. I-IV.

Chadha R, Bhandari S (2014). Drug–excipient compatibility screening —Role of thermoanalytical and spectroscopic techniques. *J Pharmaceut Biomed* 87: 82-97.

Chaudhuri B, Mehrotra A, Muzzio F J, Tomassone M S (2006). Cohesive effects in powder mixing in a tumbling blender. *Powder Technol* 165: 105-114.

Coats J (2000). Interpretation of Infrared Spectra: A practical approach. In Meyers RA (ed), Encylopedia of Analytical Chemistry. John Wiley & Sons, Chichester, pp 10815-10837.

Costas G B. (2009). Structural transitions and related physical properties of starch. In: roy lw, james nb, eugene fp. Starch: Chemistry and technology. Elsevier, USA, pp 293-372.

Dagne Y, Mulualem T, Kifle A (2014). Development of high yielding Taro (*Colocacia esculenta* L.) Variety for mid altitude growing areas of Southern Ethiopia *J Plant Sci* 2: 50-54.

Dale N, Michael L, Lev T, Lirong L (2009). Development, optimization, and scale-up of process parameters: tablet compression. In: Developing solid oral dosage forms: Pharmaceutical theory and practice, Elsevier Inc.

Dalonso N, Petkowicz C L d O (2014). Guarana powder polysaccharides: Characterization and rheological properties of starch. *Starch/Stärke* 66: 914-922.

Deborah S, Roy LW (2009). History and future of starch. In: Roy LW, James NB, Eugene FP. Starch: Chemistry and technology. Elsevier, USA, pp 1-10.

Elessandra DRZ, Cátia RS, Luis ASC, Manoel AS, Alvaro RGD (2010). Effect of heat-moisture treatment on rice starch of varying amylose content. *Food Chem 121: 358–365.*

Eliasson A-C; Wahlgrem M (2004). Starch-lipid interactions and their relevance in food products. In: Eliasson A-C. Starch in food: Structure, function and applications. Woodhead Publishing Limited, England, pp 441-460.

ElShaer A, Hanson P, Mohammed AR (2013). A systematic and mechanistic evaluation of aspartic acid as filler for directly compressed tablets containing trimethoprim and trimethoprim aspartate. *Eur J Pharm Biopharm* 83: 468-476.

FAO (1986). Manuals of Food Quality Control: Food analysis general techniques, additives, contaminants and composition. FAO Food and Nutrition paper 14/7, Rome: pp 216-217.

Fellows PJ (2000). Food Processing and Technology: Principles and Practice, 2nd ed. Woodhead Publishing Limited, England.

Flickinger MC, Drew SW (1999). Encyclopedia of Bioprocess Technology: Fermentation, Biocatalysis and Bioseparation. John Wiley & Sons, Inc, New York.

Gabaude CMD, Guillot M, Gautier J, Saudemon P, Chulia D (1999). Effects of true density, compacted mass, compression speed, and punch deformation on the mean yield pressure. *J Pharm Sci* 88: 725-729.

Gebre-Mariam T, Schmidt PC (1996a). Characterization of enset starch and its use as a binder and disintegrant for tablets. Pharmazie 51: 303-311

Gebre-Mariam T, Schmidt P C (1996b). Isolation and physico-chemical properties of enset starch. *Starch/Stärke* 48: 208-214.

Gebre-Mariam T, Schmidt P C (1998). Some physicochemical properties of dioscorea starch from Ethiopia. *Starch/Stärke* 50: 241-246.

Gunaratne A, Hoover R (2002). Effect of heat-moisture treatment on the structure and physicochemical properties of tuber and root starches. *Carbohydr Polym* 49: 425-437.

Hoover R (2001). Composition, molecular structure, and physicochemical properties of tuber and root starches: A review. *Carbohydr Polym* 45: 253-267.

Huang YB, Tsai YH, Lee SH, Chang JS,Wu PC (2005). Optimization of pH-independent release of nicardipine hydrochloride extended-release matrix tablets using response surface methodology. *Int J Pharm* 289: 87-95.

Israkarn K, Hongsprabhas P, Hongsprabhas P (2007). Influences of granule-associated proteins on physicochemical properties of mungbean and cassava starches. *Carbohydr Polym* 68: 314-322.

Johansson B, Alderborn G (2001). The effect of shape and porosity on the compression behaviour and tablet forming ability of granular materials formed from microcrystalline cellulose. *Eur J Pharm Biopharm* 52: 347-357.

Khomane KS, Bansal AK (2012). Differential compaction behaviour of roller compacted granules of clopidogrel bisulphate polymorphs. *Int J Pharm* 472: 288-295.

Kittipongpatana OS, Kittipongpatana N (2012). Preparation and physicomechanical properties of co-precipitated rice starch-colloidal silicon dioxide. *Powder Technol 217: 377-382.*

Klein B, Pinto VZ, Vanier NL, Zavareze ER, Colussi R, Evangelho JA, Gutkoskib LC, Dias ARG (2013). Effect of single and dual heat–moisture treatments on properties of rice, cassava, and pinhao starches. *Carbohydr Polym* 98: 1578-1584.

Klevan I, Nordström J, Bauer-Brandl A, Alderborn G (2009). On the physical interpretation of the initial bending of a Shapiro-Konopicky-Heckel compression profile. *Eur J Pharm Biopharm* 71: 395-401.

Kojima T, Eliott JA (2012). Incipient flow properties of two-component fine powder systems and their relationships with bulk density and particle contacts. *Powder Technol* 228: 359-370.

Lewis GA, Mathieu D, Phan-Tan-luu R (1999). Pharmaceutical Experimental Design. Marcel Dekker Inc., New York.

Makowska A, Szwengiel A, Kubiak P,Tomaszewska-Gras J (2014). Characteristics and structure of starch isolated from triticale. *Starch/Stärke* 66: 895-902.

Mîinea LA, Mehta R, Kallam M, Farina JA, Deorkar N (2011). Evaluation and characteristics of a new direct compressioin performance excipient. *Pharm Technol* 35: 1-7.

Mitrevej A, Faroongsarng D, Sinchaipanid N (1996). Compression behavior of spray dried rice starch. *Int J Pharm* 140: 61-68.

Moorthy S N (2002). Physicochemical and functional properties of tropical tuber plants. *Starch/Stärke* 54: 559-592.

Moraes J, Branzani RS, Franco CML (2014). Behavior of peruvian carrot (*Arracacia xanthorrhiza*) and cassava (*Manihot esculenta*) starches subjected to heat-moisture treatment. *Starch/Stärke* 66: 645-654.

Morin G (2012). The Effects of lubrication on pharmaceutical granules. Electronic thesis and dissertation repository. Paper 621, The University of Western Ontoria, Canada.

Müller P, Seeger M, Tomas J (2013). Compression and breakage behavior ofγ-Al_2O_3 granules. *Powder Technol* 237: 125-133.

Murakami H, Yoneyama T, Nakajima K, Kobayashi M (2001). Correlation between loose density and compactibility of granules prepared by various granulation methods. *Int J Pharm* 216: 159-164.

Nawab A, Alam F, Hasnain A (2014). Functional properties of cowpea (*Vigna unguiculata*) starch as modified by guar, pectin, and xanthan gums. *Starch/Stärke* 66: 832-840.

Odeku OA, Schmid W, Picker-Freyer KM (2008). Material and tablet properties of pregelatinized (thermally modified) Dioscorea starches. *Eur J Pharm Biopharm* 70: 357-371.

Odeku O A, Picker-Freyer K M (2010). Freeze-dried pregelatinized Dioscorea starches as tablet matrix for sustained release. *J.Excipient and Food Chem.* 1: 21-32.

Paulos G, Endale A, Bultosa G, Gebre-Mariam T (2009). Isolation and Physicochemical Characterization of Cassava Starches Obtained from Different Regions of Ethiopia. *Ethiop Pharm J* 27: 42-54.

PhEur (2005). European Pharmacopoeia. Council of Europe, Strasbourg.

Preethi J, Farhana M D, Babu B C, Faizulla M D, Bhowmik D, Duraivel S (2013). Recent trends of polymer usage in the formulation of orodispersible tablets. *IJRPB* 1: 169-174.

Puttewar T Y, Kshirsagar M D, Chandewar A V, Chikhale R V (2010). Formulation and evaluation of orodispersible tablet of taste masked doxylamine succinate using ion exchange resin. *J King Saud Univ Sci* 22: 229-240.

Raymond CR, Paul JS, Paul JW (2003). Handbook of Pharmaceutical Excipients. Pharmaceutical Press, London, and Americal Pharmaceutical Association, Chicago, pp 603-614.

Riippia M, Antikainena O, Niskanenb T, Yliruus J (1998). The effect of compression force on surface structure, crushing strength, friability and disintegration time of erythromycin acistrate tablets. *Eur J Pharm Biopharm* 46: 339-345.

Riyanto T, Aziz H (2015). Compression and mechanical properties of directly compressible pregelatinized sago starches. *Powder Technol* 269: 15-21.

Roy L, James N, Eugene F (1984). Starch: Chemistry and Technology, 2nd ed. Academic Press, USA.

Sakataa Y, Tanabeb E, Sumikawaa T, Shiraishi S, Tokudomec Y, Otsukac M (2007). Effects of solid-state reaction between paracetamol and cloperastine hydrochloride on the pharmaceutical properties of their preparations. *Int J Pharm* 335: 12-19.

Sangwan P, Petinakis E, Dean K (2014). Effects of Formulation, Structure, and Processing on Biodegradation of Starches. In: Halley PJ, Ave´rous L. Starch Polymers: From Genetic Engineering to Green Applications. Elsevier Inc, USA, pp 357-378.

Santl M, Ilic I, Vrecer F, Baumgartner S (2011). A compressibility and compactibility study of real tableting mixtures: The impact of wet and dry granulation versus a direct tableting mixture. *Int J Pharm* 414: 131-139.

Shayne C (2008). Pharmaceutical Manufacturing Handbook, John Wiley & Sons, Inc., Hoboken, New Jersey.

Shenoy P, MaximeV, Tammel K, Innings F, Fitzpatrick J, Ahrné L (2015). Effect of powder densities, particle size and shape on mixture quality of binary food powder mixtures. *Powder Technol* 272: 165-172.

Shrestha AK, Halley PJ (2014). Starch Modification to Develop Novel Starch-Biopolymer Blends: State of Art and Perspectives. In: Halley PJ and Ave´rous L. Starch Polymers: From Genetic Engineering to Green Applications. Elsevier Inc, USA, pp 105-143.

Sionkowska A (2011). Current research on the blends of natural and synthetic polymers as new biomaterials: Review. *Prog Polym Sci* 36: 1254-1276.

Subhadhirasakul S, Yuenyoungsawad S, Ketjinda W, Phadoongsombut N, Faroongsarng D (2001). Study on Tablet Binding and Disintegrating Properties of Alternative Starches Prepared from Taro and Sweet Potato Tubers. *Drug Dev Ind Pharm* 27: 81-87.

Swarbrick J (2007). Encyclopedia of Pharmaceutical Technology. Informa Healthcare, New York.

Tan I and Halley PJ (2014). "Structure-Property" Relationships of Genetically Modified Starch. In: Halley PJ, Ave´rous L. Starch Polymers: From Genetic Engineering to Green Applications. Elsevier Inc, USA, pp 31-75.

The United States Pharmacopoeia 30th ed. National Formulary 25 ed. (USP 30-NF 25) (2007). The United states Pharmacopeial Convention, Inc., Rockville, Maryland.

Wang S, Li C, Yu J, Copeland L, Wang S (2014). Phase transition and swelling behaviour of different starch granules over a wide range of water content. *LWT - Food Sci Technol* 59: 597-604.

Widodo R T, Hassan A (2015). Compression and mechanical properties of directly compressible pregelatinized sago starches. *Powder Technol* 269: 15-21.

Yong-an Y, Jun-cang Q, Wei-hua L, Lian-pu C, Zi-bu W (2012). Formation and developmental characteristics of A- and B-type starch granules in wheat endosperm. *J Integr Agr* 11: 73-81.

Yoshioka S, Stella VJ (2002). Stability of Drugs and Dosage Forms. Kluwer Academic Publishers, New York, Boston, Dordrecht, London, Moscow.

Zeng J, Li G, Goa H, Ru Z (2011). Comparison of A and B starch granules from three wheat varieties. *Molecules* 16: 10570-10591. doi: 10.3390/molecules161210570.

Zhou W, Yang J, Hong Y, Liu G, Zheng J, Gu Z, Zhang P (2014). Impact of amylose content on starch physicochemical properties in transgenic sweet potato. *Carbohydr Polym* 122: 417-427.

Zobel HF (1984). Gelatinization of starch and mechanical properties of starch pastes. In: Roy L, James N, Eugene F. Starch: Chemistry and Technology, 2nd ed. Academic Press, USA, pp 285-309.

DECLARATION

I, the undersigned, declare that this is my original work and has not been presented for a degree in any university.

Tamrat Balcha Balla

Signature: _____

This thesis has been submitted for examination with our approval as advisors

Dr. Anteneh Belete

Signature: _____

Dr Nisha Mary Joseph

Signature: _____